**UNIVERSIDAD DE CANTABRIA**

**FACULTAD DE MEDICINA**

**DEPARTAMENTO DE ANATOMÍA Y BIOLOGÍA CELULAR**


# TESIS DOCTORAL

# "Papel de los factores de transcripción Sp6 y Sp8 en el desarrollo de la extremidad"

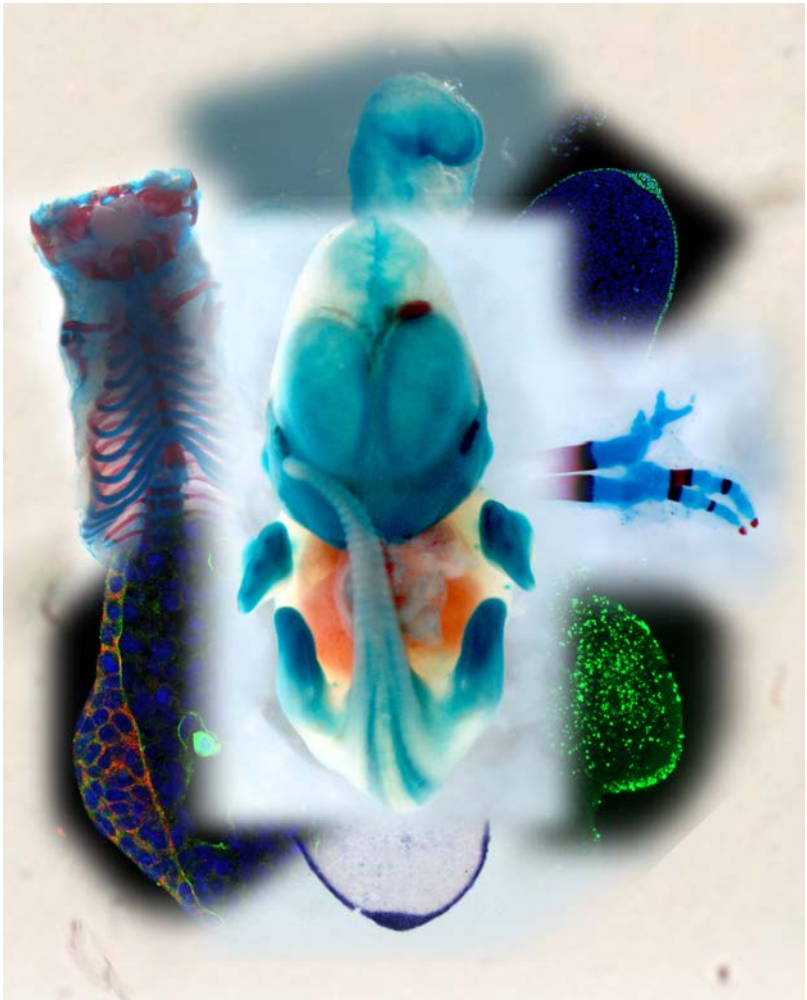


**Endika Haro Gabicagogeascoa**


**Santander 2013**

**UNIVERSIDAD DE CANTABRIA**

**FACULTAD DE MEDICINA**

**DEPARTAMENTO DE ANATOMÍA Y BIOLOGÍA CELULAR**

# "Role of Sp transcription factors Sp6 and Sp8 in limb development"

**Tesis Doctoral**

**presentada por**

**ENDIKA HARO GABICAGOGEASCOA**

**Para optar al Grado de Doctor**

**Dra. María Ángeles Ros** profesora de investigación y

**Dra. Federica Bertocchini**, contratada Ramón y Cajal

del Instituto de Biomedicina y Biotecnología de Cantabria (CSIC-UC-SODERCAN), como directoras de la Tesis Doctoral titulada "Papel de los factores de transcripción Sp6 y Sp8 en el desarrollo de la extremidad" "Role of Sp6 and Sp8 transcription factors in limb development"

**CERTIFICAN**

que dicho trabajo ha sido realizado por Don **Endika Haro Gabicagogeascoa** y consideran que se encuentra terminado y reúne los requisitos para su presentación como memoria de doctorado por el interesado, al objeto de poder optar al grado de Doctor por la Universidad de Cantabria.

*María A. Ros Lasierra* *Federica Bertocchini*

Santander a 1 de octubre de 2013

## CONTENTS

## ABBREVIATIONS

| | |
|---|---|
| **AER** | Apical Ectodermal Ridge |
| **AP** | Antero-Posterior |
| **BMP** | Bone Morphogenetic Protein |
| **DV** | Dorso-Ventral |
| ***Dlx*** | Distal-less homeobox |
| **E** | Embryonic day |
| ***En1*** | Engrailed-1 |
| **FGF** | Fibroblast Growth Factor |
| **h** | Hour |
| **GOF** | Gain of function |
| **HH** | Hamburger and Hamilton |
| **IHC** | Immunohistochemistry |
| **ISH** | In situ hybridization |
| **KO** | Knock Out |
| **LPM** | Lateral Plate Mesoderm |
| ***Lmx1b*** | LIM homeobox transcription factor 1 beta |
| **LOF** | Loss of function |

| | |
|---|---|
| ***Msx*** | msh Homeobox |
| **min** | Minute |
| **ON** | Over night |
| **PBS** | Phosphate Buffered Saline |
| **PD** | Proximo-Distal |
| **PCR** | Polymerase chain reaction |
| **PFA** | Paraformaldehyde |
| **RA** | Retinoic Acid |
| **RE** | Restriction enzyme |
| **RT** | Room temperature |
| **SEM** | Scanning Electron Microscopy |
| **SHFM** | Split hand/foot malformation |
| ***Shh*** | Sonic hedgehog |
| ***Sp*** | Specificity Protein |
| **Tam** | Tamoxifen |
| ***Tp63*** | Tumor Protein 63 |
| **TUNEL** | Terminal deoxynucleotidyl transferase–mediated dUTP nick end labeling |
| **ZPA** | Zone of Polarizing Activity |

# RESUMEN

**RESUMEN**

Durante el desarrollo, la formación de un nuevo organismo resulta de la combinación coordinada de múltiples procesos como son especificación, crecimiento y muerte celular. Entre los principales modelos para el estudio de esos procesos se encuentra la extremidad, puesto que no constituye un órgano vital y puede ser genética o experimentalmente manipulada sin comprometer la supervivencia del embrión.

Las extremidades se forman a partir de pequeños abultamientos que aparecen en la pared lateral del cuerpo embrionario y están formadas por mesodermo recubierto por una capa de ectodermo. Estos abultamientos, llamados esbozos de la extremidad, bajo la influencia de los llamados "centros señalizadores" forman una extremidad completa y con un patrón perfecto.

Uno de los centros señalizadores mas importantes en el desarrollo de la extremidad es la cresta ectodérmica apical (AER), que dirige el crecimiento a lo largo del eje próximo-distal. Se trata de un epitelio situado en el extremo mas distal de la extremidad en desarrollo. El hecho de que el desarrollo de la extremidad quede truncado cuando la AER es dañada o extirpada quirúrgicamente, demuestra claramente su necesidad para el correcto desarrollo de la extremidad. La función principal de este centro señalizador es la de regular la correcta expresión génica, supervivencia celular y proliferación en el mesodermo subyacente a ella. Estas funciones son llevadas a cabo mediante la producción de diversos miembros de la familia de Factores de Crecimiento Fibroblástico (Fgfs).

La formación de la AER comienza con la inducción de las células precursoras de la misma. En ratón, estas células están inicialmente localizadas en el ectodermo ventral del esbozo de extremidad y mediante movimientos morfogenéticos quedan compactadas en el límite dorso-ventral, dando lugar a un epitelio poliestratificado denominado AER madura. Se trata de un proceso muy complejo, estrechamente ligado al inicio del esbozo de la extremidad y al establecimiento del eje dorso-ventral. Dicho proceso está dirigido por complejas interacciones entre diferentes vías de señalización, entre las que cabe destacar

las vías de señalización por Bmp, Wnt/β-catenina y Fgf, que actúan tanto en el ectodermo como entre los componentes del ectodermo y del mesodermo.

Actualmente se acepta que una actividad Wnt/β-catenina, en ectodermo, es necesaria tanto para la inducción de la AER como para su mantenimiento. Por otra parte, la señalización por Bmp también es esencial para la inducción de la AER, actuando probablemente *"upstream"* de la señalización por Wnt/β-catenina. Paradójicamente, una vez que la AER ha sido inducida, la señalización por Bmp se vuelve perjudicial para el mantenimiento de ésta y termina por tomar parte en su regresión.

A pesar del gran número de estudios que hacen referencia a los mecanismos de inducción y mantenimiento de la AER, pocos factores de transcripción han sido descritos como mediadores en estos procesos. En particular, dos miembros de la familia de factores de transcripción Specificity Proteins (SP), Sp6 y Sp8, conocidos también como Epiprofin (Epfn) y Buttonhead (Btd) respectivamente, han sido descritos como imprescindibles para el mantenimiento y la maduración de la AER.

Ambos factores de transcripción constan de un patrón de expresión similar en el ectodermo del esbozo de extremidad, particularmente en la AER. En lo que concierne a la formación del eje próximo-distal, diversos estudios sitúan a estos dos factores de transcripción "*upstream*" de *Fgf8* y "*downstream*" de la señalización por Wnt/β-catenina en el ectodermo de la extremidad, indicando su implicación en el proceso de mantenimiento y maduración de la AER.

Las extremidades que se forman en ausencia de *Sp6* se caracterizan por la presencia de una sindactilia mesoaxial en las extremidades superiores y una sinostosis en las inferiores, además de una dorsalización parcial en la punta de los dedos. En lo referente a la AER, ésta se desarrolla con defectos de maduración. En el caso de los mutantes para *Sp8*, en el mejor de los casos el individuo llega a nacer pero muere en el periodo perinatal debido a defectos neurológicos, siendo así letal la deleción de este gen. Las extremidades aparecen con diferentes grados de truncamiento en relación a una regresión prematura de la AER.

Debido a la estrecha relación entre los genes *Sp6* y *Sp8* y su similar patrón de expresión, am factores podrían tener una función redundante en el desarrollo de la extremidad. También cabe destacar que en el "*Knock out*" (KO) de *Sp6* se mantiene la expresión de *Sp8*. Debido a esta posible redundancia en la función de estos dos factores de transcripción, es necesaria la generación del doble KO *Sp6;Sp8* para poder esclarecer su en el desarrollo de la extremidad.

Por todo ello, el objetivo de la presente Tesis Doctoral es el análisis de la función de los factores de transcripción Sp6 y Sp8, así como su posible redundancia en el desarrollo de la extremidad, particularmente en la inducción de la AER y en el establecimiento del patrón antero-posterior. Para ello hemos utilizado el ratón como animal modelo, para la generación y la caracterización del doble mutante *Sp6;Sp8,* así como mutantes condicionales de *Sp8* en un "*background*" nulo para *Sp6* con el uso de dos líneas, la *Ap2α-Cre* y la *Msx2-Cre*.

El análisis fenotípico de los mutantes y su caracterización molecular nos ha permitido determinar el requerimiento de *Sp6* y *Sp8*, así como su redundancia, en el desarrollo de la extremidad. En ausencia de ambos genes o incluso cuando sólo un alelo funcional de *Sp6* está presente (en ausencia de *Sp8*), las extremidades no se forman, dando lugar a fenotipos amélicos. La pérdida de un alelo de *Sp8* en ausencia de *Sp6,* da lugar a un fenotipo reminiscente de la malformación en humanos conocida con el nombre de mano hendida/pie hendido. El análisis de los mutantes demostró que ambos factores de transcripción son necesarios de una forma dosis dependiente aunque, probablemente, por su mayor nivel de expresión *Sp8* realiza una mayor contribución que *Sp6* al desarrollo de la extremidad.

Finalmente, los análisis moleculares mostraron que ambos factores de transcripción son necesarios para la inducción de la AER, actuando de forma redundante en la inducción de *Fgf8* mediada por Wnt/β-catenina. Además, estos factores podrían estar cooperando con la vía de señalización de Bmp en la inducción de *Engrailed1* y, por tanto, actuando en el establecimiento del patrón dorso-ventral de la extremidad

# 1. INTRODUCTION

# 1. Introduction

Developmental Biology is the field focused in the understanding of the transformation process that a fertilized egg suffers to generate a remarkable ordered cellular diversity before becoming an adult organism able to ensure the continuity of life in successive generations. Living organisms are under a constant process of progressive changes termed development, process that never ends due to the constant renewal of cells that constitute the adult organism. Although the process of generating an adult organism from a single cell differs between different species, several aspects can be gathered under the same generalized features. Through the coordination of multiple processes such as specification, growth and programmed cell death, development leads to the generation of new organisms.

Embryology is the discipline inside developmental biology that studies the development of the organism from fertilization to the fetus stage. During this period of time the organism is called embryo. In the human, the term embryo refers to the developing organism from the moment the zygote is implanted until the eight week after conception (tenth week of pregnancy), from this point onwards it is termed fetus. Embryology is focused on the description of the processes that the embryo suffers during development, while developmental biology centers its attention trying to understand the causality of the developmental processes within an organism.

The generation of a new organism starts with the fecundation. In this process, the fusion of the genetic material provided by two gametes (the sperm and the egg) leads to the formation of a fertilized egg or zygote. Once the fertilized egg is formed, a phase known as cleavage occurs. During cleavage, the zygote undergoes several mitotic divisions and develops into a morula, a compact sphere composed of blastomers. This phase finishes with the generation of the blastula, a fluid filled sphere known as blastocoel surrounded by a cell layer termed the trophoblast that nourishes the blastocyst and will develop the embryonary part of

the placenta. A group of blastomers concentrated in one of the poles of the blastocyst (the animal pole) forms the inner cell mass that will develop into the fetus.

The cleavage is followed by gastrulation. The gastrulation is the phase where the gastrula is generated and drastic cell rearrangements occur. These cellular movements give rise to the formation of the three germ layers typical of triploblastic embryos: ectoderm, endoderm and mesoderm. After gastrulation, cellular interactions lead to the generation of the organs. During this process termed organogenesis the ectoderm, the outer layer of the gastrula, is responsible for the development of the epidermis and the nervous system, the endoderm or inner layer gives rise to the digestive system and associated organs, such as liver, pancreas and lungs and the mesoderm, located between the ectoderm and the endoderm, produces the heart, the gonads and the kidney but also blood cells and vessels, bones, tendons and muscles.

During development a single cell, the zygote, will give rise to more than 200 different types of cells that will form part of the more than 30 different organs that constitute about more than 10 systems or apparatus present in an organism. The influence of different signalling pathways orchestrates the generation of the cellular diversity and pushes cells to acquire morphological and functional characteristics according to their different fates. All these interactions enable the generation of the different tissues and organs, through a process known as differentiation.

Previous to differentiation cells acquire a commitment to a certain fate. This commitment can be divided into two states, specification and determination. Specification is the reversible state of the cells that precedes determination. In this state the information to acquire morphological and functional characteristics according to a specific commitment is established. However, the exposure to different signals could break the commitment and change their fate. Determination

instead, is an irreversible state and is often closely followed by differentiation. A cell is determined when the commitment to its fate cannot be broken, the cell will continue towards the specified fate even when transplanted into a different environment.

Despite the bewildering number of cell types and patterns found during development, few signalling pathways have been shown to be responsible for generating them. The vast majority of the signalling molecules, ligand, receptor and signal transducer belong to the same five families: WNT, Notch, Transforming Growth Factor-ß (TGF-ß), Fibroblast Growth Factor (FGF) and Hedgehog (Hh) families. Hence, developmental biology tries to understand the role of these signalling pathways during development, as well as, the interactions amongst them.

Over many decades, animal models have been used as tools to figure out the regulatory mechanisms behind developmental processes. Based on the high homology between different animal models and humans, the use of these models has become an incredibly helpful tool to gain insights into several aspects of human biology and diseases.

Since vertebrate limb is an easily accessible organ and it's experimental manipulation does not affect embryo survival, it has become a popular system for the study of the mechanisms orchestrating the organogenesis. Grafting and recombination experiments in chicks as well as gene-targeted manipulation assays in mice have provided incredibly helpful insight concerning the intricate interactions between the different signalling pathways that pattern the limb. Moreover, the possibility to extrapolate the relation amongst the different signalling pathways during limb development to other developmental process makes the limb a very useful tool.

## 1. 1 Limb development

The first morphological evidence of limb development is appreciable when differences in proliferation rates between cells of the flank and those of the prospective limb fields occur. By the time proliferation rates are maintained in the prospective limb area but decrease in the flank of the embryo, cells from the lateral plate mesoderm (LPM) start to accumulate under the ectoderm, leading to the appearance of slight bulges in the lateral body wall of the embryo (Fig. 1)(Searls and Janners, 1971).

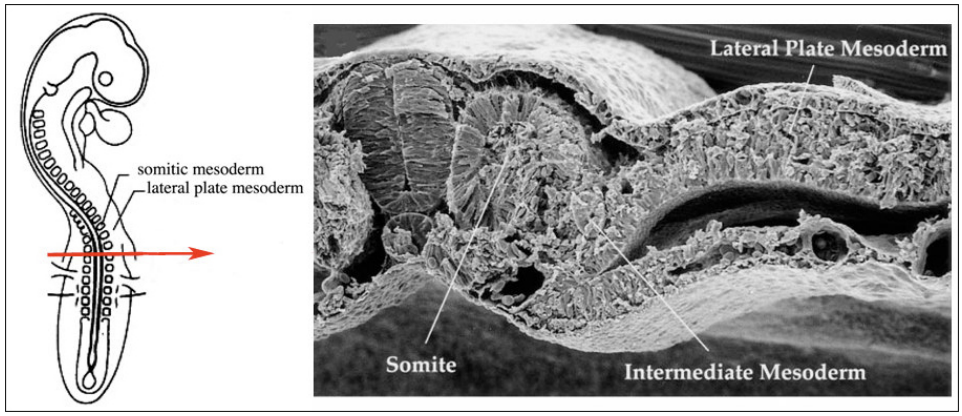


**Figure 1. The limb is formed by cells from the lateral plate mesoderm (LPM; limb skeletal precursor) and from the somitic mesoderm (limb muscle precursors).** Representation of a 16HH chick embryo (left) and scanning electron microscopy (SEM) section (right). The SEM photograph corresponds to a transversal section at the level of the wing (indicated with a red arrow). The limb develops from the LPM and the muscular precursors cells colonize the limb form the somitic mesoderm. The intermediate mesoderm lies between them. From Johnson and Tabin, 1997.

Vertebrate limb development is a complex process governed by several interactions mainly between the ectoderm and the mesoderm but also within the ectoderm and within the mesoderm. Interactions amongst multiple signalling pathways establish pattern along the three main axes of the limb; the proximo-distal (PD) axis (from the shoulder/hip to the tip of the digits), the anterior-posterior (AP) axis (from the thumb to the little finger) and the dorso-ventral (DV) axis (from knuckle to palm)(Fig. 2A).

Outgrowth and patterning along the three axes is controlled by three signalling centers that arise in the limb bud as it emerges (Mariani and Martin, 2003; Niswander, 2003; Tickle, 2003). These signalling centers are the Apical Ectodermal Ridge (AER), the Zone of Polarizing Activity (ZPA) and the non-AER ectoderm. These signalling centers control development and patterning in each one of the three axes through the production of specific signalling molecules responsible for the developmental behavior of neighbouring cells.

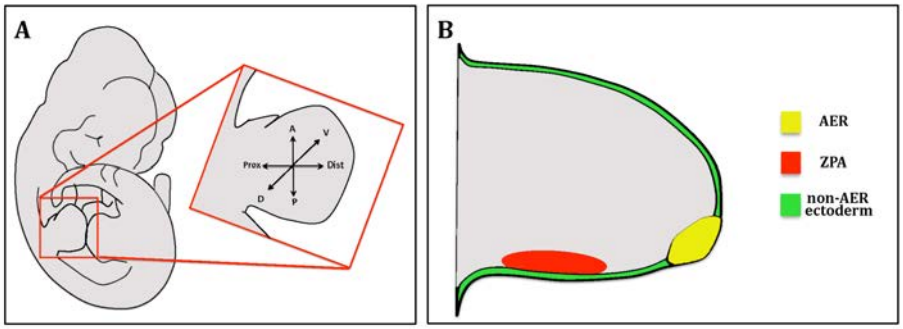


**Figure 2. Illustration of limb axes and signalling centers.** A) Illustration of a mouse embryo depicting the three spatial limb axes Proximo-distal (PD), anterio-posterior (AP) and dorso-ventral (DV). B) Schematic representation of a mouse limb bud showing the signalling centers AER (yellow), ZPA (red) and non-ectoderm AER (Green).

Members of the Fgf family emanating from the AER located at the distal tip of the limb, promotes outgrowth and patterning of the limb along the PD axis (Saunders, 1948; Sun *et al.,* 2002; Boulet *et al.,* 2004; Mariani *et al.,* 2008). The ZPA, a signalling center formed by a group of mesodermal cells located at the posterior limb border drives patterning along the AP axis through the production of Sonic Hedgehog (Shh) (Saunders and Gasseling, 1968; Riddle *et al*., 1993; Yang *et al.,* 1997; Gritli-Linde *et al.,* 2001; Zeng *et al.,* 2001). Finally, the non-AER ectoderm is responsible for DV asymmetries of the limb through the specific expression of *Wnt7a* in the dorsal limb ectoderm and *Engrailed1* (*En1*) in the ventral limb ectoderm (Fig. 2B)(Parr and McMahon, 1995; Loomis *et al*., 1996; Cygan *et al*., 1997). Importantly, coordination and interaction amongst these centers is

indispensable for proper pattern establishment and development of the skeletal elements that form the limb (Laufer *et al*., 1994; Niswander *et al.*, 1994; Parr and McMahon, 1995; Yang and Niswander, 1995).

The limb bud mesoderm is mainly composed of cells from the LPM that will give rise to the connective tissue and the skeletal precursors (Michaud *et al*., 1997). However, from a very early stage it is quite heterogeneous due to the colonization of endothelial and muscular precursor cells from the somitic mesoderm that will develop into muscles and tendons, whereas hair, nails, feathers and eccrine glands are ectodermal derivatives (Chevallier *et al.*, 1977; Christ *et al*., 1977).

During limb development mesenchymal cells condense in a proximal to distal fashion to form a continuous branching. Later on, this branching differentiates into cartilage and subsequent joint formation leads to the segregation of individual elements (Cohn and Bright, 1999; Shubin, 2002). Finally, due to an ossification process, cartilage is replaced by bone and the basic organization of the vertebrate limb is acquired.

Although forelimbs and hindlimbs differ in morphology and acquire their own and unique identity during development, they are formed by homolog elements. A well-developed vertebrate limb consists of three main skeletal segments termed in a proximal to distal sequence, the stylopod, the zeugopod and the autopod. The stylopod is the most proximal segment and contains one skeletal element, the humerus in the forelimb and the femur in the hindlimd. The zeugopod corresponds to the intermediate skeletal segment localized between the stylopod and the autopod. It contains two skeletal elements, radius and ulna in the forelimb, and tibia and fibula in the hindlimb. Finally the third segment corresponds to the autopod. The autopod is the most distal element of the limb and contains several elements as carpals/tarsals, metacarpals/metatarsals and phalanges (from proximal to distal)(Fig. 3). While the stylopod and the zeugopod are highly

conserved across tetrapods, the autopod displays a more variable organization amongst different species.

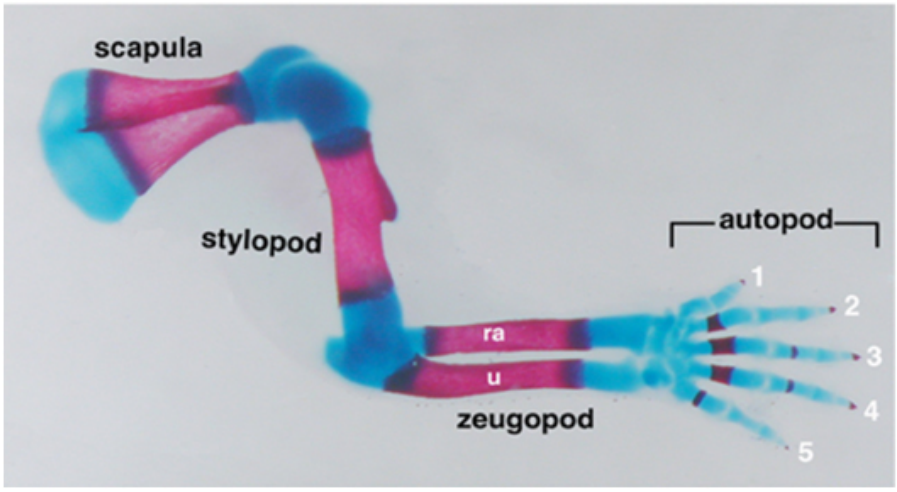


**Figure 3. Skeletal elements of the mouse limb.** Alizarin red (bone) and alcian blue (cartilage) skeletal staining showing the forelimb skeletal pattern of a newborn mouse. The stylopod containing a unique element the humerus, the zeugopod containing the ulna (u) and the radius (ra) and the autopod containing carpals, metacarpals and phalanges. The numbers indicate the identity of each digit.

## 1. 2 Limb initiation

Although limb-forming capacity before getting restricted to the prospective limb mesoderm is broadly distributed along the LPM, limbs arise from very precise locations along the body axes (Burke *et al.,* 1995; Cohn *et al.,* 1997). Interestingly, only four limbs per embryo are specified in all vertebrates and they are always located opposite to each other in respect to the midline.

In the chick, the limb buds are first appreciable by stage 16 of Hamburger and Hamilton (HH; Hamburger and Hamilton, 1951) after 51-56 hours of incubation, while in the mouse they are first evident around embryonic day E9.5 of gestation. In most tetrapods, forelimb always lies at the cervical to thoracic transition and the hindlimb at the lumbosacral transition (Burke *et al.,* 1995). The

protuberances are present in the embryo trunk extending opposite to somites 15-20 in chick and 7-12 in mouse for the upper limbs, while lower limbs developed opposite to somites 26-32 in chick and 23-28 in mouse (Fernandez-Teran and Ros, 2008).

Prospective limb field positioning along the embryo body axes is under a rigorous specification process in which intricate interactions between different molecules establish their location. Therefore, limb fields and thus limbs, do not form anywhere along the body axis. Several reports have proposed different possible candidates for the specification of prospective limb fields, although this is not fully clear.

Retinoic acid (RA) was proposed as the most upstream molecule involved in limb field specification, but its role remains quite controversial. Supernumerary limb developed after administration of RA in mice at early stages, suggested a role for RA in limb induction (Niederreither *et al*., 1996; Rutledge *et al*., 1994). However, it was later demonstrated that RA treatments were responsible for tail bud duplication rather than supernumerary limb formation. The absence of upper limbs in both, mice lacking *Retinaldehyde dehydrogenase* (*Raldh2*; gene encoding the enzyme necessary for the synthesis of RA) (Niederreither *et al*., 2002, Zhao *et al*., 2009) and experiments in chick where RA inhibitors were applied, reinforced the possible role of RA in limb induction (Stratford *et al*., 1996; Helms *et al*., 1996). Very recently, RA has been proposed to be required prior to limb bud induction to antagonize *Fgf8* signal emanating from the heart and the caudal proliferative zone to enable limb bud induction (Cunningham *et al*., 2013).

Finally, it was shown that RA administration led to homeotic vertebral transformation, due to the alteration of the expression boundaries of *Homeobox* (*Hox*) genes in the paraxial mesoderm. This, together with its ability to induce the expression of the Hox transcription factors *"in vitro"*, supports that RA would act

upstream of *Hox* genes in the initiation of limb development (Kessel and Gruss, 1990; Deschamps, 2007).

*Hox* genes were first identified in *Drosophila melanogaster*. They can appear dispersed in the genome or as a single *Hox* complex or cluster composed of 8 transcription factors arranged in a split tandem as in *D. melanogaster*. Tetrapod vertebrates can have up to 13 Hox transcription factors arranged in tandem and organized in 4 different clusters (HoxA-D) (Duboule and Dolle, 1989; Tarchini and Duboule, 2006)(Fig. 4).

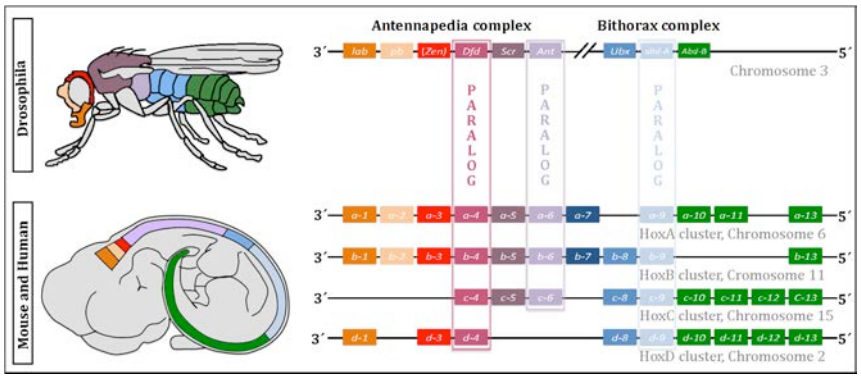


**Figure 4. Hox genes in *Drosophila* and their phylogenetic counterparts in mouse.** In *Drosophila* Hox cluster is composed of 8 genes arranged in tandem in a split-cluster. In the mouse there are 39 *Hox* genes organized in four clusters A, B, C and D in four chromosomes (6, 11, 15 and 2 indicated under each cluster). Three sets of paralogs and their corresponding ancestral genes are designated in color boxes. Spatial colinearity with the embryonic craneo-caudal axis is illustrated (color match between genes and their expression domains along the embryonic axis). From Pang *et al.*, 2010.

Within a single cluster, a 3´ located *Hox* gene is expressed first during development and in a more anterior position along the AP axis of the embryo than a 5´ located one (Kessel and Gruss, 1990; Duboule and Dolle, 1989; Gaunt, 1988; Krumlauf, 1992). This intrinsic property of spatial and temporal collinearity produces nested overlapping expression domains of the *Hox* genes along the AP axis of the vertebrate embryos in correlation with their genomic arrangement. The staggered boundaries in the expression of *Hox* genes have been shown to play

determinant roles in the specification of positional identity along the body axis of insect segments and chordate neural tube and axial skeleton, because modifications in the expression patterns of *Hox* genes resulted in homeotic transformations (Akam *et al.,* 1994; Krumlauf, 1994).

The analysis of *Hoxb9*, *Hoxc9* and *Hoxd9* expression in the LPM after inducing ectopic limbs in chick, suggested the involvement of the staggered and dynamic expression of these *Hox9* paralogs in the specification of the prospective wing, flank and leg territories (Cohn *et al.,* 1997). In addition, *Hoxb5*, *Hoxc6* and *Hoxc8* anterior expression boundaries located at the level of the upper limbs (Oliver *et al*., 1990; Rancourt *et al*., 1995; Nelson *et al*., 1996), together with an anterior shift of the forelimbs observed in mice lacking *Hoxb5* supported the implication of the expression boundaries of *Hox* genes in limb positioning (Rancourt *et al.*, 1995). Moreover, lack of morphological evidence of forelimb development in snakes was correlated with an extended expression domain of *Hox* genes, in both the paraxial and the LPM (Cohn & Tickle, 1999).

Although the proposal for the implication of *Hox* genes in limb positioning, gene targeting analysis carried out in mouse disrupting different combinations of *Hox* genes did not verify the involvement of any member of this family in the specification of limb positioning. The only case regarding the role of *Hox* genes in this aspect is the mentioned deletion of *Hoxb5* in mouse (Rancourt *et al*., 1995). However, a cervico-thoracic homeotic transformation could account for the anterior shift of the forelimb. In spite of this controversy, *Hox* genes in the LPM have been shown to be required upstream of the T-box transcription factors (Minguillon *et al*., 2005).

The members of the T-box family of transcription factors were shown to play multiple roles during limb development (Rallis *et al.,* 2005; Papaioannou and Silver 1998). Expression of several members of this family in the developing limb was reported to be spatially and temporally consistent with a role in the limb

specification process (Gibson-Brown *et al.,* 1996; Gibson-Brown *et al.*, 1998; Isaac *et al*., 1998; Logan *et al.,* 1998; Takeuchi *et al.*, 2003). Further analysis in mice, demonstrated that expression of *Tbx5* in the forelimb LPM was directly regulated by *Hox* genes supported by the presence of *Hox* binding motifs in the *Tbx5* promoter (Minguillon *et al*., 2012).

*Tbx5* and *Tbx4* are expressed in the prospective forelimb and hindlimb mesoderm respectively and have been shown to be required for forelimb and hindlimb induction (Agarwal *et al.*, 2003; Rallis *et al*., 2003; Naiche and Papaioannou, 2007). Disruption of *Tbx5* leading to absence of pectoral fin induction in zebrafish (Ahn *et al.*, 2002; Ng*. et al*., 2002; Garrity *et al.,* 2002), together with missexpression experiments in chick and lack of forelimbs in mice in which *Tbx5* has been disrupted, demonstrated that *Tbx5* was absolutely required, and sufficient, for forelimb and pectoral fin induction (Ng *et al*., 2002; Takeuchi *et al*., 2003; Rallis *et al*., 2003).

It has been assumed that *Tbx4* in the hindlimb function similar to *Tbx5* in the forelimb. However, while disruption of *Tbx5* abolished forelimb development, in the absence of *Tbx4* the hindlimb still formed (Hasson *et al.,* 2007; Minguillon *et al.,* 2005; Minguillon *et al.,* 2009; Naiche and Papaioannou, 2007). Thus, some additional factor must be cooperating with *Tbx4* for hindlimb induction (Agarwal *et al.,* 2003, Rallis et al., 2003, Minguillon *et al*., 2005). In chick, hindlimb restricted expression of the paired homeodomain factor, Pitx1, was shown to precede that of *Tbx4*. Further analysis in mice demonstrated that it was responsible for *Tbx4* expression and that both were conjointly required for proper hindlimb development (Logan and Tabin, 1999; Kioussi *et al*., 1999; Lanctot *et al.,* 1999; Szeto *et al.,* 1999; Duboc and Logan, 2011).

In the current model limb induction is a tightly regulated process that relies on intricate ephitelial-mesenchymal interactions in which a Wnt/ß-catenin activity restricts the limb forming ability to the prospective limb mesoderm where a

regulatory loop between Fgf signalling from the mesoderm and the ectoderm components of the limb is established (reviewed by Tabin 1995). The ability of the members of the Fgf family to develop ectopic limbs when applied to the flank (Cohn *et a*l., 1995; Crossley *et al*., 1996; Vogel *et al*., 1996) together with the dynamic expression pattern of *Fgf10* in the LPM during chick development focused the attention on it as a possible candidate responsible for the induction of Fgf signalling in the limb ectoderm (Ohuchi *et al*., 1997). At early stages of chick development prior to the appearance of the bud, *Fgf10* is expressed in a broad domain of the LPM, as well as, in the segmental plate and the intermediate mesoderm. However, by 14HH in chick, just prior to limb bud appearance and *Fgf8* expression in the limb ectoderm, *Fgf10* gets restricted to the prospective limb mesoderm (Ohuchi *et al*., 1997).

Expression of *Tbx5* and *Tbx4* was shown to be required upstream of *Fgf10* in the prospective limb forelimb and hindlimb mesoderm, respectively (Agarwal *et al*., 2003; Rallis *et a*l., 2003; Takeuchi *et al*., 2003). In chick, *Tbx5* has been shown to be necessary for *Wnt2b* expression in the prospective forelimb mesoderm, whereas *Wnt8c* requires previous *Tbx4* expression in the hindlimb prospective mesoderm (Takeuchi *et al*., 2003). In chick, *Wnt2b* is required to restrict or maintain *Fgf10* expression in a Wnt/ß-catenin dependent manner at the appropriate level of the LPM where forelimb buds developed, while Wnt8c acts in the same manner in the hindlimb (Kawakami *et al*., 2001). In mouse, mesodermal requirement of Wnt/β-catenin activity previous to restriction of *Fgf10* expression to the LPM has been also suggested (Kawakami *et al*., 2011). However, the epistatic relation between *Tbx* and Wnt/β-catenin signalling in the LPM upstream of *Fgf10* is not clear. Studies in mice and chick support the requirement of the *Tbx* genes upstream of Wnt/β-catenin signalling, whereas gene inactivation studies in zebrafish positioned *Wnt2b* upstream of *Tbx5* (Ng. *et al*., 2002). In addition, *Hox* genes have been recently involved in the direct regulation of *Fgf10* in the LPM (Sheth *et al*., 2013).

The limbless phenotype of mice lacking *Fgf10* demonstrated its requirement for limb outgrowth and development, consistent with a failure in *Fgf8* induction in the limb ectoderm (Min *et al*., 1998; Sekine *et al*., 1999). However, although mice lacking *Fgf10* have no limbs, an initial bulge is formed implying the irrelevance of *Fgf10* for the initial accumulation of LPM cells under the ectoderm (Sekine *et al*., 1999).

Once *Fgf10* expression gets restricted to the prospective limb mesoderm, it induces *Fgf8* expression in a set of specific cells of the overlying ectoderm, in a Wnt/β-catenin dependent manner. The induction of *Fgf8* in the ectoderm establishes a positive regulatory feedback loop between *Fgf8* and *Fgf10* signalling (Ohuchi *et al*., 1997; Kawakami *et al*., 2001). Mesodermal *Fgf10* signalling to the ectoderm through its receptor Fgfr2b (Xu *et al.,* 1998; Arman *et al*., 1999; Yu *et al*., 2008; Lu *et al*., 2008) induces the expression of *Wnt3a* in the chick limb ectoderm (Kengaku *et al.*, 1998). In mouse, gene-targeting analysis demonstrated that *Wnt3* fulfills the role of *Wnt3a* in chick (Barrow *et al*., 2003). Next, these Wnt signalling molecules in the limb ectoderm activate *Fgf8* expression in certain limb ectodermal cells, in a Wnt/β-catenin dependent manner (Kengaku *et al.*, 1998; Soshnikova *et al*., 2003; Barrow *et al*., 2003; Yu *et al*., 2008; Lu *et al*., 2008). As the limb grows ectodermal cells expressing *Fgf8* developed into a mature AER. Once *Fgf8* is induced in the limb ectoderm it maintains *Fgf10* expression in the underlying mesoderm (Ohuchi *et al.,* 1997), establishing a positive regulatory loop between *Fgf8* in the ectoderm and *Fgf10* in the mesoderm, absolutely required for limb bud outgrowth (Ohuchi *et al*., 1997; Xu *et al.,* 1998)(Fig. 5).

The current model predicts that disruption of any component of this regulatory Wnt/Fgf loop will result in limbless phenotypes due to a failure in Fgf expression in the limb ectoderm, as occurs in mice lacking *Tbx5* (Agarwal *et al*., 2003; Rallis *et a*l., 2003), *Fgf10* (Min *et al*., 1998; Sekine *et al*., 1999), *Fgfr2* (Xu *et al.,* 1998; Arman *et al*., 1999; Yu *et al*., 2008; Lu *et al*., 2008), Wnt/ß-catenin (Barrow *et al*., 2003; Soshnikova *et al*., 2003) or *Wnt3* (Barrow *et al*., 2003).

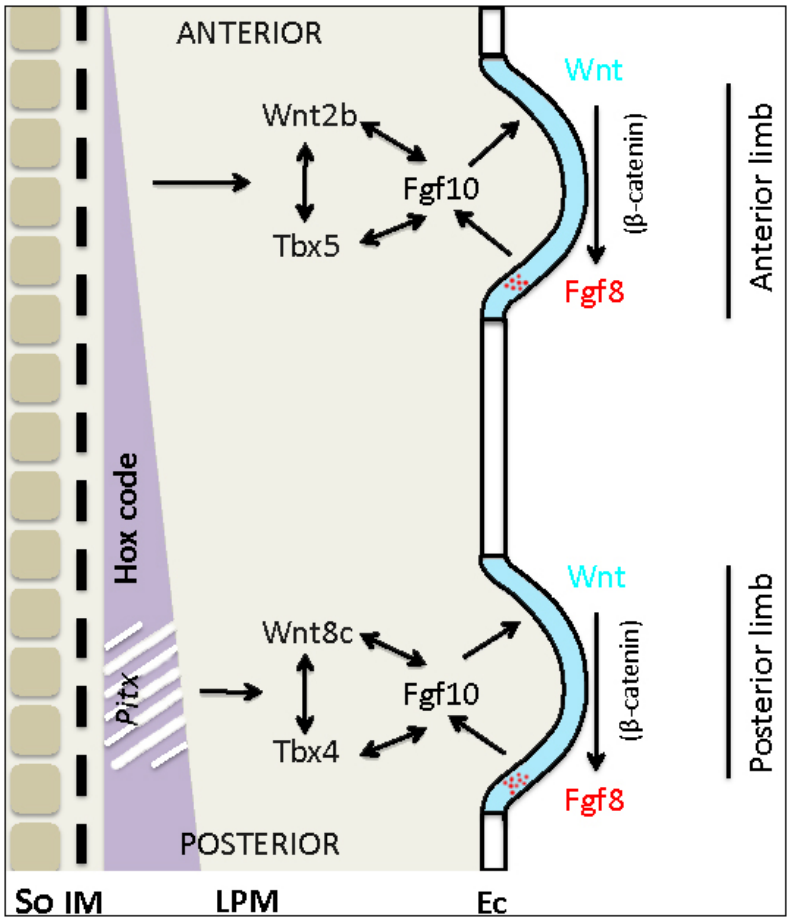


**Figure 5. Illustration of the regulatory cascade involved in limb initiation.** A *Hox* code in the lateral plate mesoderm and *Pitx1* in the hindlimb territory acting upstream of the Tbx transcription factors and a Wnt activity in the lateral plate mesoderm, *Wnt2b* and *Wnt8c* in the forelimb and hindlimb respectively, are required for the restriction of *Fgf10* expression in the prospective limb mesoderm. Fgf10 signalling from the mesoderm induces the expression of *Wnt3* in chick or *Wnt3a* in mouse limb ectoderm that in turns activates the expression of *Fgf8* in the limb ectoderm in a Wnt/β-catenin dependent manner. Then, Fgf8 signalling to the mesoderm maintains *Fgf10* expression and a regulatory loop is established. So, Somite; IM, Intermediate mesoderm; LPM, Lateral plate mesoderm; Ec, Ectoderm. Based on Kawakami *et al.,* 2001.

## 1.3 Signalling centers

### 1.3.1 Proximo-Distal axis and the AER

The AER is the thickened epithelium running along the DV boundary of the limb bud (Fig. 6A), responsible for the PD elongation and patterning of the limb through the maintenance of the underlying mesenchyme in a proliferative and undifferentiated state (Saunders *et al.,* 1948; Dudley *et al.,* 2002; Sun *et al.,* 2002; Niswander *et al.,* 2003; Tickle, 2003; Boulet *et al.,* 2004; Mariani *et al.,* 2008). It is

an embryonic transitory and very dynamic structure subject to morphogenetic changes during development (Guo *et al*., 2003). A mature AER consists of a thickened pseudostratified columnar epithelium in birds and polystratified in mammals (Fig. 6B,C).

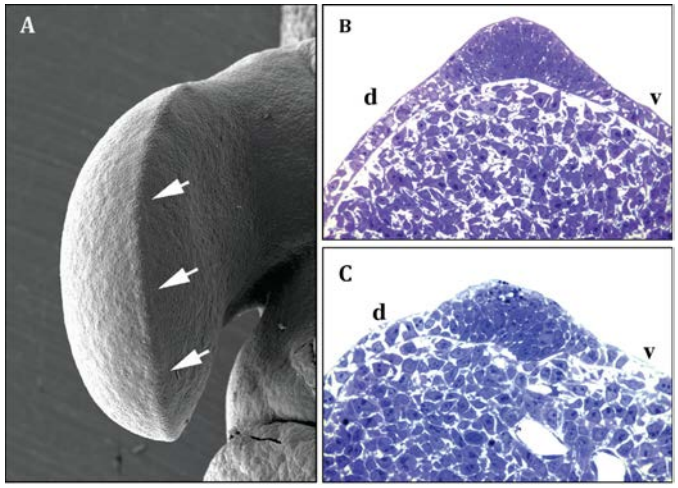


**Figure 6. AER Morphology.** 26HH chick limb scanning microscopy photograph showing a distal view of the AER prominence indicated by arrows (A). Semithin sections of 20HH chick wing where the pseudostrtaified organization is appreciable (B) and E10.5 mouse where a polystratified organization is visible (B). From Fernandez-Teran and Ros, 2008.

Surgical AER removal experiments in chick demonstrated the importance of this structure during limb development. While surgical removal during early stages of limb development led to the formation of severely truncated limbs, progressively removal at later stages resulted in the formation of more distal elements in a progressive fashion. These experiments unveiled the relevance of this signalling center during limb outgrowth along the PD axis (Saunders, 1948; Rowe *et al*., 1982; Cohn *et al.,* 1995). Since limb PD outgrowth and patterning was shown to be an AER dependent developmental process, understanding the

processes concerning its formation and maintenance, as well as, the identification of the mechanism involved in the function that exerts in the underlying mesoderm has became one of the major objectives within the limb field.

Interestingly, members of the Fgf family were shown to be expressed within the AER and the finding that beads soaked in Fgf induced ectopic limb formation when applied into the flank and also that development of truncated limbs after AER removal was rescued by either application of Fgf soaked beads or Fgf expressing cells, demonstrated that AER activity was mediated by Fgf signalling (Fallon *et al.,* 1994; Niswander *et al.,* 1993).

Several members of the Fgf family *Fgf4*, *Fgf8*, *Fgf9* and *Fgf17* exhibits a restricted pattern of expression in the AER and are termed the AER-Fgfs. However, while *Fgf8* expression spatially and temporally accompanies the whole existence of the AER, the rest of AER-Fgfs showed a lower level of expression and a more posteriorly restricted pattern of expression in time and space (Heikinheimo *et al.,* 1994; Ohuchi *et al.,* 1994; Mahmood *et al.,* 1995; Crossley *et al.,* 1995).

Combinatorial deletions of the different AER-Fgfs demonstrated that they are functionally redundant (Fig. 7) (Sun *et al*., 2000; Mariani *et al.*, 2008). *Fgf8* is the major contributor to the Fgf dose provided by the AER, followed by *Fgf4*, *Fgf9* and *Fgf17* and it is considered the principal mediator of AER function, because it is sufficient for proper limb development (Mariani *et al.*, 2008). Amongst the *Fgfs* expressed in the AER, *Fgf8* is the only one that leads to limb defects when disrupted (Moon and Capecchi, 2000; Lewandoski *et al.*, 2000; Sun *et al.*, 2002; Mariani *et al.*, 2008).

In absence of *Fgf8*, the limb bud is reduced in size and exhibited aplasia or hypoplasia of specific skeletal elements (Moon and Capecchi, 2000; Lewandoski *et al.*, 2000). Remarkably, additional removal of *Fgf4* resulted in amelic phenotypes implying that the AER exerts its function through the production of the members of Fgf family (Sun *et al.,* 2002; Boulet *et al.,* 2004). In addition, the mild limb

phenotype observed after *Fgf8* removal can be explained due to the upregulation of *Fgf4* that was expressed earlier and in a more anterior fashion than in normal circumstances (Moon and Capecchi, 2000).

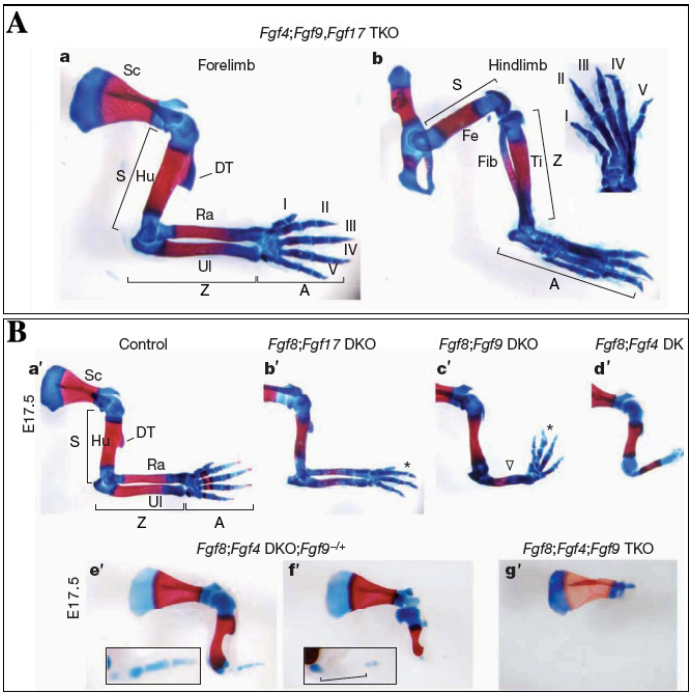


**Figure 8. Effects of AER-Fgf inactivation in mouse limb development.** A) Forelimb (a) and hindlimb (b) skeleton phenotype of *Fgf4;Fgf9;Fgf17* triple KO mutants. B) Combinations of different AER-Fgf inactivation leading to limb phenotype. a´ corresponds to control, b´ to *Fgf8;Fgf17* DKO, c´ to *Fgf8;Fgf9* DKO (Asterisks in b´ and c´ indicates that the mutant autopod has only four digits), d´ *Fgf8;Fgf4* DKO, e, and f´ illustrates the two different phenotypes obtained for *Fgf8;Fgf4 DKO;Fgf9*$^{-/+}$ the more and the less common respectively (the inset is a higher magnification of the distal elements and the bracket in f indicates a gap between the distal humerus and the digit-like element), g´ *Fgf8;Fgf4;Fgf9*$^{-/-}$ TKO. From Mariani *et al*, 2008.

### 1.3.1.1 Fgf signalling

Fgf is a large family composed at least of 23 known different growth factors in which alternative splicing produces further diversity (Martin, 1998; Ornitz, 2000; Ornitz and Marie, 2002). Signalling by Fgf members is mediated through 4 different fibroblast growth factor receptor (Fgfr). Each of *Fgfr* encodes a tyrosine kynase receptor which is further diversified by the production of alternative spliced forms containing 2 to 3 inmunoglobulin (Ig) extracellular domains (Hou *et al*., 1991; Werner *et al*., 1992; Orr-Urtreger *et al*., 1993; Ornitz *et al*., 1996). The

alternative splicing isoforms have different binding affinities for the different Fgfs. Fgfr are selectively distributed in the limb bud (Orr-Urtreger *et al*., 1993), *Fgfr1* expression is restricted to the limb mesoderm (Partanen *et al*., 1998), different isoforms of the *Fgfr2* are expressed in both the mesoderm and the AER (Xu *et al*., 1998) and *Fgfr3* is expressed in the growth plate of long bones, whereas *Fgfr4* is not expressed in the limb bud (Weinstein *et al*., 1998). The distribution and the high variability of both, the ligands and the receptors, together with the different affinities between them increase the complexity of the Fgf signallig pathway.

Intracellular signal transduction downstream of Fgf signalling is highly variable and leads to the phosphorylation of several target signal transducers. Heparin Sulfate Proteoglycans (HSPG) promotes ligand binding and receptor dimerization (Ornitz, 2000; Lin, 2004). Dimerization and subsequent autophosphorylation of the receptor activates the Growth factor receptor-bound protein (*Grb2*) or the *Fgfr* stimulated *Grb2* binding protein (*Frs2*) and leads to the formation of membrane associated complexes responsible for the recruitment of either Ras or phosphatydil-inositol 3´-OH kynase (PI3K). This recruitments leads to the activation of the mitogen activated protein kynase pathway (MAPK) that includes ERK, JNK or p38 signal transducers (Roux and Blenis, 2004) or the AKT pathway, respectively (Datta *et al*., 1999). In addition, *Fgfr* signal transduction can act through JAK/STAT, as well as, PLC-γ1 (Mohammadi *et al*., 1991).

#### 1.3.1.2 Proximo-Distal patterning

Despite intensive studies have given important clues regarding different signalling molecules and transcription factors involved in limb PD pattern establishment, the mechanisms behind are still unknown and several models have been proposed. Interestingly, *Meis1*, *Hoxa11* and *Hoxa13* exhibit a restricted pattern of expression in the stylopod, the zeugopod and autopod respectively, and

are considered the best markers of each of the limb segments, although they are not responsible for their specification (Tabin and Wolpert, 2007).

Experiments in chick, in which the AER was progressively removed at different stages resulting in progressively more distal truncations corresponding to later AER removals, led to the proposal of the first model to explain the manner in which the limb is specified along its PD axis, the **Progress zone model** (PZM) (Summerbell *et al*., 1973). According to this model, mesodermal cells located under the AER form the progress zone (PZ). Fgf emanating from the AER maintains the cells of the PZ in a continuous proliferative an undifferentiated state. While the limb grows, the size of the PZ remains constant and cells from PZ are progressively released from the influence of the AER and start to differentiate. This model predicts that the longer the cells stay in the PZ under the influence of the AER, the more distal elements they are specified into. It also assumes that distal elements are specified after the specification of the proximal ones and also that the number of divisions should be the way by which cells from the PZ realize the time spent in the PZ.

Transplantation experiments where the PZ from an old chick wing was transplanted into a young chick wing and *vice versa* led to loss and duplication of limb elements respectively (Summerbell and Lewis, 1975), reinforcing the prevalence of the PZM. After 30 years, conditional disruption of *Fgf8* and *Fgf4* resulted in a phenotype incompatible with the PZM and led to the proposal of a new model, the **Early specification model**. Conditional removal of *Fgf8* and *Fgf4* was performed with the use of the *Msx2-Cre* line. The kinetics of this line enables the removal of both Fgfs prior to their induction in the hindlimb, while allowed early and transient expression of both Fgfs in the forelimb. While amelic phenotype resulted from removal of both Fgfs in the hindlimb, the forelimb developed the three segments of the limb with proximal elements being severely hypoplastic and one or two perfectly developed digits (Sun *et al*., 2002). This phenotype was difficult to explain with the PZM. The ESM postulates that from

very early stages the three segments of the limb are already specified and as the limb develops they expand. This model proposed that AER removal experiments that support the PZM could be explained through the increase in cell death observed in the distal mesenchyme after AER removal (Rowe *et al*., 1982; Dudley *et al*., 2002). The lack of early markers for the progenitor cells of the specified segments did not make of this model a very popular model.

The **Differentiation front model** was proposed with the aim to reconcile mouse genetics and manipulation experiments in chick (Tabin and Wolpert, 2007). This model was merely based in the main characteristics of the two-signal model with the difference that it postulates that the state of the early limb is proximal by default. Specification of distal elements is then achieved through the modification of the default state by the action of the AER-Fgfs as indicated by the induction of zeugopod and autopod markers, *Hoxa11* and *Hoxa13* respectively. While proximal cells are progressively determined distal cells are maintained in an undifferentiated state through the influence of the AER-Fgfs until they are specified. The boundary between both states corresponds to the differentiation front, boundary that becomes progressively shifted distally as the limb grows.

The phenotype resulting from the triple conditional deletion of *Fgf8;4;9*$^{+/-}$ lacking the zeugopod in the forelimb while reduced stylopod and autopod are developed was incompatible with the previous models proposed and led to the formulation of the **Two-signal model** (Mariani *et al*., 2008). According to this model, it was proposed that the limb bud develops under the influence of instructive opposing diffusible signals emanating from the trunk and the AER, possibly RA and Fgf signalling respectively. RA was proposed responsible for the specification of proximal elements and Fgf for distal elements. Finally, cellular interactions between proximal and distal domains might be responsible for the specification of the zeugopod. A modified version of this model has been proposed in which as the limb bud grows the distal part of the limb get rid of the influence of

the proximalizing factor and it is subdivided into zeugopod and autopod compartments (Rosello-Diez *et al.,* 2011; Cooper *et al.,* 2011).

Interestingly, regarding RA role in PD establishment, recent analysis carried out in zebrafish and mouse where RA emanating from the trunk has been abolished, implies that RA is not required as an instructive signal for proximal specification of limb segments as assessed by Meis1/2 expression in the proximal mesoderm. Thereby, argues against an opposing diffusible gradient between RA and Fgf, where RA specifies proximal fates (Cunningham *et al*., 2013).

### 1.3.2 Anterio-Posterior axis and the ZPA

Limb AP axis is established very early in development prior to the appearance of the limb bud (Hamburger, 1938). Classical experiment in chick demonstrated that the asymmetry of the vertebrate limbs along its AP axis was controlled by the ZPA. This signalling center is composed of mesodermal cells located at the posterior limb border. The ability to perform mirror image digit duplications when transplanted into the anterior limb mesenchyme, demonstrated that the ZPA was the signalling center responsible for the establishment of the limb polarity along the AP axis (Saunders and Gasseling, 1968).

The first model to explain how digit identity is specified was the classical **Morphogen gradient model**. This model assumes that an unknown diffusible molecule emanating from the ZPA was responsible for the AP polarity through the establishment of a concentration gradient along the AP axis. In addition, it proposed that digit identity corresponded to the positional value acquired by the cells according to their position within the gradient. The model determined that posterior digits required the highest concentrations of the morphogen (Yang *et al*., 1997).

Mirror image digit duplication after RA administration led to the assumption that RA was the mediator of the ZPA responsible for AP pattern establishment (Tickle *et al*., 1982; Tickle *et al.,* 1985; Wanek *et al.,* 1991). Later, Shh, a signalling molecule emanating from the ZPA establishing a gradient along the limb AP axis, was shown to be the morphogen responsible for AP limb polarity (Riddle *et al*., 1993; Lopez-Martinez *et al.,* 1995; Gritli-Linde *et al.,* 2001).

Further analysis demonstrated that Shh elicited the same effect of the ZPA and that AP duplications resulting from RA treatments were due to the induction of *Shh* in the anterior limb mesenchyme (Riddle *et al*., 1993; Helms *et al*., 1996; Lopez-Martinez *et al*., 1995; Yang *et al*., 1997).

Gene-targeting analysis in mice supported the role of *Shh* as the critical morphogen essential for AP pattern establishment of the autopod regulating both digit number and identity, while AP patterning of the stylopod was independent of Shh. In the absence of *Shh* the stylopod is developed in both the forelimb and the hindlimb. However, the zeugopod lacks one element in the forelimb and the autopod is not developed, whereas in the hindlimb both elements of the zeugopod are partially present but fused and only digit 1 is developed (Chiang *et al*., 2001; Chiang *et al*., 1996; Kraus *et al*., 2001).

#### 1.3.2.1 Shh Signalling

Shh signalling transduction is mediated by its receptor Patched (Ptc). In absence of *Shh*, Ptc inhibits the trans-membrane protein Smoothened (Smo) and avoids the activation of target genes. Shh binding to Ptc, enables Shh signalling transduction through the release of Smo. In vertebrates, Gli1, Gli2 and Gli3 transcription factors members of the Glioma associated oncogenes family, were shown to mediate Shh signalling transduction downstream of Smo. Since the limb was correctly developed in absence of *Gli1* and disruption of *Gli2* lead to a delay in

ossification (Mo *et al.,* 1997), whereas mice lacking *Gli3* developed polydactilous limbs (Schimmang *et al.,* 1992; Hui and Joyner, 1993), *Gli3* is the principal mediator of Shh signalling during limb development.

*Gli3* expression is independent of Shh signalling and is uniformly expressed along the AP axis of the limb, except in the ZPA where it is not expressed. In absence of Shh signalling cleavage of the Gli3 full length (Gli3FL) protein to a truncated transcriptional repressor form occurs (Gli3R) (Wang *et al.,* 2000), whereas Shh signalling inhibits the cleavage of the Gli3FL generating a Gli3R gradient along the AP axis with higher concentrations in the anterior mesenchyme, translating the extracellular gradient of Shh into an opposite intracellular gradient of Gli3R. *Shh* dependent gradient of Gli3R was shown to be responsible for digit patterning of the autopod (Wang *et al.,* 2000). Moreover, the analysis of *Gli3* and the double *Shh;Gli3* mutant mice that display the same polydactilous phenotype (Huy and Joyner, 1993; Litingtung *et al.,* 2002; te Welscher *et al.,* 2002), suggested that one the of major roles of *Shh* during limb development was to avoid *Gli3* processing.

#### 1.3.2.2 Digit patterning

Apart from the classical morphogen model, several models have been proposed in order to explain how digit patterning (number and identity) occurs. In chick, the sequence in which extra digit were induced in mirror-image duplications obtained after application of Shh in the anterior limb mesenchyme, led to the formulation of the **Promotion-morphogen gradient model**. This model is a modification of the morphogen gradient model in which apart of the concentration, the exposure time to Shh is also critical for digit identity specification. Anterior digits are specified first and then promoted to more posterior fates as the exposure time increases. This model suggests that specification of posterior digits requires a longer exposure time to higher concentrations of Shh than anterior ones and also

that lower concentrations of Shh even if maintained for longer are not able to specify posterior digits (Yang *et al*., 1997).

Later, fate map experiments determined that Shh descendants' cells contributed to the formation of digits 4 and 5 and half of digit 3. In addition, it was shown that these digits transcribed *Shh* for longer in a progressive posterior fashion and also that they have been exposed to Shh for a longer period of time in an autocrine manner. Thus, the most posterior digit is the one in which its precursors have transcribed *Shh* for longer. Based on these observations, the **Temporal-spatial gradient model** was proposed. According to this, a gradient of Shh signalling is established along the AP axis, where longer exposure time to Shh signalling is critical for posterior digit identity. Digit 1 specification is independent of Shh signalling, digit 2 requires a spatial gradient of Shh signalling, digit 3 requires a spatial and temporal gradient and digit 4 and 5 have transcribed *Shh* for longer and requires only a temporal gradient (Harfe *et al.,* 2004). The generation of a mutant mice with normal lasting but reduced *Shh* expression, where digit 2 was lost but digit 4 and 5 were specified supported this model (Scherz *et al.,* 2007).

More recently, the analysis of mutant mice in which *Shh* transcription was arrested at different time points without affecting its level of expression led to the proposal of the **Biphasic model**. These experiment demonstrated that the reduction in digit number was proportional to the stage at which Shh expression was arrested. The analysis of digit condensations in this mutants showed that the order in which digit were lost (d3, d5, d2 and d4) was the inverse to normal digit formation (d4, d2, d5 and d3). According to this, the model proposed that Shh is required for the specification of digit identity in an early and transitory phase, while the expansion of the digital plate requires continuous *Shh* expression in order to generate sufficient digit precursor cells (Zhu *et al.,* 2008).

In addition, recent studies in chick led to the transformation of the Promotion-morphogen gradient model into a new **Growth-morphogen model** in

which Shh through the control of cell-cycle regulators integrates proliferation and specification of digit precursor cells. In chick, progressive inhibition at early stages of Shh signalling with the use of the *Smo* inhibitor Cyclopamine, resulted in loss of more posterior digits and confirmed that shorter exposures to Shh are required for the specification of anterior digits in comparison to posterior digits (Scherz *et al.,* 2007; Towers *et al.,* 2008). In addition, blocking proliferation through the application of Trichostatin A (TSA) resulted in reduction in limb size with only posterior structures present. Application of TSA abolished *Shh* expression, but, when the effect of the TSA was ended *Shh* expression was recovered and maintained as in non-manipulated circumstances, though temporally shifted, implying that *Shh* expression was controlled by cell proliferation and also that the recovery of Shh signalling after TSA application was enough to determine posterior digit identity (Towers *et al.*, 2008).

### 1.3.3 Dorso-Ventral axis and the non-AER ectoderm

The presence of morphological distinguishable characteristics in the dorsal and ventral regions of the limb reflects its established DV polarity. In mouse limbs, hair only appears on the dorsal surface of the autopod and nails are present in the dorsal surface of digit tips, while footpads and eccrine glands are developed in the ventral surface. Moreover, the internal DV organization is also appreciable due to the dorsal location of extensor muscles and ventral location of the flexor ones.

DV patterning establishment is a complex process involving interactions within the ectoderm but also between the mesoderm and the ectoderm. The stage at which the limb acquires its DV polarity is not fully determined. Surgical manipulation experiments in chick demonstrated that DV polarity of both ectoderm and mesoderm is already established before the initial bud emerges (Altabef *et al*., 1997; Altabef and Tickle, 2002; Kimmel *et al.,* 2000; Michaud *et al.,* 1997). Two different phases can be defined. The earliest one where mesodermal

influences impart the DV limb polarity to the ectoderm, whereas a latest one when this information has been acquired by the ectoderm and this impose it polarity to the limb bud mesoderm (Kieny *et al.,* 1971; Saunders & Reuss, 1974; Geduspan and MacCabe, 1989).

#### 1.3.3.1 Polarizing the limb ectoderm

Whether the information required for the establishment of DV limb polarity resides in the mesoderm remains controversial. Experiments carried out by Kieny and colleagues in which DV inversion of presumptive limb mesoderm grafted under the flank ectoderm resulted in limbs with the same DV polarity of the ipsilateral non-manipulated ones, suggested that influences from the environment were responsible for limb DV polarity (Kieny *et al.,* 1971). However, similar grafting experiment carried out by Saunders and Reuss suggested that from very early stages the ability to establish the DV polarity of the limb resides in the presumptive limb mesoderm. In these experiments, DV inversion of 12HH wing presumptive mesoderm transplanted under the flank ectoderm, resulted in limbs with reverse DV polarity. In contrast to Kienys results, this DV inversion led to the assumption that DV information resides in the presumptive limb mesoderm by this stage and that the mesoderm was able to impose its polarity to the covering ectoderm (Saunder and Reuss, 1974).

In view of the controversial results obtained in the experiments mentioned above, further experiments in chick where bidorsal limbs developed either by positioning the limb prospective field between two rows of somites or by the insertion of a barrier between the prospective limb field and the lateral somatopleure, confirmed the hypothesis that signals emanating from the somitic mesoderm and the LPM were responsible for the DV polarity of the limb between stage 13 and 15HH. Le Douarin and colleagues proposed that molecules emanating from the somitic mesoderm dorsalized the limb ectoderm, whereas inductive

signals emanating from the somatopleure exerted a ventralizing effect over the limb ectoderm (Michaud *et a*l., 1997). These experiments led to a possible explanation for the different results obtained by previously mentioned experiments regarding DV polarity establishment. Since the ectoderm covering the somites could be the source of dorsalizing factors responsible for limb dorsal identity, it is possible that in grafting experiments carried out by Reuss and Saunders a portion of somites attached to the presumptive limb mesoderm when grafted into the flank led to the reversed DV polarity of the grafts. Nevertheless, the molecular mechanisms that mediate mesodermally derived signals responsible for limb DV polarity remains unknown. Bmps in the ventral LPM and its antagonist Noggin in the somitic mesoderm were proposed as candidates for polarizing the ventral and dorsal limb ectoderm respectively (Michaud *et a*l., 1997).

Regarding later stages in development, Geduspan and MacCabe´s experiments in chick demonstrated that by 15/16HH when limb bud starts to be appreciable, the ability to polarize the limb has been already acquired by the ectoderm. In chick 180º rotation of the limb ectoderm after 16HH led to DV inverted limb polarity, while inversion before this stage had no effect implying that the information required for DV establishment resides in the ectoderm by 16HH and that the ectoderm is able to imposed its polarity to the mesoderm. Hence, from this stage on the ectoderm is responsible for limb DV polarity.

#### 1.3.3.2 The non-AER ectoderm

The ectoderm covering the dorsal and ventral sides of the limbs responsible for DV pattern establishment constitute the signalling centre called the non-AER ectoderm. The restricted domains of expression of *Wnt7a,* a secreted signalling molecule member of the Wnt family, expressed in the dorsal ectoderm (Dealy *et al*., 1993; Riddle *et al*., 1995) and the homeodomein transcription factor *En1* expressed in the ventral limb ectoderm (Davis *et al*., 1991; Gardner and Baral,

1992), are responsible for the DV limb pattern establishment and impose its polarity to the underlying mesoderm (Fig. 8) (Riddle *et al*., 1995; Vogel *et al*., 1995; Parr and McMahon, 1995; Rodriguez-Esteban et al., 1997; Cygan *et al*., 1997; Loomis *et al*., 1996; Loomis *et al*., 1998).

*Wnt7a* expression in the dorsal ectoderm has been shown to be required for the expression of the LIM homeodomain transcription factor (*Lmx1b)* in the underlying distal dorsal limb mesenchyme and it is both necessary and sufficient for dorsal limb specification as revealed by gene inactivation studies in mouse and misexpression experiments in chick (Parr and McMahon, 1995; Riddle *et al*., 1995; Vogel *et al*., 1995; Rodriguez-Esteban et al., 1997).

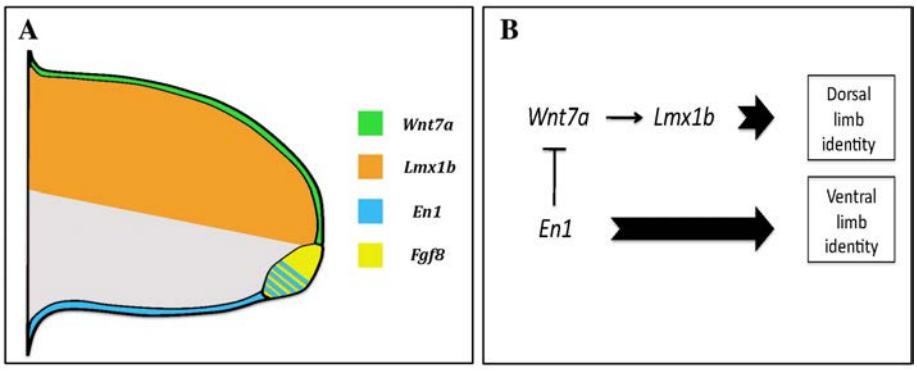


**Figure 8. DV pattern establishment.** A) Pattern of expression of the genes involved in DV pattern establishment in ectodermal and mesodermal compartments. B) Schematic model of the genetic interaction responsible for DV pattern establishment.

Null mutations in the *En1* gene leads to dorsalization of the ventral limb ectoderm due to ectopic activation of *Lmx1b* in the ventral limb mesoderm triggered by ectopic *Wnt7a* expression in the ventral ectoderm. Remarkably, the phenotype of the compound *Wnt7a;En1* mutant displayed a double ventral limb phenotype very similar to that of *Wnt7a* mutant (Wurst *et al*., 1994; Loomis *et al*., 1996; Cygan *et al*., 1997; Loomis *et al*., 1998). In addition, *En1* overexpression in

chick limb dorsal ectoderm was shown to repress *Wnt7a* expression with the subsequent downregulation of *Lmx1b* in the mesoderm (Logan *et al*., 1997; Laufer *et al*., 1997). Hence, *En1* expression in the ventral ectoderm confers ventral identity through the restriction of *Wnt7a* to the dorsal ectoderm that is responsible for limb dorsal identity through its requirement for *Lmx1b* expression in the underlying dorsal limb mesoderm (Fig. 8B)(Davis *et al*., 1991; Gardner and Barald, 1992; Parr and McMahon *et al*., 1995).

Manipulation experiments and gene-targeting analysis in chick and mouse respectively suggest that additional molecules to *Wnt7*, *En1* and *Lmx1b* might be involved in DV pattern establishment (Pautou and Kieny, 1973; MacCabe *et al.,* 1974; Geduspan and MacCabe, 1989; Akita, 1996). Interestingly, *Lmx1b* is expressed all over the dorsal mesoderm, but only the expression on the distal part of the limb depends on *Wnt7a* expression in the dorsal ectoderm, as revealed by the lack of *Lmx1b* expression in the most distal part of the limb in *Wnt7a* mutant, from E11.5 on (Cygan *et al*., 1997; Loomis *et al*., 1996; Loomis *et al*., 1998). In addition, while *Wnt7a* dependent *Lmx1b* expression is restricted to the most distal part of the limb, ectopic expression of *Wnt7a* in the ventral ectoderm of *En1* mutant mice leads to ectopic expression of *Lmx1b* all over the ventral mesoderm (Cygan *et al*., 1997; Loomis *et al*., 1996; Loomis *et al*., 1998). Finally, after 16HH in chick the later the ectoderm is inverted, the more distally restricted DV inversions are developed, implying the ability of the ectoderm to polarize only the distal limb mesoderm (Geduspan and MacCabe, 1989).

#### 1.3.3.3 Dorso-Ventral boundaries in the limb ectoderm

Chick-quail chimeras and cell labeling experiments in chick, as well as gene-targeting manipulation assays in mouse, revealed the existence of three different DV boundaries located at different levels in the AER that are essential for its proper development (Fig. 9)(Michaud *et al*., 1997; Altabef *et al*., 1997; Altabef and Tickle, 2002; Kimmel *et al*., 2000).

Experiments in chick demonstrated the existence of a boundary that operates along the presumptive limb and flank ectoderm. The boundary is present at least from the anterior part of the wing to the posterior part of the leg. The presence of this boundary prevents mixing of cells and splits the ectoderm into dorsal and ventral domains. This boundary is supposed to mark the location at which limbs arise. As the limbs emerge and the AER develops, the boundary localize into the DV middle extent of the AER (Michaud *et al*., 1997; Altabef *et al*., 1997; Altabef and Tickle, 2002). However, cell lineage restriction along this boundary remains quite controversial. While chick-quail graft experiments supported the existence of a sharp boundary localized in the middle DV extent of the AER avoiding cell mixing between dorsal and ventral ectoderm, DiI cell marking experiments in chick showed that dorsal AER cells extended all over the AER while ventral ectodermal cells were restricted to the ventral half of the AER (Michaud *et al*., 1997; Altabef *et al*., 1997; Altabef and Tickle, 2002).

The use of Cre-LoxP based fate maps and retroviral cell-marking experiments carried out in mouse supported the existence of a boundary located at the middle of the AER. The boundary, separates *En1* expressing cells that constitutes the ventral half of the AER from the dorsal half of the AER and dorsal ectoderm that does not express *En1* (Kimmel *et al*., 2000). Interestingly, this boundary is established previous to and independently of *En1* activity in the ectoderm (Altabef and Tickle, 2002; Kimmel *et al*., 2000). In addition, the boundary starts to disappear when the AER reaches its maximum height by E11.5. Thus, based on this transient property of the boundary its role was related with AER integrity, by the stage the boundary disappears the AER starts to regress (Kimmel *et al*., 2000). Based on this observation, the authors proposed that the controversy behind the experiments carried out in chick in which dorsal ectodermal cells were found in the ventral half of the AER in DiI cell marking experiments could be explained due to later analysis compared to chimera analysis.

Additional experiments in mice demonstrated two additional boundaries present in the AER. At very early stages a boundary appears at the dorsal edge of the AER. This boundary avoids mixing between cells expressing *Wnt7a* located in the dorsal ectoderm and cells that do not express *Wnt7a*. The other one appears in the ventral edge of the AER when the AER acquires morphologically distinguishable characteristics (Kimmel *et al*., 2000).

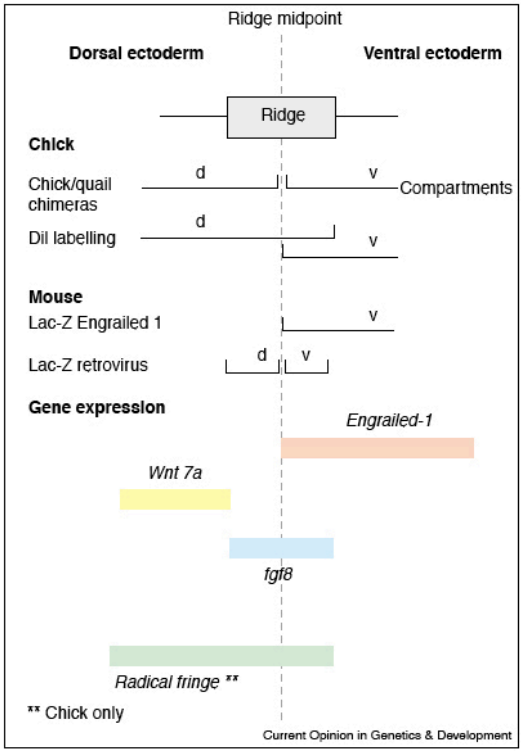


**Figure 9. Illustration showing the compartment boundaries and also gene expression within mouse and chick AER.** Cell lineage compartments defined by mouse and chick experiments. The dashed line represents the DV midline of the AER. The extent of the ventral compartment correlates with *En1* expression, *Fgf8* is expressed through the entire ridge and *Wnt7a* is expressed in the dorsal ectoderm whereas *Radical fringe* is expressed in the dorsal ectoderm and the AER. From Tickle 2001.

## 1.4. AER development

Studies in chick and mouse limb buds have characterized the dynamics of AER morphology (Todt and Fallon, 1984; Bell *et al*., 1998; Loomis *et al*., 1998). Several phases can be considered during AER development: AER induction, AER maturation and AER regression.

### 1.4.1 AER induction

The induction of the AER corresponds to the specification of AER precursor cells, termed the "pre-AER" cells. In this phase *Fgf8* is induced in a patchy pattern in the limb ectoderm. The "pre-AER" cells are defined as cells that express *Fgf8* but are not yet anatomically distinguishable from the rest of the neighbouring ectodermal cells (Bell *et al*., 1998, Loomis *et al*., 1998). By E9 and 16HH in mice and chick respectively, a patchy pattern of *Fgf8* expression becomes appreciable in the limb ectoderm. While in mouse this initial expression of *Fgf8* is restricted to the ventral ectoderm (Loomis *et al*., 1998; Kimmel *et al*., 2000) (Fig.10A), in chick it is induced distally in both dorsal and ventral ectoderm opposite to somites 15-20 (Crossley *et al*., 1996, Ohuchi *et al*., 1998). As previously mentioned, in the current model *Fgf10* signalling from the LPM is absolutely required for the induction of *Fgf8* in the limb ectoderm, through the induction of *Wnt3a* or *Wnt3* in chick and mouse limb ectoderm respectively (Ohuchi *et al*., 1997; Min *et al*., 1998; Sekine *et al*., 1999; Soshnikova *et al*., 2003; Barrow *et al*., 2003), in which Bmp signalling plays also a critical role (Ahn et al., 2001; Pizette *et al*., 2001; Soshnikova *et al*., 2003; Pajni-Underwood *et al*., 2007).

### 1.4.2 AER maturation

Once the AER is induced and the limb develops, a "mature-AER" is formed. Morphogenetic movements of the ectoderm compact the pre-AER cells towards the DV boundary of the limb bud. In mice, by E10 movement and compaction of "pre-AER" cells located first in the ventral ectoderm developed into a bi-layered epithelium to form a pronounced thickening of the ectoderm close to the DV interface (Crossley and Martin, 1995; Loomis *et al*., 1998)(Fig. 10D). At E10.5-11 a mature-AER is first appreciable confined along the DV boundary of the developing limb and formed a polystratified epithelium composed of 3-4 cell layers (Meyer *et al*., 1997; Bell *et al*., 1998). In chick, by 18HH the columnar shape of AER cells in

the wing bud ectoderm makes them distinguishable from the neighbouring non-AER cells that exhibit cuboidal morphology. Later on by 20HH this columnar cells form a pseudostratified epithelium, the mature AER.

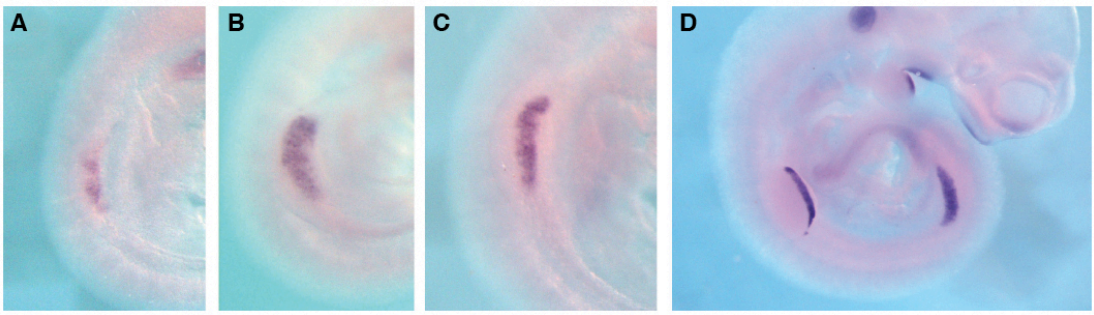


**Figure 10. *Fgf8* expression during early mouse limb development.** *Fgf8* is first detected in the ventral limb ectoderm by E9. (A), *Fgf8* expression spreads along the ventral limb ectoderm occupying a broad territory (B-C) and becomes confined to the distal tip of the limb by E10.5 (D). From Fernandez-Teran and Ros, 2008.

### 1.4.3 AER regression

Finally, regression of the AER occurs. By E11 once the AER reaches it maximum height, it begins to regress to the point that no AER descendants are present at birth as revealed by cell lineage analysis in mice (Guo *et al.,* 2003). Fgf expression in the AER decays starts first over the interdigital spaces and remains over the digits until the last phalanges are laid down (Pizette and Niswander *et al*., 1999; Ganan *et al*., 1996; Khokha *et al*., 2003; Zuñiga *et al*., 1999; Wang et al., 2004; Pajni-Underwood *et al*., 2007).

### 1.4.4 AER maintenance

Once the AER is induced two regulatory feedback loops established in the limb became critical for its maintenance. The first is the previously mentioned loop between Fgf10 in the mesoderm and Fgf8 in the limb ectoderm responsible for AER induction (Min *et al*., 1998; Sekine *et al*., 1999; Xu *et al.,* 1998; Arman *et al*., 1999; Girovodsky *et al*., 2003; Lu *et al*., 2008; Soshnikova *et al*., 2003; Barrow *et al*., 2003). Since removal of any component of this loop once the AER is established resulted in AER regression, demonstrated its requirement also for AER maintenance (Lu *et al*., 2008).

The other regulatory feedback loop is related to the role that Bmp exerts in the AER after its induction. Bmp signalling becomes detrimental for the AER and a regulatory loop between Shh from the ZPA and Fgf from the AER is responsible for blocking the negative effects that Bmps exert over the AER, required for the correct outgrowth and patterning of the limb. Shh emanating from the ZPA induces the Bmp antagonist *Gremlin* (*Grem1*) in the limb mesenchyme. Grem1 blocks the negative effect that Bmp exerts over the AER allowing Fgf expression in the AER (Pizette and Niswander *et al*., 1999; Ganan *et al*., 1996; Khokha *et al*., 2003; Zuñiga *et al*., 1999)(Fig. 11). Subsequently, Fgf maintains *Shh* expression in the ZPA establishing the regulatory feedback loop. Remarkably, the correct cessation of this loop is determinant for the correct development of the limb. The fact that cells that have expressed *Shh* are not able to express *Grem1* generates a gap between these two domains. As the limb grows this gap becomes bigger allowing the regression of the AER mediated by Bmp signalling (Scherz *et al*., 2004). On the other hand, it has been proposed that high levels of Fgf expression inhibit *Grem1* expression. Thus, as the limb bud grows and the Fgf expression level in the AER becomes higher, the gap between these two domains becomes bigger allowing Bmp function and subsequent regression of the AER (Verheyden and Sun 2008).

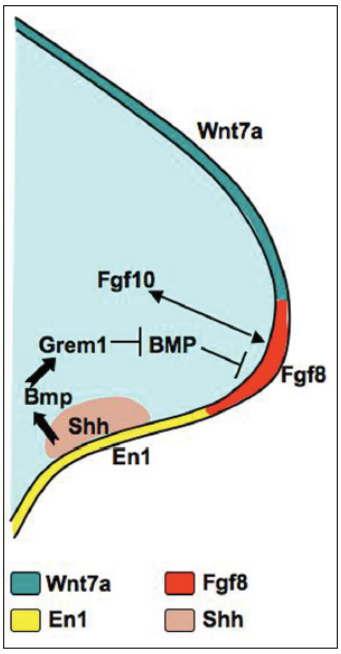


**Figure 11. Illustration of regulatory interactions involving the process of AER maintenance.** The arrows indicate induction and the bars repression. The color code is indicated in the bottom, for more detail see the text. Taken from Fernandez-Teran and Ros 2008.

### 1.4.5 Split hand/foot malformation

Split hand/foot malformation (SHFM) is a human congenital malformation, affects to the distal portion of the upper and lower limbs that is characterized by the absence of central digits and fusion of the remaining ones. It is believed that it is the consequence of a failure in the maintenance of the medial region of the AER that lacks *Fgf8* expression (Temtamy and McKusick, 1978; Sifakis *et al*., 2001)(Fig.12). The incidence of SHFM is about 1:18,000 live births and can appear as an isolated entity or as part of a syndrome. In human at least 6 loci have been associated to non-syndromic SHFM. Isolated forms of SHFM are commonly inherited in an autosomic dominant fashion, with incomplete penetrance and variable expressivity (Scherer *et al*. 1994), with the exception of SFHM type VI that is inherited in an autososmal recessive fashion and SHFM type II that is linked to the X chromosome (Ahmad *et al.,* 1987; Faiyaz-Ul-Haque *et al*. 1993).

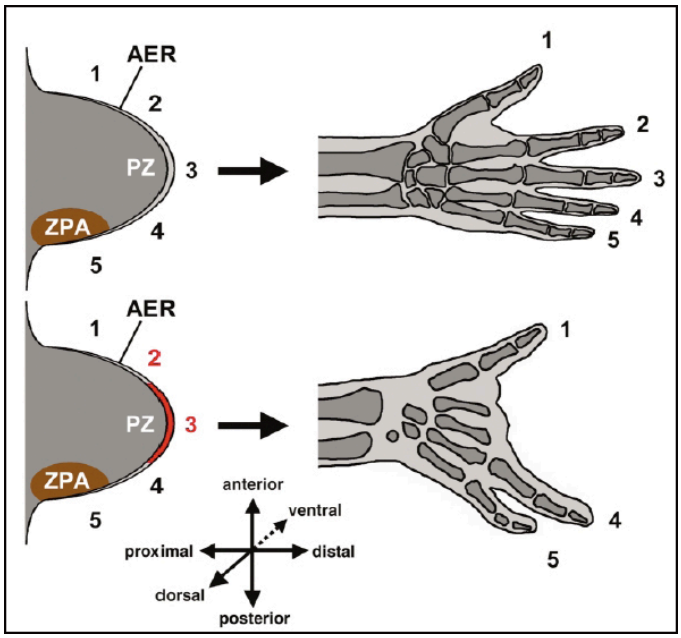


**Figure 12. AER defect leading to Split hand/foot malformation (SHFM).** Normal development of the autopod (top) and SHFM phenotype (bottom). A failure to maintain AER activity (red) in the developing limb bud leads to the absence of the central rays and causes an SHFM phenotype. AER, apical ectodermal ridge; PZ, progress zone; ZPA, zone of polarizing activity. From Duijf *et al.,* 2003.

SHFM type I is commonly linked to minimal deletion of *DSS1* in human and to *distal-less homeobox* genes *Dlx5* and *Dlx6* in mouse (Simeone *et al.,* 1994; Scherer *et al.*, 1994; Crackower *et al.,* 1996). The *Dlx5;Dlx6* double KO resembles the limb phenotype characteristic of SHFM (Robledo *et al.,* 2002; Merlo *et al.*, 2002), confirming the implication of the human orthologs *DLX5* and *DLX6* in this pathology. Based on the phenotype of the *Dactylin* (*Dac*) mutant mice and posterior mapping analysis the *Dac* gene was proposed as the gene responsible for SHFM type III, although it is not fully clear (Johnson *et al.,* 1995; Sidow et al., 1999; de Mollerat *et a*l., 2003). In humans mutations in *Tp63*, the homolog of the cell-cycle regulator *p53*, have been shown to be the cause of the SHFM type IV. Finally, the HoxD cluster has been related to SHFM type V and *Wnt10b* to SHFM type VI whereas no gene has been associated to SHFM type II. Despite the identification of 6 loci involved in SHFM, only *Tp63* (SHFM IV) and *Dlx5* and *Dlx6* (SHFM I) have been unequivocally involved in this malformation. Disruption analyses in mice revealed that *Tp63* is required for AER formation (Mills *et al.*,

1999; Yang *et al*., 1999). Further analysis of the role of *Tp63* and *Dlx* genes helped to clarify the epistatic relation between them. It has been shown that *Tp63* acts upstream of the *Dlx* genes, for proper AER development (Lo Iacono *et al*., 2008; Kouwenhoven *et al*., 2010).

### 1.4.6 AER induction and DV pattern establishment

As mentioned, mouse pre-AER cells are induced in a patchy pattern of expression in the ventral limb ectoderm by the time the DV polarity is acquired by the ectoderm (Kimmel *et al*., 2000). In contrast, chick *Fgf8* expressing cells are initially detectable in a wider domain along the limb DV border (Crossley and Martin, 1995; Crossley *et al*., 1996). As the limb bud develops, *Fgf8* expressing cells committed to form the AER are confined to the DV limb interface, at the distal tip of the limb bud. Chick-quail chimera experiments revealed that the whole ectoderm covering the prospective limb field forms the AER. In addition these experiments demonstrated that the ectoderm overlaying the somites and the intermediate mesoderm give rise to the dorsal ectoderm of the limb, while cells from the ventral ectoderm are originated in the ectoderm overlying the lateral somatopleure (Michaud *et al*., 1997). However, while cell lineage analysis in chick confirmed the origin of dorsal and ventral ectoderm, whether these cells contributed to the AER remains controversial. In contrast to chimera experiments, DiI cell-labeling experiment in chick supported a mingled origin of the AER, constituted by ventral and dorsal ectodermal cells mixed with AER cells (Altabef *et al.,* 1997). In addition, cell-marking experiments in mouse indicated that only part of the initial pre-AER cells were committed to form the mature AER (Guo *et al*, 2003; Kimmel *et al*., 2000).

The fact that AER induction and DV pattern establishment occurs concomitantly and also the positioning of the mature AER at the DV interface, lead

to the hypothesis that these two processes are under common regulatory mechanisms. This is supported by the fact that ectopic limbs developed after application of Fgf soaked beads in the flank ectoderm arise at the DV boundary, in precise alignment with normal limbs independently of the position of the bead (Cohn *et al*., 1995; Vogel *et al*., 1996; Ohuchi *et al*., 1997).

This notion came from the study of the chicken mutant *limbless* that fails to develop an AER as a possible consequence of a failure in DV pattern establishment (Ros *et al*., 1996; Grieshammer *et al*., 1996; Noramly *et al*., 1996). *Limbless,* is an autosomic recessive mutation in chick affecting the ectodermal component of the limb. It is characterized by the absence of *Fgf8* expression in the limb ectoderm and lack of the AER that leads to the regression of the limb bud by 19HH. *Limbless* limb buds lack *En1* expression in the ventral ectoderm with the subsequent ectopic *Wnt7a* expression in the ventral ectoderm, leading to the development of bidorsal limb buds. It has been suggested that the failure in DV polarity establishment in *limbless* limb buds could be the reason for the absence of *Fgf8* expression in the limb ectoderm and the subsequent bud regression (Ros *et al*., 1996; Noramly *et al*., 1996; Grieshamer *et al*., 1996). In addition, grafting experiments in chick in which confrontation of ventral and dorsal limb ectoderm resulted in the induction of ectopic AERs supported the requirement of the DV interface for AER induction (Laufer *et al*., 1997; Tanaka *et al*., 1997).

In contrast, *eudiplopodia,* another recessive mutation in chick, it is characterized by the development of ectopic AERs in the dorsal limb ectoderm. Interestingly, the digits developed from these ectopic AERs are characterized by a double dorsal phenotype (Goetinck, 1964), denoting the absence of DV patterning, implying that DV pattern establishment is not a prerequisite for AER induction. It was further supported by the development of an AER in double dorsal limbs developed when prospective limb mesoderm was grafted between two rows of somites, or even when a filter was placed proximal to the somatopleure (Michaud *et a*l., 1997).

In addition, if limb DV polarity is a prerequisite for AER induction, it would be expected that mice lacking DV specification markers such as *Wnt7a* or *En1* should develop defects in AER induction. Nevertheless, AER induction is not affected in either *Wnt7a* or *En1* mutant mice, neither in the double mutant *Wnt7a;En1*. Interestingly, in mice lacking *En1*, ectopic *Wnt7a* expression in the ventral ectoderm prevents the compactation of the AER, leading to a ventrally extended AER (Cygan *et al*., 1997; Loomis *et al*., 1996; Loomis *et al*., 1998; Parr and McMahon, 1995).

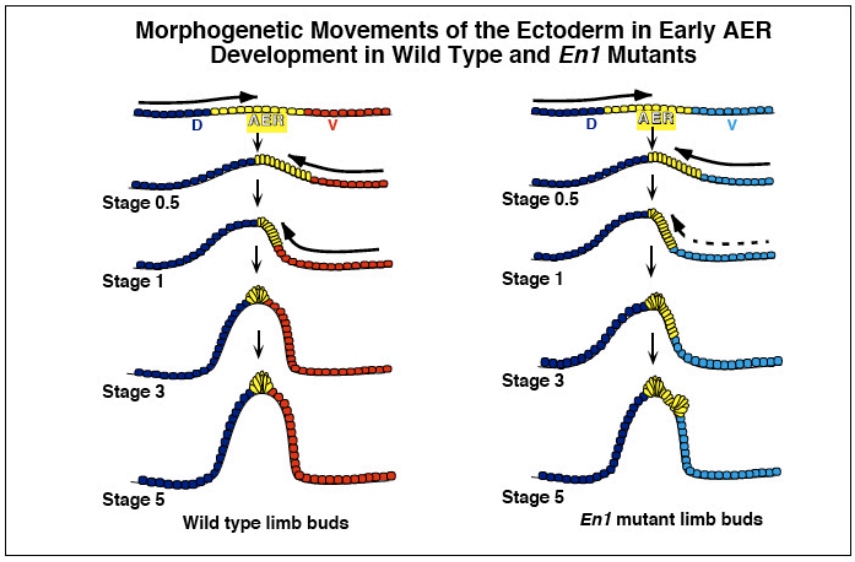


**Figure 13. Illustration for the morphogenetic movements during the formation of the AER in mouse.** Sequential convergent movements of the ectoderm. An initial wave of lateral morphogenetic movements of the ectoderm confined AER precursor cells into the ventral ectoderm. Afterwards, a second wave compresses these cells to the distal 1/3 of the ventral ectoderm and finally the last wave constricts the cells at the DV limb boundary. Lack of *En1* leads to ventrally extended AER. From Loomis *et al,.* 1998.

The phenotypes in which AER maturation defects arise due to lack of *En1* expression in the ventral ectoderm supports the notion that Bmps emanating from the LPM are the molecules required for the establishment of ventral limb polarity

and proper AER positioning (Michaud *et al*., 1997; Ahn *et al.,* 2001; Soshnikova *et al*., 2003; Pajni-Underwood *et al*., 2007; Maatouk *et al*., 2009; Choi *et al.,* 2012). Based in the ventrally extended AER morphology of *En1* mutant mice, Loomis and colleagues proposed a model in which convergent morphogenetic movements are required for the mature AER morphology. In this model, lateral convergent movements would initially compact the pre-AER cells in the ventral ectoderm. Afterward, morphogenetic movements from the ventral ectoderm compacts the AER cells and confine them to the DV interface. *En1* has been proposed as the candidate responsible for the morphogenetic movements required to confine the ventrally located AER cells to the DV boundary (Loomis *et al*., 1998)(Fig. 13). However, AER maturation defects present in *En1* mutant mice are rescued by additional removal of *Wnt7a*, suggesting that neither *En1* nor *Wnt7a* are required for proper AER induction and positioning at the DV limb interface (Parr and McMahon, 1995; Cygan *et al*., 1997; Loomis *et al*., 1996; Loomis *et al*., 1998).

In contrast, *En1* misexpression experiments in chick led to the proposal that a boundary between cells expressing *En1* and non-expressing could be an indispensable prerequisite for AER induction. While low levels of *En1* missexpresion in the dorsal ectoderm led to the development of additional AERs, high levels of missexpression abolished endogenous AER formation (Laufer *et al*., 1997; Logan *et al*., 1997; Rodriguez-Esteban *et al*., 1997; Pizette *et al*., 2001). Thus, it was proposed that *En1* could be responsible for the specification of the ventral ectoderm through cell lineage restriction in the ventral ectoderm. Nevertheless, either retroviral overexpression in the chick ectoderm or its missexpression with the use of the *Msx2*-Cre line in mice that drives expression all over the AER did not affect the DV cell lineage boundaries present in the limb ectoderm (Altabef and Tickle, 2002; Kimmel *et al*., 2000). Hence, it is possible that common signalling mechanisms responsible for DV pattern establishment and AER induction lies upstream of *En1*.

The common parallelism between vertebrates AER and *Drosophila´s* wing margin, both arise at the DV boundary and are required for PD growth (Diaz-Benjumea *et al*., 1993), led to the proposal that *Radical Fringe* (*R-fng)* in the chick performed the same role to *Fringe* in *Drosophila* that is responsible for PD growth and DV positioning of the wing margin (Brook *et al*., 1996). *R-fng* is expressed in the limb dorsal ectoderm reaching the ventral boundary of the AER and it was proposed that the boundary between *R-fng* expressing and non-expressing cells was responsible for the correct positioning of the wing margin at the DV boundary (Laufer *et al*., 1997; Rodriguez-Esteban *et al*., 1997). However, limb developmental defects were not appreciable after its disruption.

#### 1.4.6.1 The role of the Bmp signalling pathway

In agreement with Le Douarin and colleagues´ proposal that Bmp signalling in the LPM could act as a ventralizing factor providing ventral identity to the ventral limb ectoderm, *En1* has been shown to be a downstream effector of Bmp signalling pathway in ventral limb specification (Pizette *et al*., 2001; Ahn *et al*., 2001).

Bmps are a large family of growth factors members of the Transforming Growth Factor-β superfamily (TGF-β) together with TGF-βs, Activins/Inhibins, and Müllerian Inhibiting Substance (Kingsley, 1994). Bmps are implicated in several processes governing vertebrate limb development, such as chondrogenesis or programmed cell death (Dudley *et al*., 1995; Dunn *et al*., 1997; Kawakami *et al*., 1996; Luo *et al*., 1995; Pizette and Niswander, 1999; Pizette and Niswander, 2000; Zou and Niswander, 1996). Intracellular transduction of the Bmp signalling is transmitted by the type I and type II receptors. The Bmp ligands have been shown to signal through three different types II receptors, the BmprII, the ActR-IIa and the ActR-IIb (Yamashita *et al*., 1995; Hoodless *et al*., 1996). In addition, four different type I receptors have been described for Bmp signal transduction,

*BmprIa*, *BmprIb, ALK2* and *ALK1*. *BmprIa* is a ubiquitously expressed type Ia receptor also termed activin receptor-like kinase-3 or ALK-3 and *BmprIb,* also termed ALK-6, is responsible for cartilaginous condensations (Zou *et al*., 1997; ten Dijke *et al*., 1994; Koenig *et al*., 1994). Remarkably, *Bmp2*, *Bmp4* and *Bmp7* are ligands binding the type Ia receptor and are expressed in the limb during development (Yamaji *et al*., 1994). However, two of them, *Bmp2* and *Bmp7*, have been also shown to bind to the activin type II receptors (Yamashita *et al*., 1995; Hoodless *et al*., 1996).

Both *Bmpr,* type I and II, are required for intracellular signal transduction. Binding of Bmp ligands to the single pass transmembrane sherine-treonine kinase receptors type II, phosphorylates and activates the type I receptors which in turns phosphorylates Smad transcription factors for subsequent nuclear translocation and activation or repression of target genes (Heldin *et al*., 1997; Massagué, 1998; Attisano and Wrana, 1998; Derynck *et al*., 1998; Padgett *et al*., 1997; Whitman, 1997). Three major classes of Smads have been described. One is the receptor regulated Smads (R-Smad). They are the substrates of the kynase receptors and are critical for biological response. TGF-ß and activin receptors are responsible for Smad2 and Smad3 phophorylation for transduction of their specific signal, whereas Bmp signalling is propagated through Bmpr mediated phosphorylation of Smad1, Smad5 and Smad8. After phosphorylation of the R-Smad a heteromeric complex with the second class of Smad, the common mediator (co-Smads) is formed. In mammals only co-Smad4 has been described. Once the heteromeric complex (R-Smad/co-Smad) is formed translocates into the nucleus and regulates gene expression. Finally, Smad6 and Smad7 belong to the inhibitor Smads (I-Smads) class that prevents the access or phosphorylation of R-Smads.

Even though intensive studies focused in the role of Bmp signalling in limb induction, its role is not fully understood. Missexpresion in chick of the constitutively active form of the *BmprIa* led to either ectopic AER development or disruption of the endogenous AER induction, suggesting that a boundary of Bmp

signalling and non-signalling was required for AER induction (Pizzete *et al.*, 2001). Further analysis revealed that missexpression of the constitutively active *BmprIa* in the dorsal limb ectoderm induced *En1* expression and also the *Msx1* and *Msx2* transcription factors, transcriptional mediators of the Bmp signalling (Suzuki *et al.*, 1997; Pizette and Niswander, 1999; Pizzete *et al.*, 2001).

*BmprIa* overexpression led to the expression of *Fgf8* triggered by the induction of either *En1* or *Msx1/2.* Moreover, missexpression of *En1* or *Msx1/2* led also to the development of ectopic AERs. However, the etymology of the ectopic AER developed after missexpression of either *Msx* or *En-1* was different. It was suggested that ectopic AER developed after *En1* missexpression in limb dorsal ectoderm arise as a misplacement of the endogenous AER, whereas the ectopic AERs resulting from *Msx* missexpression arise in a patchy pattern scattered through the dorsal ectoderm independently of the endogenous AER (Pizette *et al.*, 2001). Thus, it was suggested that Bmp signalling through the *BmprIa* could link DV patterning and AER induction through the activation of *En1* and *Msx* transcription factors respectively (Fig. 14)(Pizette *et al.*, 2001).

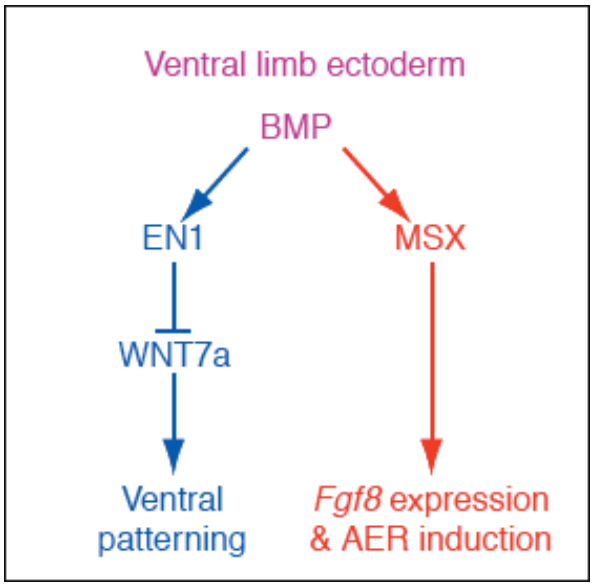


**Figure 14. Role of Bmp signalling in the ventral limb ectoderm.** BMP through the induction of *En1* is responsible for ventral patterning, while its role in AER induction is mediated by the Msx transcription factors. From Pizette *et al.*, 2001.

In contrast to missexpression experiments in chick, the analysis of the double *Msx1;Msx2* knock out mutant that exhibited a disruption of the anterior region of the AER and a failure in DV boundary establishment at that region, consistent with a role for the *Msx* transcription factors in DV pattern establishment rather than in AER induction (Lallemand *et al*., 2005).

Early lethality due to defects in gastrulation in mice lacking *BmprIa (*Mishina *et al.,* 1995), forced researchers to investigate its role in limb development using conditional approaches with the use of the Cre/LoxP system. Conditional removal of *BmprIa* in the limb has been performed with the use of different Cre lines. Removal of the *BmprIa* from the limb mesoderm has been performed with the use of the *Prx1Cre* line. This line drives Cre activity in the limb mesoderm (Logan *et al.,* 2002). *Prx1Cre* dependent *BmprIa* removal led to AP defects, decrease in growth of the autopod and minor DV defects with slight ectopic expression of *Lmx1b* in the ventral limb mesoderm (Ovchinnikov *et al*., 2006).

Regarding the ectoderm, removal of the *BmprIa* has been also performed with the use different Cre lines (Ahn *et al*., 2001; Shosnikova *et al*., 2003; Pajni-Underwood *et al*., 2007). The use of the *Msx2*-Cre line that drives Cre expression in the ventral limb ectoderm and the AER, before AER induction in the hindlimb (19 Somites) and after its induction in the forelimb (21 Somites)(Sun *et al*., 2000; Barrow *et al.,* 2003), suggested a dynamic role for Bmp signalling during development. At early stages it is required for AER induction while at later stages mediates AER regression (Fig. 15)(Pajni-Underwood *et al*., 2007).

*Msx2-Cre* dependent *BmprIa* removal at early stages, prior to AER induction in the hindlimb, resulted in absence of *Fgf8* induction and lack of the AER with the subsequent complete agenesis of the hindlimbs, implying its requirement for AER induction (Pajni-Underwood *et al*., 2007). Requirement that was first demonstrated with the use of the *Brn4-Cre* deleter line that drives expression of

Cre in the dorsal and ventral ectoderm of the limb buds by E9.75, with highest expression levels in the AER (Ahn *et al*., 2001; Soshnikova *et al*., 2003). Noteworthy, while *Msx2-Cre* removal of the *BmprIa* led to agenesis of the hindlimbs in all affected individuals, the use of the *Brn4Cre* line resulted in a wide range of phenotypes, ranging from agenesis of the hindlimbs with no detectable *Fgf8* expression, to grossly malformed limbs with severely reduced *Fgf8* expression levels. The differences in the phenotypes of both conditional mutants are explained due to the specific kinetics of each Cre line used (Ahn *et al*., 2001; Pajni-Underwood *et al*., 2007). Interestingly, while *Brn4-Cre* mediated *BmprIa* removal exhibited variable penetrance in AER disruption, the penetrance in DV patterning establishment defects was complete, implying that AER induction and DV pattern seems to be independent processes (Ahn *et al*., 2001).

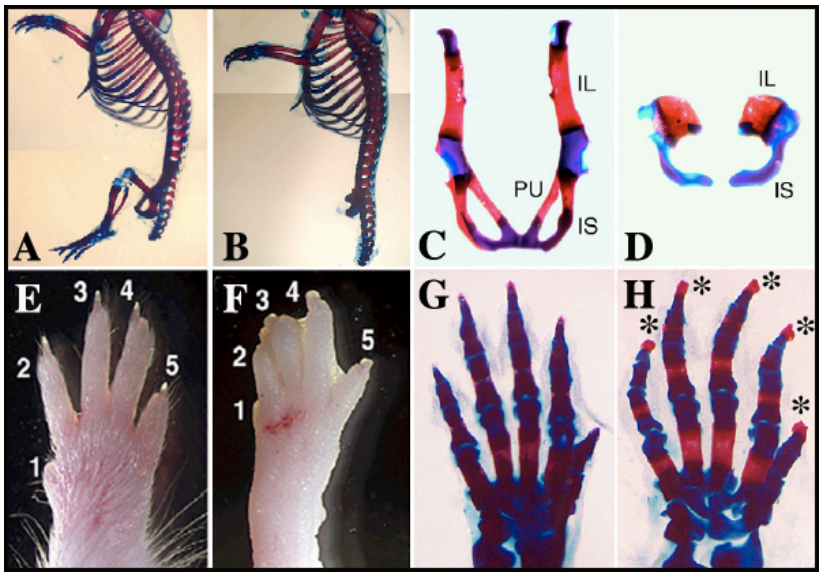


**Figure 15. Skeletal phenotype of *Msx2-Cre;BmprIA$^{flox}$* conditional mutant mice.** Skeletal preparations of normal (A,C,G) and mutant newborns(B,D,H) and dorsal view of gross morphology of normal (E) and mutant (F) forelimbs. In mutants, hindlimb elements are absent and pelvic bones are reduced or absent, while all the forelimb elements are developed. The autopd shows interdigital webbing (F) and broader digit tips with double-dorsal phenotype (asterisks in H). From Pajni-Underwood *et al.,* 2007.

The role of Bmps at later stages once the AER is formed, is related to AER regression. At later stages of limb development Bmp signalling becomes detrimental for the AER and regulates the cessation of *Fgf8* expression in the AER (Zuñiga *et al*., 1999; Pizette *et al.,* 2001; Pajni-Underwood *et al*., 2007; reviewed in Fernández-Teran and Ros, 2008). *Msx2-Cre* removal of the *BmprIa* led to soft tissue syndactyly in forelimbs as a consequence of reduced programmed cell death in the interdigital tissue mediated by prolonged *Fgf* expression in the AER (Fig. 15F). Noteworthy, soft tissue syndactyly present in *BmprIa*;*Msx2-Cre* conditional mutant forelimbs was rescued by additional removal of *Fgf8* and *Fgf4* from the AER (Pajni-Underwood *et al*., 2007). According to this results, *Brn4-Cre;BmprIa* conditional mutant forelimbs exhibited subtle defects (Ahn *et al*., 2001). Interestingly, DV pattern was properly established in these forelimbs, as assessed by expression of *Lmx1b*, *En1* and *Wnt7a* (Ahn *et al*., 2001). Absence of DV pattern defects in these forelimbs implies that the DV pattern is already established before E10, when the *BmprIa* has been widely removed and also that once it is established Bmps are no longer required for proper DV pattern (Wong *et al*., 2012; Ahn *et al*., 2001). In contrast, *Msx2-Cre* dependent removal in forelimbs resulted in digit tips with double dorsal phenotypes implying its continuous requirement for proper DV pattern establishment (Pajni-Underwood *et al*., 2007)(Fig. 15F,H).

Based on the kinetics of the different Cre deleter lines used to abolish Bmp signalling through the removal of the *BmprIa* in the limb ectoderm, a temporal window between E9.5 and E9.75 was suggested for the requirement of Bmp signalling in the hindlimb ectoderm for both AER induction and establishment of the ventral limb polarity (Ahn *et al.,* 2001; Soshnikova *et al*., 2003; Pajni-Underwood *et al*., 2007). Based on this hypothesis, *Bmp4*, and *Bmp7* expressed in the LPM were proposed as candidate molecules emanating from the lateral somatopleure responsible for *BmprIa* activity in the ventral limb ectoderm required for the DV patterning of the limb ectoderm through the induction of *En-1* in the ventral ectoderm (Ahn *et al.,* 2001).

The functional redundancy and the overlapping expression domains between the Bmp ligands expressed in the limb makes it difficult to analyze the role of particular Bmps during limb development. In order to assess their role, several combinations of conditional removals of the different Bmp ligands expressed in either the limb ectoderm or mesoderm have been performed (Selever *et al.*, 2004; Bandyopadhyay *et al.*, 2006; Maatouk *et al.*, 2009; Choi *et al.,* 2012). However, none of the conditional deletion of the *Bmp* ligands in either the limb ectoderm or mesoderm mimicked the amelic hindlimb phenotype obtained with the *Msx2-Cre* conditional removal of the *BmprIa* from the limb ectoderm.

Single KO mice for either *Bmp2* or *Bmp4* died at early stages prior to limb bud induction (Winnier *et al.,* 1995; Zhang and Bradley, 1996), while polidactylous hindlimbs arise in the *Bmp7* null mice (Dudley *et al.,* 1995; Luo *et al.,* 1995; Hofmann *et al*., 1996). *Bmp4* conditional removal from the mesoderm with the use of the *Prx1Cre* line resulted in polydacytilous limbs with defects in both, the AER and DV pattern establishment. AER defects corresponded to ventrally expanded *Fgf8* expression, as a result of the absence of *En1* expression and ectopic *Wnt7a* expression in the ventral limb ectoderm, followed by ectopic *Lmx1b* expression in the ventral mesoderm (Selever *et al.*, 2004). Chondrogenic condensations failed to form when *Bmp2* was additionally removed in addition to a longer-lived AER without reported DV patterning defects. Finally, removal of *Bmp2* in a null background for *Bmp7* exhibited subtle malformation (Bandyopadhyay *et al.*, 2006).

Removal of different Bmp ligands in the limb ectoderm was performed with the use of the *Msx2-Cre*. Conditional deletion of *Bmp2* and *Bmp4*, resulted in polydactilous limbs with double-dorsal digit tips due to lack of *En1* expression in the ventral ectoderm and ectopic expression of *Lmx1b* in the ventral mesoderm. These mutants also displayed elongated and thinner AER as judged by CD44 expression and expanded expression of *Fgf4* and *Fgf8* along the DV and the AP axes (Maatouk *et al*., 2009). Triple deletion of *Bmp2*, *Bmp4* and *Bmp7* resulted in the same DV an AER defects with an ectrodactylous limb phenotype (Choi *et al.,* 2012).

Unexpectedly, conditional removal of the Bmps expressed in the AER resulted in a more severe forelimb phenotype than that of *BmprIa* removal, even though both are removed with the use of the *Msx2-Cre* line. The downregulation of *Msx1/2* expression observed in both the mesoderm and the ectoderm when Bmps are removed from the ectoderm, downregulation not appreciable when *BmprIa* is removed, could be explained due to additional receptors apart form the *BmprIa* by which Bmp signalling maintains the expression of *Msx1/2* (Choi *et al.,* 2012)

In conclusion, early removal of the Bmp ligands expressed in either the ectoderm or the mesoderm did not result in agenesis of the hindlimbs shown in *Msx2-Cre* dependent conditional *BmprIa* removal. One possible explanation is that removal of the Bmp ligands expressed in the ectoderm could be masked by the expression of those ligands in the underlying mesoderm and vice versa or by additional ligands apart form Bmp2/4 and 7 signalling through the *BmprIa*. However, as mentioned it has been demonstrated that Bmp signalling and its downstream effectors are required for proper DV establishment and AER induction (Ahn *et al.,* 2001; Soshnikova *et al*., 2003; Selever *et a*l., 2004; Bandyopadhyay *et al*., 2006; Pajni-Underwood *et al*., 2007; Maatouk *et al*., 2009; Choi *et al.,* 2012). Nevertheless, AER induction and DV pattern establishment relies on intricate interactions between different signalling pathways. Disruption of Bmp signalling in the ectoderm is not the only signalling pathway that results in loss of Fgf signalling from the AER and failure of DV polarity establishment (Barrow *et al.,* 2003; Soshnikova *et al.,* 2003).

#### 1.4.6.2 The role of the WNT signalling pathway

Disruption of the Wnt/ß-catenin signalling pathway led also to both, limbless phenotypes, due to failure of AER induction and DV patterning defects (Soshnikova *et al*., 2003; Barrow *et al*., 2003). The vertebrate Wnt ligands homologs of wingless in *Drosophila*, represent a large family of signalling

molecules. Through the control of cell proliferation and differentiation it regulates several aspects of limb development (Eastman and Grosschedl, 1999; Huelsken and Burchmeier, 2001).

Wnt signalling transduction is carried out by a number of seven pass transmembrane receptors of the Frizzled family (Fzd). Depending on the co-receptor associated, either Lrp5 and Lrp6 or Knypek and orphan receptors like Ror and Ryk, the binding of Wnt ligands to Fzd receptor leads to the activation of either canonical or non-canonical pathways respectively (Pinson *et al*., 2000; Tamai *et al*., 2000; Wehrli *et al*., 2000; Halford *et al*., 2000; Topczewski *et al*., 2001; Yoda *et al*., 2003).

Canonical Wnt signalling transduction through the Fzd/Lrp complex results in the stabilization of ß-catenin. Binding of the ligand leads to the activation of the Dishevelled (Dvs) protein and results in the inhibition of the docking proteins Axin, APC (adenomatous polyposis coli) and GSK-3beta (Glycogen Synthetase Kinase 3beta) complex. In absence of Wnt signalling this complex phosporylates ß-catenin in its N-terminus and promotes its ubiquitination for posterior degradation via proteasome (Zeng *et al*., 1997; Korinek *et al*., 1997; Liu *et al*., 2002; Schwarz-Romond *et al*., 2002). Hence, activation of Dsv leads to the stabilization of ß-catenin through the inhibition of its phosphorylation that allows its translocation to the nucleus. Once in the nucleus, interactions with Lef1 (Lef) and Tcf1 (Tcf), members of the lymphoid enhancer factor and the T cell factor families of transcription factors respectively, activates target genes (Behrens *et al*., 1996; Galceran *et al*., 1999).

Ectopic induction of *Fgf8* and subsequent limb outgrowth after misexpression of *Wnt3a, ß-catenin* or *Lef1* in the chick limb ectoderm was the first evidence for the requirement of the Wnt/ß-catenin signalling pathway for limb outgrowth. Moreover, misexpression of a *Lef1* construct lacking DNA binding domain, used as dominant negative form that competes with the endogenous Lef1

for ß-catenin, led to AER disruption (Kengaku *et al*., 1998). The finding that induction of *Fgf8* expression in the limb ectoderm was preceded by the expression of *Wnt3a* in the limb ectoderm, and that *Wnt3a* was able to induce *Fgf8* when missexpressed, positioned *Wnt3a* upstream of *Fgf8* induction in limb bud development (Kengaku *et al*., 1998).

In mouse, disruption of *Wnt3a* stunted trunk development caudal to the forelimb, but did not interfere with limb development (Takada *et al*., 1994; Greco *et al*., 1996). However, the lack of limbs in the *lef1;Tcf1* double KO supported the implication of the canonical Wnt signalling in mouse limb development (Galgeran *et al*., 1999). Nevertheless, the ubiquitous expression of these transcription factors in ectodermal and mesodermal compartments, did not allow to determined whether they were specifically required in either the mesoderm or the ectoderm.

The finding that conditional removal of *Wnt3* in the limb ectoderm resulted in an amelic phenotype indicated that the function described for *Wnt3a* in chick was performed by *Wnt3* in the mouse (Barrow *et al*., 2003). *Wnt3* is expressed all over the limb ectoderm at least from E9.5 to E11.5. Because *Wnt3* null homozygous mice fail to develop due to defects in gastrulation, conditional approaches were undertaken with the aim to unravel its requirement during limb development (Roelink and Nusse, 1991; Barrow *et al*., 2003). *RAR-Cre* and *Msx2-Cre* deleter lines were used to remove *Wnt3* from the limb ectoderm. The *Msx2-Cre* line drives expression of the Cre in the limb ectoderm before and after induction of the AER, in hindlimb and forelimb respectively, whereas the *RAR-Cre* drives Cre activity in the forelimb ectoderm and mesoderm prior to AER induction (Moon and Capecchi 2000; Barrow *et al.,* 2003). As expected, the forelimb phenotype of *RAR-Cre* conditional mutants was much more severe than that of the *Msx2-Cre* due to the earlier activation of Cre activity. Variable defects ranging from oligodactyly of one digit and absence of the ulna, to development of three digits and normal zeugopod were obtained with the *RAR-Cre* forelimbs, while removal with the *Msx2-Cre* line exceptionally resulted in absence of digit 5 in the forelimb, whereas the hindlimb

phenotype was quite variable ranging from completely normal to total absence of the hindlimbs (Barrow *et al.,* 2003).

The analysis of *RAR-Cre* mutant forelimbs revealed that the lack of anterior and posterior digits correlated with lack of *Fgf8* expression and lack of thickened ectoderm in those regions, similarly to *Msx2-Cre* mutant hindlimbs. Cre monitorization of both *RAR-Cre* and *Msx2-Cre* with the use of Rosa26 reporter (R26R) line that bears a LoxP flanked DNA STOP sequence preventing expression of the downstream *LacZ*, in the *R26R* locus, until Cre mediated recombination (Soriano, 1999), revealed that lack of *Fgf8* expression was restricted to domains were Cre expression was active in both dorsal and ventral ectoderm. Therefore, they demonstrate that removal of *Wnt3* from dorsal and ventral abolished *Fgf8* induction. However, despite ubiquitous *Wnt3* expression in the limb ectoderm, it was suggested that its signalling was restricted to the pre-AER cells (Barrow *et al.,* 2003). Remarkably, human mutations in *Wnt3* result in a tetramelic phenotype (Niemann *et al*., 2004).

To further assess the implication of Wnt/ß-catenin signalling in the limb ectoderm, conditional removal of *ß-catenin* was performed with the use of the *Msx2-Cre* and the *Brn4-Cre* lines (Fig. 16)(Barrow *et al.,* 2003; Soshnikova *et al.,* 2003). Removal of *ß-catenin* prior to AER induction led to limbless phenotypes with no detectable expression of *Fgf8*, *Bmp4* and *Bmp2* (Fig. 16B.D,E). In addition, DV pattern establishment defects with loss of *En1* and ventrally expanded *Wnt7a* expression were also appreciable. Moreover, its removal after AER induction led to truncated limbs and double dorsal forelimb implying that canonical Wnt signalling is required for AER induction, but it is also continuously required for AER maintenance and DV pattern establishment (Barrow *et al.,* 2003; Soshnikova *et al.,* 2003).

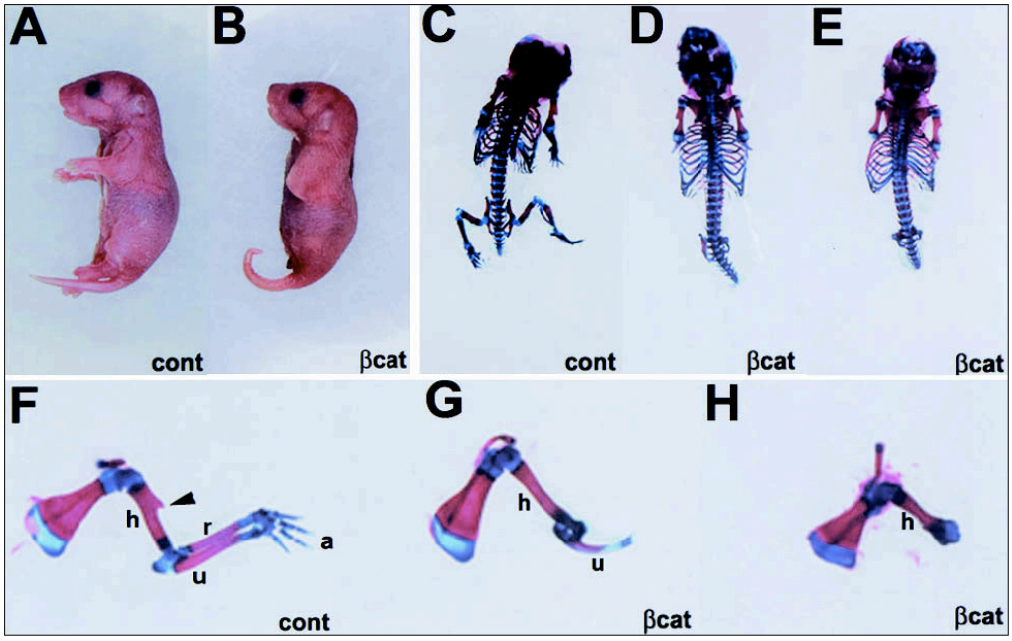


**Figure 16. Limb phenotype of loss of function of *β-catenin* with the *Msx2-Cre* driver line.** Newborn gross morphology and skeletal phenotype of control (A,C,F) and mutant mice (B,D,E,G,H). *β-cat, β-catenin* loss of function; cont, control; u, ulna; h, humerus; r, radius; a autopod. From Barrow *et al*., 2003.

Consistent with its role in AER induction, *ß-catenin* gain of function (GOF) mutation with the use of the *Brn4-Cre* exhibited ventrally expanded AERs with expanded expression of *Bmp4* and *Fgf8*, while DV defects were not appreciable (Soshnikova *et al*., 2003). Remarkably, *Msx2-Cre* dependent *ß-catenin* GOF rescues the stunted limb development due to the removal of *Fgfr2* from the limb ectoderm. Hence, this GOF approaches confirmed that Wnt/ß-catenin was absolutely required and sufficient for *Fgf8* induction, downstream of *Fgf10* (Soshnikova *et al*., 2003, Barrow *et al*., 2003; Lu *et al*., 2008).

### 1.4.6.3 Epistatic relationship between Wnt and Bmp signalling pathways

The epistatic relation between Wnt and Bmp signalling pathways in DV pattern establishment and AER induction remains quite controversial (Soshnikova *et al*., 2003; Barrow *et al*., 2003). Based on overexpression experiments in chick in

which the dominant active form of *ß-catenin* resulted in the induction of the *Fgf8, Bmp2/4* and *7* together with lack of expression of these ligands when Wnt/ß-catenin signalling is disrupted, led to the proposal that Wnt/ß-catenin signalling lies upstream of Bmp signalling in the limb ectoderm in both, AER induction and DV patterning (Barrow *et al*., 2003).

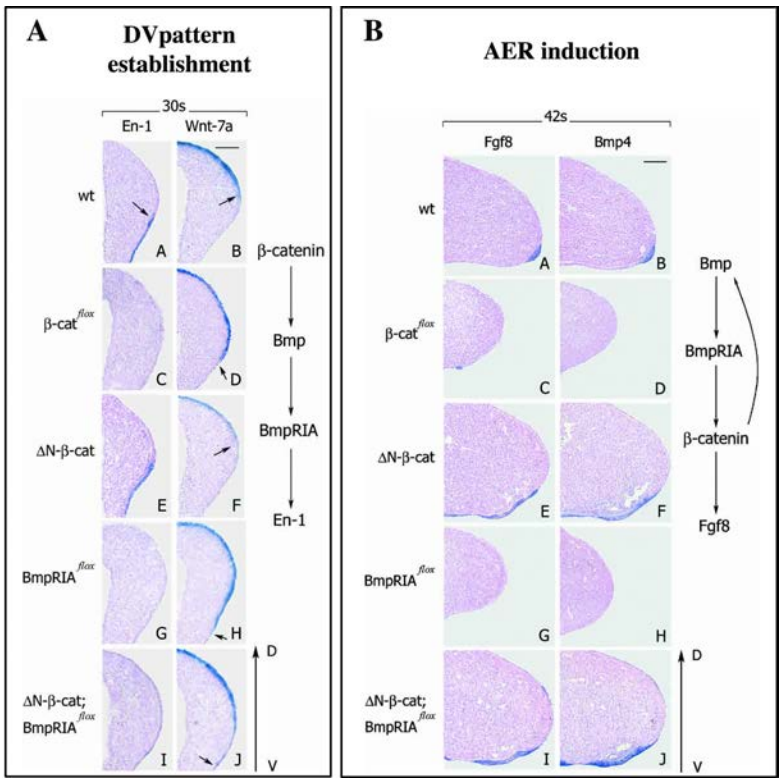


**Figure 17. Epistatic relationship between Wnt/β-catenin and Bmp signalling pathways in DV pattern establishment and AER induction.** A) Wnt/β-catenin acts upstream or in parallel to Bmp signalling in DV establishment as assessed by *En1* (A,C,E,G and I) and *Wnt7a* (B,D,F,H and J) expression in wild type (wt) (A,B), *β-catenin* loss of function *(β-cat$^{flox}$)* (C,D), *β-catenin* Gain of function (*ΔN-β-cat*)(E,F), *BmprIA* mutant (*BmprIA$^{flox}$*) (G,H) and Gain of function of *β-catenin* in the absence of *BmprIA (ΔN-β-cat;BmprIA$^{flox}$)* (I,J). *En1* expression is lost from the ventral limb ectoderm and *Wnt7a* is ectopically expressed in the ventral ectoderm at 30 somites stage in both *β-cat$^{flox}$* and *BmprIA$^{flox}$* mutants and it is not rescued in the *ΔN-β-cat;BmprIA$^{flox}$*. B) Wnt/β-catenin acts downstream of Bmp signalling in AER induction (See scheme at right) as assessed by *Fgf8* (A,C,E,G and I) and *Bmp4* (B,D,F,H and J) expression in wild type (wt) (A,B), *β-catenin* loss of function *(β-cat$^{flox}$)* (C,D), BmprIA mutant (*BmprIA$^{flox}$*), *β-catenin* Gain of function (*ΔN-β-cat*)(E,F), (G,H) and Gain of function of *β-catenin* in the absence of *BmprIA (ΔN-β-cat;BmprIA$^{flox}$)* (I,J). Gain of function mutation of Wnt/β-catenin in absence of the *BmprIA* rescues *Fgf8* and *Bmp4* expression lost in *BmprIA* mutants. From Soshnikova *et al*, 2003.

However, the observation that the *ß-catenin* GOF was able to rescue the limb phenotype of the *BmprIa* mutant suggested that Wnt/ß-catenin signalling lies downstream of Bmp signalling in AER induction and in parallel or downstream in DV pattern establishment. *ß-catenin* GOF mutation in absence of the *BmprIa* rescued the loss of *Bmp4* and *Fgf8* expression in the limb ectoderm of *BmprIa* mutants while lack of *En1* expression and ventrally expanded expression of *Wnt7a* were not rescued (Soshnikova *et al.,* 2003) (Fig. 17). Thus, the linkage between AER induction and DV pattern establishment must lie somewhere between Wnt/ß-catenin and Bmp signalling pathways, because disruption of either of them results in both, lack of AER induction and DV patterning defects (Soshnikova *et al.,* 2003; Barrow *et al*., 2003). However, further analysis of the crosstalk between both signalling pathways should be necessary to determine their epistatic interactions.

## 1.5. The family of the Specificity Protein of transcription factors

The number of transcription factors that belong to this family is highly variable amongst different species, ranging from two Sp-members like *btd* and *D-SP1* in *Drosophila* to up to 13 like in same teleost fishes (Wimmer *et al*., 1996). In mammals, 9 members of the Specificity Protein (Sp) family of transcription factors have been described (Zhao and Meng, 2005). There is evidence for the relevance of several members of this family for the correct development of the embryo. Interestingly, the human *Sp1* was the first identified and cloned binding-specific transcription factor (Dynan and Tjian, 1983; Kadonaga *et al*., 1987). Targeted disruptions of several members of this family have been reported. Animals lacking *Sp1* died at E10.5 (Marin *et al*., 1997). *Sp3* null mice develop to term and die due to a respiratory failure and exhibited teeth and ossification defects (Gollner *et al*., 2001; Bouwman *et al*., 2000). Disruption of *Sp4* led to reduced viability and cardiac defects (Supp *et al*., 1996; Nguyen-Tran *et al*., 2000). No overt phenotype was shown in *Sp5* mutants (Harrison *et al*., 2000). Disruption of *Sp6* led to mild limb

defects restricted to the autopod and also in the teeth and skin (Nakamura *et al*., 2004; Hertveldt *et al*., 2008; Talamillo *et al*., 2010). Targeted mutation in *Sp7* resulted in impaired osteoblast differentiation (Nakashima *et al*., 2002) and *Sp8* null mice develop to term and die due to defects in the closure of the neural tube (Bell *et al*., 2003; Treichel *et al*., 2003).

The distinctive features of the proteins of this family are a highly conserved carboxy terminal DNA-binding domain, characterized by three Cys2His2 zinc finger motifs (which recognize a commonly known structures, GC and GT boxes, within the promoter region of the genes) and a Btd box located in close proximity to it (Wimmer *et al*., 1996). In addition, all the members of the family, with the exception of *Sp6,* contain a Sp box located in their N-terminus (Zhao and Meng, 2005; Runko and Sagerstrom, 2003). The role of the Sp box has not been determined but has been related to proteolytic cleavage or transcriptional activity. There is also an amino-terminal region, which is more variable that includes transcriptional activation or repression domains (Fig. 18).

Release of the human genome, revealed the linkage between *Sp4* and *Sp8*, separated by 545kb with their promoters located face to face, similar to *Sp1*-*Sp7*, *Sp2*-*Sp6* and *Sp3*-*Sp9* gene pairs, whereas *Sp5* is located at distance of 2564bp from *Sp3,* independently of the rest of the Sp family members. Interestingly, the Sp transcription factors are located in the same chromosomes of the *Hox* genes. Of most interest, genetic evolutionary analyses amongst different species suggested the existence of an ancestral Sp cluster linked to the Hox cluster during metazoan evolution (Schaeper *et al.,* 2010).

Recently, the group of Earnst Wimmer based on phylogenetic protein domain structures, expression patterns and genomic localization of the Sp members in different species proposed that previously designated orthologs for *D-SP1* and *btd* in *Drosophila*, *Sp1* and *Sp8* in human respectively, are not directly

homologs. They proposed that *D-SP1* is more closely related to human *Sp8*, the ortholog of mouse *Btd*, and that *btd* is the ortholog of *Sp5* (Schaeper *et al.,* 2010).

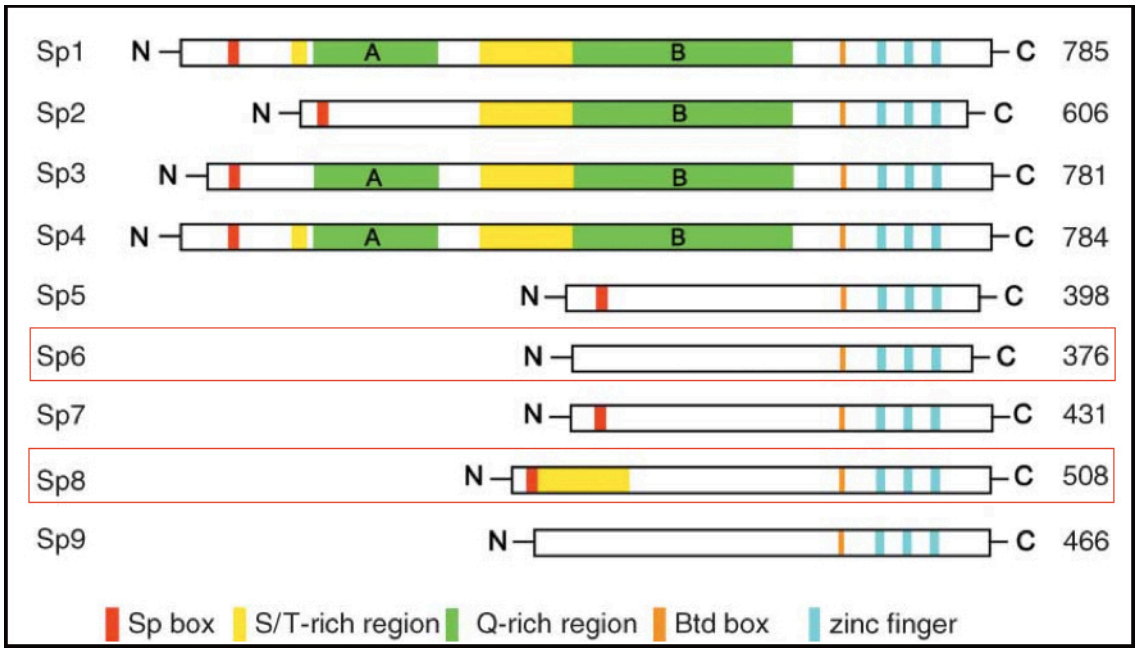


**Figure 18. Specificity Protein family of transcription factors.** The Btd box and three zinc finger domains located at the C-terminus are conserved in all the members of the family. In the N-terminus an Sp box characteristic of the members of this family is conserved in all the members with the exception of *Sp6* and *Sp9*. Two transactivation domains (glutamine (Q)-rich regions) and serine/ threonine (S/ T)-rich regions for proteasome-dependent degradation are present in some members of the family. From Zhao and Meng, 2005.

So far only two members of the Specificity Protein (Sp) family of transcription factors, Sp6 and Sp8, also known as Epiprofin (Epfn) and Buttonhead (Btd) respectively, have been suggested as possible candidates mediating the Wnt/ß-catenin dependent induction of *Fgf8*. Both transcription factors have been demonstrated to function downstream of Wnt/ß-catenin signalling and upstream of *Fgf8* in the limb ectoderm (Kawakami *et al*., 2004; Sahara *et al*., 2007; Talamillo *et al.*, 2010).

Disruption of *Sp6* prevents AER maturation and results in syndactyly with partial dorsalization of the digital tips whereas disruption of *Sp8* results in limb truncation due to the premature regression of the AER. During limb development both are expressed in the entire prospective limb ectoderm prior to *Fgf8* induction and become progressively confined to the AER as the limb bud develops (Bell et al., 2003; Treichel et al., 2003; Talamillo et al., 2010).

The role of *Sp6* and *Sp8* during limb development is not completely determined. Several reports indicate that they are required for Wnt/β-catenin dependent maintenance of *Fgf8* expression in AER cells, but not for its induction (Bell *et al.,* 2003; Treichel *et al.*, 2003; Kawakami *et al.,* 2004; Talamillo *et al.,* 2010; Lin *et al.,* 2013). Based on their overlapping patterns of expression and on their LOF phenotypes, it has been previously suggested that both factors may act in a redundant manner in the induction and maintenance of the AER. In addition, the fact that AER induction and DV pattern establishment occurs concomitantly, DV defects present in mice lacking *Sp6* (Talamillo *et al.,* 2010) and the fact that the orthologs in *Drosophila* of the Sp family have been shown to be able to induce the entire genetic network required for ventral imaginal disc development, including the establishment of a sharp boundary of *En1* expression (Estella *et al.,* 2003; Estella and Mann, 2010), led us to hypothesize that *Sp6* and *Sp8* could be the molecules responsible for coordinating AER induction and DV pattern establishment.

# 2. AIM OF THE PRESENT THESIS

## 2. Aim of the present Thesis

Since *Sp6* and *Sp8* are close related genes and have similar patterns of expression during limb development, the aim of the present Thesis is the analysis of the function and possible redundancy between the Sp family members *Sp6* and *Sp8* in limb development, particularly in the induction of the AER and the DV pattern establishment. Therefore, we have used mouse genetics to study the requirement and the possible redundancy between Sp6 and Sp8 transcription factors during limb development through the generation of double *Sp6*;*Sp8* null mutants and also *Sp6*null;*Sp8* conditional mutants using the *Ap2-Cre* and the *Msx2-Cre* lines.

# 3. MATERIALS & METHODS

# 3. Materials & methods

## 3.1 Mouse strains

The *Epfn-null* (*Sp6*), the *Sp8*$^{CreERT2}$, the *Sp8*$^{flox}$, the *Catnb*$^{lox(ex3)}$, the *Apα2-Cre*, the *Msx2-Cre*, , and the *ROSA26* reporter (R26R) mouse lines were used in this study. All animal procedures were conducted accordingly to the EU regulations and 3R principles and reviewed and approved by the Bioethics Committee of the University of Cantabria. All mice were maintained in a mixed genetic background (C57BL6/CD1) and genotyped based on previously published reports.

The ***Sp6*-null (*Sp6*)** allele is characterized by the absence of the 2$^{nd}$ exon of the *Sp6* gene that encodes the entire coding sequence (CDS) of the *Sp6* gene (Nakamura *et al.,* 2004).

The ***Sp8*$^{CreERT2}$** allele bears a tamoxifen inducible Cre recombinase in substitution of the *Sp8* allele. This line expresses the CreERT2 recombinase in the Sp8 locus. The CreERT2 is a modification of the Cre that contains a G400V/M543A/L544A triple mutation in the Estrogen Receptor ligand-binding domain (ER-LBD) that makes it more sensitive to Tamoxifen (Tam) than the mutant ER LBD with a single G521R substitution.

The ***Sp8*$^{flox}$** allele contains the *Sp8* gene flanked by two LoxP sites that enable conditional removal with the use of Cre driver lines. The first LoxP site is located 5´ to exon 1 and the second one 3´ to exon 3. Cre dependent rearrangement between the two LoxP sites results in the excision of the 3 exons of the *Sp8* gene, completely disrupting it (Zembricky *et al*., 2007).

The ***Catnb*$^{lox(ex3)}$** (*ß-catenin)* allele contains two LoxP sites that flanks the third exon of *ß-catenin* gene. Cre dependent excision of this exon avoids phosphorylation of ß-catenin and results in stabilization of the protein (Harada *et al*., 1999).

The ***Ap2α-Cre*** **driver line** bears an IRESCre cassette into the 3´untraslated region of the *Ap2α* locus between the Stop codon and the polyadenilation sequence allowing the regulation of the Cre under the *Ap2α* locus without affecting the *Ap2* gene function (Macatee *et al.,* 2003). This line drives Cre expression in the limb ectoderm prior to *Fgf8* expression in both forelimb and hindlimb (Boulet *et al.,* 2004).

The ***Msx2-Cr*****e driver line** is a transgenic line that bears a 439bp fragment of the *Msx2* AER specific enhancer followed by the Cre with a nuclear localization sequence that allows specific Cre expression in the limb ectoderm by 19 and 21 So in hindlimb and forelimb respectively (Sun *et al.,* 2000).

The ***Rosa26 reporter*** **(*R26R*) line** bears a floxed 4x polyadenilation sequence that avoids LacZ expression in the ubiquitously expressed *ROSA26* locus (Soriano, 1999). By mating these mice with Cre-expressing transgenic mice, excision of the LoxP flanked STOP sequence occurs allowing expression of the LacZ reporter. This line is a reporter for cells in which Cre dependent rearrangement has occurred and also their descendants.

### 3.2 Mouse mating strategies

*Sp8*$^{CreERT2}$ heterozygous mice were mated to *Sp6* heterozygous mice for the generation of double heterozygous mice (*Sp6*$^{+/-}$;*Sp8*$^{+/\mathrm{CreERT}}$) for posterior analysis of double Knock Out mutant mice (*Sp6*$^{-/-}$;*Sp8*$^{\mathrm{CreERT/CreERT}}$) obtained from crosses between double heterozygous mice, with the aim to unravel their role and their possible redundancy in AER induction and DV pattern establishment.

*R26R* heterozygous mice were mated to *Ap2αCre* heterozygous to define the expression pattern of the Cre under the *Ap2α* promoter, to determine its suitability for conditional removal of *Sp8* from the limb ectoderm. In addition, *R26R* heterozygous mice were matted to *Sp8*$^{CrERT2}$ heterozygous mice to analyze it suitability for temporally deletion of genes from the limb ectoderm.

Conditional removal of the *Sp8*$^{flox}$ allele was performed with two different deleter lines the *Ap2αCre* line and the *Msx2-Cre* line. *Sp8* limb conditional mutants, in an *Sp6* null background, were generated by mating double heterozygous females (*Sp6*$^{+/-}$;*Sp8*$^{+/flox}$) with double heterozygous males carrying the Cre recombinase under the *Ap2α* promoter (*Sp6*$^{+/-}$;*Sp8*$^{+/flox}$;*Ap2α*$^{+/Cre}$) or under the *Msx2* AER specific enhancer (*Sp6*$^{+/-}$;*Sp8*$^{+/flox}$;*Msx2*$^{+/Cre}$). The followed matting strategies are shown below, in each cross the expected Mendelian fraction of the genotypes of interest is indicated in brackets. Both Cre lines are active in the germ cells, thus DNA rearrangement occurs between the LoxP sites flanking the floxed alleles leading to the generation of deleted (D) alleles. In order to ubiquitously ablate the floxed allele, we decided to bear the Cre in the males because the penetrance for Cre activation in the germ cells is of the 100% (Weng *et al*., 2008).

**1st cross: Generation of double *Sp6*$^{+/-}$;*Sp8*$^{f/+}$ heterozygous mice**

| MALE | FEMALE |
|---|---|
| *Sp6*$^{+/-}$ | *Sp8*$^{f/f}$ |
| X | |
| *Sp6*$^{+/-}$;*Sp8*$^{f/+}$ (1/2) | |

**2nd cross: Generation of double *Sp6*$^{+/-}$;*Sp8*$^{f/+}$ heterozygous mice bearing the Cre under the Ap2α locus.**

| MALE | FEMALE |
|---|---|
| *Ap2α*$^{+/Cre}$ | *Sp6*$^{+/-}$;*Sp8*$^{f/+}$ |
| X | |
| *Sp6*$^{+/-}$;*Sp8*$^{f/+}$;*Ap2α*$^{Cre}$ (1/8) | |

**3rd mating: Generation of double *Sp6*$^{-/-}$;*Sp8*$^{f/D}$ homozygous mice bearing the Cre under the Ap2α locus.**

| MALE | FEMALE |
|---|---|
| *Sp6*$^{+/-}$; *Sp8*$^{f/+}$; *Ap2α*$^{Cre}$ | *Sp6*$^{+/-}$;*Sp8*$^{f/+}$ |
| X | |
| *Sp6*$^{-/-}$;*Sp8*$^{f/D}$;*Ap2α*$^{Cre}$ (1/32) | |

**Finall mating for the generation of double *Sp6*$^{-/-}$;*Sp8*$^{f/D}$ homozygous bearing the Cre under the Msx2 locus.**

| MALE | FEMALE |
|---|---|
| *Sp6*$^{+/-}$; *Sp8*$^{f/+}$;*Msx2*$^{Cre}$ | *Sp6*$^{+/-}$;*Sp8*$^{f/+}$ |
| X | |
| *Sp6*$^{-/-}$;*Sp8*$^{f/D}$;*Msx2α*$^{Cre}$ (1/32) | |

Since *Sp6* and *Sp8* have been shown to act downstream of Wnt/ß-catenin, conditional *ß-catenin* GOF approaches were performed with the use of the $Sp8^{CreERT2}$ line (Talamillo *et al*., 2010, Kawakami *et al.,* 2004). $Catnb^{lox(ex3)}$ heterozygous mice were mated to $Sp8^{CreERT2}$ heterozygous mice for the generation of double $Catnb^{+/lox(ex3)}$;$Sp8^{+/CreERT2}$ heterozygous embryos.

### 3.3 Mouse embryos

Noon of the day the vaginal plug was detected was design as embryonic day (E) 0.5. Embryos were harvested by caesarean section from pregnant mice at the desired developmental stage and dissected in Phosphate Buffered Saline (PBS- 137mM NaCL, 2.7mM KCL, 10mM $Na_2HPO_4$, 2mM $KH_2PO_4$) for posterior fixation in Paraformaldehyde-4% (PFA) between 4 hours (h) to overnight (ON) at 4ºC. Genotyping was performed with DNA obtained from the yolk sac or from tail biopsies.

### 3.4 DNA extraction

Mice were genotyped by the polymerase chain reaction (PCR) analysis. The DNA was obtained from tail biopsies or from embryonic membranes.

#### 3.4.1 DNA extraction form tail biopsies

For tail DNA extraction, 0.5cm length tail biopsies were placed in a solution containing 400 µl Tail buffer (10 mM Tris.Cl pH8.0, 50mM EDTA, 100mM NaCl, 5%SDS) and 20 µl of proteinase K (stock 20mg/ml, Merck, # 24568) and incubated at 55ºC ON. The next day, once the tissue was digested the volume was brought to 750µl adding Tail buffer and additional 250µl of NaCl 6M. Samples were then centrifuged 10 minutes (min) at 12.000G, at room temperature (RT). Then, 750µl of the supernatant were transferred to a new tube for posterior DNA precipitation. 500 µl of isopropanol were added and spin down for 10 min at 4ºC. The supernatant was discarded and the pellet was

washed with 1ml of 70% ethanol (EtOH) and centrifuged for 5 min at 4ºC. Then, the pellet was resuspended in 500µl TE buffer (10 mM Tris.Cl pH8.0, 100 µM EDTA) and incubated at 55ºC for 20 min with the lid open the first 5 min to evaporate traces of EtOH.

In general, 1µl of extracted DNA obtained from tail biopsies and resuspended in TE was used for the PCR reaction.

### 3.4.2 Yolk sac DNA extraction

For yolk sac DNA extraction, the yolk sac was dissected and transferred to an eppendorf tube containing 100µl of lysis buffer (50mM KCl, 10mM Tris pH 8.3, 2 mM $MgCl_2$, 0,1mg/ml gelatin, 0,45%NP-40, 0,45% Tween 20) and 0,5 µl of proteinase K (stock 20mg/ml) and incubated ON at 55ºC. Then, the proteinase K was heat inactivated at 95ºC for 10 min and 1µl of this solution was used directly for mice genotyping by the PCR reaction.

## 3.5- Mice Genotyping by the PCR reaction

Mice were genotyped following standard PCR protocols, varying the annealing temperature and the annealing time according to the melting temperature (Tm) of the primers used. The PCR reaction was performed in a total volume of 25µl with the use of ReadyMix™ Taq PCR Reaction Mix with $MgCl_2$ mastermix (Sigma-Aldrich). The primers were used in a final concentration of 200nM. PCR products were run in a 1% agarose gel containing Red Safe for DNA staining and visualized in the Gel-Doc under ultraviolet light and the use of the Quantity–One software (Bio-Rad). Finally, the molecular weight of the products was determined with the use of MassRuler DNA Ladder (Fermentas). The set of primers used to genotype each mouse strain is specified below and it is indicated into 5' to 3' orientation.

*Msx2-Cre* driver line

*Msx2-Cre*-F: AAC AAC TCT GCT GAC TGC TCC TG

*Msx2-Cre*-R: CCT GGC GAT CCC TGA ACA TGT CC

*Ap2αCre* driver line

*Ap2αCre*-F: TGGAAAATGCTTCTGTCCGTTTGC

*Ap2αCre*-R: AACGAACCTGGTCGAAATCAGTG

*R26R* line

R26R-F: ACC CTG GCG TTA CCC AAC TT

R26R-F: CTG TCC CCG TAA CCG AC

*Sp8$^{CreERT2}$* allele

Sp8$^{CreERT}$ wt-F: CAA GCA CGT GAA GAC ACA CAG T

Sp8$^{CreERT}$ wt-R: TGT GTG CTA CTT ACT GTC CAC ATC C

Sp8$^{CreERT}$ mt-F: GAA GTC TCT GGA AGA GAA GGA CCA T

*Sp8$^{flox}$* allele

Sp8$^{Flox}$-F: CCA ATG GGA GAA AAA CAC ACC CCC TCT TAC TCC TC

Sp8$^{Flox}$-R: CCA GCT TCC TGG ACT CTT TCA GTA TAG TTT TGA AG

*Epfn* (*Sp6*) allele

Epfn mt-F: GCTTCCTCGTGCTTTACGGTATC

Epfn wt-F: GCTGGAAACCGTGAAGGAAAGG

Epfn R: GGGTTAGGGGTCATAAGGGATAGG

*Catnb$^{lox(ex3)}$* allele

Catnb$^{lox(ex3)}$-F:GACACCGCTCTGGACAATG

Catnb$^{lox(ex3)}$-R:GTGGCTGACAGCAGCTTTTCTG

### 3.6 Skeletal preparations

Newborn mice were collected and dissected in PBS. Once the skin was removed newborns were eviscerated and fixed in EtOH-96% ON. For cartilage staining, EtOH-96% was replaced by Alcian Blue Staining solution (80% EtOH-96%, 20% glacial acetic acid and 0.3mg/ml Alcian Blue) for the next 2-3 days.

Next, excess staining was removed through successive changes in EtOH-96%. Once the replaced EtOH appeared clear Etoh was replaced by Potassium Hydroxide 1% (KOH) for 3-4h. For bone staining, once the bones become visible, KOH 1% was replaced by Alizarin Red staining solution (0.05mg/ml Alizarin Red in KOH-1%) for about 20 h. Once the bones acquired the desired Alizarin Red staining, the samples were cleared for approximately 24h in 20% KOH-1% in glycerin and followed by additional successive changes of EtOH-70%/glycerin/$H_20$ (1:2:7, 3:3:4, 4:4:2 and 5:5:0), every 24 h. Skeletal preparations were observed with the use of an Olympus SZX12 stereoscopic scope and photographs were taken with a Nikon DS-Fi1 camera.

## 3.7 RNA probe synthesis

### 3.7.1 Transformation

Specific DNA sequences for RNA probe synthesis are cloned in plasmidic vectors. For transformation, 1-3µl of the vector bearing the target DNA was added to an eppendorf containing 30 µl of Dh5α (*E. coli*) competent bacteria. Bacteria were incubated on ice for 30 min and transformed by heat shock for 20 seconds at 37ºC.

### 3.7.2 Mini-prep

For amplification of target DNA transformed bacteria were grown in LB at 37ºC for one hour before being plated in a Petri dish containing LB-Agar (LB 20mg/ml, Agar 15mg/ml, X-gal 0.04mg/ml and IPTG 0.04 mg/ml) and cultured ON at 37ºC. Antibiotic resistant gene encoded by the plasmids enables selective growth of transformed bacteria, depending on the plasmid used the corresponding antibiotic was added to the medium, whereas X-gal and IPTG were used to differentiate between transformed bacteria with plasmids containing an insert (white colonies) from those with an empty plasmids (Blue colonies) when colony screening by PCR was performed. The next day, a positive colony was selected from the Petri dish and transferred to an Erlenmeyer

containing 10 ml LB (Amp 1/1000) and incubated ON at 37ºC in a rocking platform. Finally, plasmidic DNA extraction was performed using the "Quiakit Spin Mini-prep Kit" (Quiagen) following manufacturers recommendation.

### 3.7.3 Plasmid linearization

The target DNA is cloned into the polylinker region of the plasmid flanked by Sp6, T3 or T7 RNA polymerase promoters. Purified plasmidic DNA containing the target DNA sequence for probe synthesis was linearised for *"in-vitro"* sense and antisense-transcription using the appropriate specific restriction enzymes (RE).

### 3.7.4 In vitro transcription

Once the plasmid containing the target DNA sequence for probe synthesis was lienarised, *"in-vitro"* sense and antisense-transcription in presence of digoxigenin labeled ribouridiltriphospahate nucleotides (Dig-UTP) were performed using the appropriate specific polymerase for each plasmid.

## 3.8 Whole mount in situ hybridization

Whole mount in situ hybridization (ISH) was performed to analyze gene expression in mutant embryos. After fixation in PFA between 4h to ON at 4ºC, embryos were rinse in PBS 5 min (twice) for removal of the fixative. Before incubation in hybridization buffer containing digoxigenin labeled antisense mRNA probe several steps for permeabilization were performed. Embryos were first washed for 5 min in PBS-Tween (PBT- 0.1%Tween in PBS) and dehydrated by successive changes in rising methanol (MetOH) concentrations diluted in PBT; 25%, 50%, 75%, and two of 100% prior to store ON at -20ºC. The period of time spent in each dehydration steps varies depending on the size of the embryo, for example 5 and 10 min for E9.5 and E10.5 embryos respectively.

Embryos were rehydrated by successive changes in decreasing MetOH concentrations diluted in PBT; 100%, 75%, 50%, 25% and rinsed in PBT twice for 5 min per step. Afterwards, samples were bleached in hydrogen peroxide-6% diluted in PBT for 60 min. Then, embryos were rinsed in PBT for 5 min and incubated in proteinase K buffer (50mM Tris pH 7,4, 5mM EDTA) containing proteinase K (10µg/ml). The incubation time varies among different developmental stages and also between the ectoderm and the mesoderm. To check gene expression in the ectoderm we have performed 5 min digestion of proteinase K (5µg/ml). Proteinase K was replaced by PBT for the next 5 min and post-fixed with Glutaraldehyde-0,2% in PFA-4% for 20 min. After fixation, embryos were rinsed twice in PBT for 5 min each. Finally, PBT was replaced by hybridization buffer (50% formamide, 5x SSC, 2% blocking powder, 0.1% Triton X-100; 0.1% Chaps, 1mg/ml tRNA, 50ug/ml Heparin pH4.5, 500mM EDTA pH8) and embryos were prehybridazed ON at 65ºC.

The next day, embryos were frozen at -20ºC at least for 6h and then hybridized. For hybridization, previous hybridization buffer was replaced by hybridization buffer containing the desired amount of probe for each experiment and hybridized ON at 65ºC. Before being replaced, the hybridization buffer containing the probe was previously heated at 90ºC for 2 min to avoid possible secondary structures present within the probe.

The following day, to get rid of unspecific binding post-hybridization washes were performed. Hybridization buffer was replaced by Chaps-0.1% in 2xSSC (1M NaCL, 100mM Sodium Citrate, 0.1% Chaps) and washed 3 times for 30 min each at 65ºC. Then, embryos were rinsed three times in Chaps-0.1% in 0.2xSSC (10mM NaCl, 1mM Sodium Citrate, 0.1% Chaps) for 1h and 10 min. Afterwards, embryos were washed twice for 10 min in KTBT buffer at RT (50mM TrisHCL pH7,4, 150mM NaCL, 10mM KCL, triton-1%) for posterior preblock with 20% sheep serum in KTBT for 6h. For the next step, embryos were incubated at 1/2000 anti-Digoxigenin Alkaline Phosphatase (anti-DigAP) antibody (Ab.) diluted in 20% sheep serum in KTBT and rock ON at 4 ºC.

For post-antibody washes embryos were rinsed at RT in KTBT for 1h, 5 or more times and then ON at 4ºC. The next day, embryos were rinsed twice in NTMT buffer (100mM TrisHCL pH9.5, 50mM $MgCl_2$; 100mM NaCL, Triton-1%) for 15 min. Finally, detection of alkaline phophatase activity was obtained incubating the embryos in the dark with NTMT solution containing 3 μl/ml of NBT and 2,3 μl/ml of BCIP stock solution. When the desired signal level was obtained, embryos were rinsed in KTBT for 5 min and fixed in PFA-4%. The embryos were observed with the use of the Olympus SZX12 stereoscopic scope and photographs were taken with a Nikon DS-Fi1 camera.

### 3.9 Paraffin embedding and histological sections

Embryos were embedded in paraffin for posterior sectioning, either to analyze the LacZ staining in more detail, to perform ISH in sections, TUNEL assay or inmunohistochemistry (IHC). After fixation, embryos were rinsed in PBS twice for removal of the fixative solution and progressively dehydrated in rising EtOH concentrations in PBS (50%, 70%, 96% and 100% twice). The embryos were cleared with two changes of Xilol (10 min each) and finally embedded in paraffin at 60ºC for 1h 30 min. A Leica RM2125RT microtome was used to perform 7 μm embryo sections.

### 3.10 Araldite embedding and semithin sections

Araldite embedding was performed following standard procedures. Briefly, tissue was fixed ON at 4ªC in a fixative solution containing PFA-4%, glutaraldehyde-0.016%, $CaCl_2$ 0.002% and phosphate buffer 0.12M. For removal of the fixative, tissue was washed for several times with 0.4M phosphates buffer and post-fixed in osmium tetroxide (Glucose 0,04M, phosphate buffer 0,14M $Cl_2Ca$ 0,0125% and $O_4Os$ 2%). After 2h, osmium tetroxide was removed and tissue was washed ON. Then, tissue dehydration was performed by the use of rising acetone concentrations. Afterwards, tissue was embedded in 50%

araldite-50% anhydride acetone and finally kept in 100% araldite for 3 days at 60ºC to allow araldite polymerization for posterior semithin sectioning.

### 3.11 In Situ Hybridization in sections

To perform ISH in paraffin sections, paraffin was removed from the tissue sections by two washes of Xilol of 10 min each and routinely rehydrated. Next, permeabilization with proteinase K (10 µg/ml) was performed for 7 min and 30 seconds. Slides were immediately rinsed in PBS for 5 min and post-fixed for 20 min in PFA-4%. Afterwards, the slides were rinsed in PBS for 5 min twice. PBS washes were followed by an acetylation step (0,1M Triethanolamine, 0,066mM Acetic Anhydride) of 10 min to reduce background. Then, the slides were rinsed twice in PBT for 5 min each and washed for additional 5 min in distilled water ($dH_2O$) before allowing them to air dry.

Once the slides were dried, hybridization buffer containing the desired amount of probe for each experiment was added and a coverslip was applied over the slides for posterior hybridization ON at 65ºC, in a humid chamber. The hybridization buffer containing the desired amount of probe was previously heated at 90ºC for 2 min to avoid secondary structures.

The next day, slides were rinsed in 5xSSC at RT (2.5M NaCL, 250mM Sodium Citrate) until the covers were removed and post-hybridization washes were then performed to remove unspecific bindings. Slides were washed for 30 min in 1xSSC/Formamide (500mM NaCL, 50mM Sodium Citrate and 50% formamide), afterwards 20 min in 2xSSC (1M NaCL, 100mM Sodium Citrate) and two additional 20 min washes in 0.2xSSC (10mM NaCL, 1mM Sodium Citrate) were performed. All the post-hybridization washes were done at 65ºC. Finally, three washes of 5 min each at RT in MABT pH7,5 (NaCL 150mM, Maleic Acid 100mM, 0.04% Tween) were performed previous to incubation with blocking solution (20% sheep serum in MABT) for 1h, at RT. The blocking solution was replaced by 5% sheep serum in MABT, containing 1/2500 dilution of the anti-DigAP. Ab., for posterior incubation ON at 4ºC in a humid chamber.

Finally, for post-antibody washes embryos were rinsed at RT in MABT for 5 min, 3 times. Then, MABT was replaced by NTM pH9.5 for 10 min. Detection of alkaline phophatase activity was obtained incubating the embryos in the dark with NTM containing 3 μl/ml of NBT and 2,3 μl/ml of BCIP stock solution. When the desired signal level was obtained, embryos were rinsed in PBS for 5 min treated with osmium tetroxide-0.02% for 1 min, washed 5 min in PBS and fixed in PFA-4%. After 20 min, slides were washed in PBS for 5 min, then in $dH_2O$ other 5 min and stained with eosin for 3 min for posterior progressive dehydration using changes of 10 min in rising EtOH concentrations (50%, 70%, 96%, 100% twice and Xilol twice). Cytoseal was used as mounting media. Samples were observed with the use of the Nikon ECLIPSE 80i microscope and photographs were taken with a Nikon DS-Ri1 camera.

RNA probes used in this study:

*Fgf8* (Crossley *et al*., 1996), *Bmp4* (Bandyopadhyay *et al*., 2006), *Tp63* (Mills *et al*., 1999), *Dlx5* (Robledo *et al*., 2002), *Wnt7a* (Cygan *et al*., 1997), *En1* (Loomis *et al*., 1996), *Msx2* (Robert *et al*., 1991), *Shh* (Lopez-Martinez *et al*., 1995), *Fgf10* (Sekine *et al*., 1999), *Sp6* (Nakamura *et al*., 2004), *Sp8* (Treichel *et al*., 2003).

### 3.12 LacZ Staining

LacZ staining was performed to visualize Cre dependent removal of the STOP codon that avoids LacZ expression in *R26R* mice. Embryos were dissected in cold PBS and transferred to a numbered 2 ml eppendorf tube containing PBS and keep in ice until all embryos were collected. Then, the PBS solution was replaced by fixative solution (1% Formaldehyde, 0.2% Glutaraldehyde, 0.02% NP40, 0.01% Sodium deoxycholate in PBS) for 20-30 min (depending on the stage) at 4 ºC on a rocking platform. After fixation, the embryos were rinsed with two changes of PBS for 10 min each and washed with two changes of LacZ buffer pH 7,3 (Sodium phosphate dibasic 75mM, Sodium phosphate monobasic monohydrated 30mM, $MgCl_2$ 2mM, 0.1% sodic deoxichalate (Merck, reference

1.06504.0250), 0.2% igepal (Aldrich, reference 542334), Tris HCL 20mM) for 10 min each, at 37ºC. LacZ buffer was replaced by the staining solution (potassium ferrocyanide ($K_4Fe(Cn_6)$) 5mM, potassium ferrocyanide ($K_3Fe(Cn_6)$) 5mM, X-Gal 0,1%) and the embryos were kept in this solution for 90 min on a rocking platform at RT. Staining reaction was stopped replacing the staining solution by PBS. After several washes in PBS, the embryos were fixed in PFA-4% and stored at 4ºC. The embryos were observed with the use of the Olympus SZX12 stereoscopic scope and photographs were taken with a Nikon DS-Fi1 camera.

### 3.13 Tamoxifen administration

Tamoxifen administration was used to activate nuclear translocation of the CreERT2 enzyme in experiments were the *Sp8*$^{CreERT2}$ line was mated either to *R26R* mice, to evaluate it use for temporally controlled deletion of genes specifically from the limb ectoderm, or to *Catnb*$^{lox(Ex3)}$ mice, to generate a GOF of mutation *β-catenin*. 40mg Tam were dissolved in 400µl of absolute EtOH. This required extensive vortex to obtain complete solution. Then 3.6 ml of autoclaved sunflower oil were added. To evaluate the use of the *Sp8*$^{CreERT2}$ line for temporally controlled deletion of genes specifically from the limb ectoderm, intraperitoneal administration of 1mg (100 µl) to pregnant mice with a tuberculin syringe and 25-gauge needle, at E7.5, was performed. Embryos were obtained by caesarean section 48h later (E9.5). Tam oral gavage was performed for the analysis of the GOF mutation of *ß-catenin* with the *Sp8*$^{CreERT}$ line. For oral gavage 0.05 Tam mg per mice gram weight were administrated. Three consecutive tamoxifen oral administrations every 24h were performed from E7.5 to E9.5. and embryos were obtained by cesarean section of pregnant mice at E10.5.

### 3.14 mRNA extraction

Mouse E10.5 mRNA was used for the quantitative analysis of the expression levels of *Sp8* and *Sp6* in the limb ectoderm by quantitative-PCR

analysis (q-PCR), as well as for the generation of *Fgf8* and *Bmp4* probes by PCR and to clone *Sp8*.

For mRNA extraction tissue weight was measured and 500 µl of Trizol (Invitrogen) per 100mg were added to each sample for posterior homogenization of the tissue. Once homogenized, samples were laid for 5 min at RT and incubated in 0.1 ml of chloroform per volume of Trizol. After 3 min, samples were centrifuged at 12.000G for 15 min at 4ºC. After centrifugation, the supernatant was collected and incubated with 0.5ml isopropanol per volume of Trizol. After 10 min, samples were centrifuged at 12.000G for 10 min at 4ºC. The supernatant was discarded and the pellet washed with EtOH-70% and resuspended in RNA-ase free water after the EtOH was evaporated. Samples were then stored at -80ºC before measuring the concentration at the Nanodrop (Nanodrop technologies ND-1000).

### 3.15 Retro Transcription

cDNA was use as template for q-PCR, PCR probes generation and *Sp8* cloning. To perform the retro-transcriptase PCR (rt-PCR), two mix were prepared. In the first, 1ug of total RNA, obtained from E10.5 mouse embryos, was diluted in 10.5µl RNA-ase free water and heated at 65ºC for 5 min. Afterwards, 9.5µl of the second mix containing the reaction buffer (DTT (0,1M), dNTP, random primers, RNA-ase inhibitor and M-MLV retro-transcriptase (Invitrogen)) were added and immediately incubated for 50 min at 42ºC and additional 5 min at 70ªC, before storing at -20ºC.

### 3.16 Quantitative PCR

Mouse E10.5 limb RNA samples were used for rt-PCR and posterior analysis of *Sp6* and *Sp8* expression level by q-PCR. E10.5 embryos were harvested in PBS and forelimbs and hindlimbs were removed. RNA was extracted separately from 3 pools of 8 forelimbs or 8 hindlimbs each, and then

retrotranscribed as described above. 3 pools were analyzed for either forelimbs or hindlimbs and two replicates for each pool were performed.

After rt-PCR cDNA concentration was measured with the Nanodrop (Nanodrop technologies ND-1000) and adjust to 1µg/µl. q-PCR was performed with the use of the Mx3005P cycler and MxPro software analysis (Stratagene). For q-PCR reaction, 40µl reaction mix containing 2µg of cDNA, 20µl of SYBRgreen mix and 18µl of water was prepared. Final concentration of the specific primers for each gene analyzed was of 125nM. Afterwards, the samples were divided in two, obtaining two 18µl replicates of each sample.

The housekeeping gene used as a control to normalize the expression levels of each one of the genes measured in this experiment was the 18sRNA. The relative expression levels were calculated using the equation $2^{-\Delta Ct}$ (Livak and Schmittgen, 2001), were the threshold for each cycle (Ct) is defined as the cycle in which the fluorescence reaches a stable threshold level.

The primers used to analyze *Sp6*, *Sp8* and *18sRNA* expression levels by qPCR SYBRGreen are indicated below:

Sp6 qPCR primers (5´to 3´orientation):

Sp6-F: tgctaaccgctgtctgtgg

Sp6-R:ctggtatgtctggagaggttgc

Sp8 qPCR primers (5´to 3´orientation):

Sp8-F: ttatctccaaggtgcacacg

Sp8-R:gcttgaaccaggactcatacg

18sRNA qPCR primers (5´to 3´orientation):

18sRNA-R: ttggcaatgtttcgctc

18sRNA-F: cgccgctagaggtgaaattt

### 3.17 Generation of antisense probes for ISH by PCR

A 384bp length *Fgf8* and a 597bp length *Bmp4* specific probes for ISH were generated by PCR, using cDNA samples obtained from E10.5 embryos.

Specific primers for PCR amplification of *Fgf8* and *Bmp4* from cDNA samples were designed using on line bioinformatics tools such as sequence analysis and BLAST programs, together with the sequence manipulation suite website (www.bioinformatics.org.). Once amplified, the PCR product was run in 1% agarose gel and gel purified following manufacturer instructions of the Quiaquick gel extraction kit (Quiagen). Addition of recognition sites for the Sp6 polymerase to 5´ends of specific reverse primers used to amplify each of the genes, enables direct *"in-vitro"* transcription of the antisense probe for ISH directly from gel purified PCR products. Primer-sequences used are specified below, whereby Sp6 polymerase promoter-sequence is underlined and in upper case.

Fgf8 antisense PCR probe primers (5´to 3´orientation):

Fgf8-F: gcacttgctggttctctgc

Fgf8-R: ATTTAGGTGACACTATAGAAggtagttgaggaactcgaagc

Bmp4 antisense PCR probe primers (5´to 3´orientation):

Bmp4-F: tcattccggattacatgagg

Bmp4-R: ATTTAGGTGACACTATAGAAcggcagttcttattcttcttcc

### 3.18 Isolation and cloning of the *Sp8* coding sequence

1516bp fragment corresponding to the CDS of the *Sp8* gene was amplified from cDNA samples from E10.5 embryos with the use of PCR extender system (5Prime) using the primers specified below. The PCR product was run in 1% agarose gel for posterior purification with the use of the Quiaquick gel extraction kit (Quiagen) following manufacturers recommendations and cloned with the used of the TOPO-TA cloning kit (Invitrogen) into provided pCR2.1-Topo vector.

For plasmid amplification, 4µl of the pCR2.1-Topo vector bearing the PCR product were used for transformation of Dh5α (*E. coli*) competent bacteria. After incubation of transformed bacteria, colony PCR screening of individual colonies was performed with the use of M13 primers that recognized flanking regions of the polylinker from the pCR2.1-Topo vector. Among the screened colonies, three

colonies that carried an insert of the correct size were sequenced. The sequence confirmed 100% homology to *Sp8*. Once the CDS of the *Sp8* gene was confirmed, it was cloned into the expression vector pCIG (Megason and McMahon, 2002), a pCAGGS modified vector containing an internal ribosomal entry site (IRES) followed by a cDNA encoding EGFP (pCAGG-IRES2-nucEGFP), useful for electroporation in chick and mouse.

To release the Sp8 CDS from the pCR2.1-Topo vector, the vector was linearised with the use of the BamHI RE. Then, fill in of the 3´end was performed with the use of the Klenow Fragment (Thermoscientific) before releasing the insert performing a second digestion with XhoI RE. Once the insert was released the digestion product was run in 1% agarose gel and purify with the Quiaquick gel extraction kit (Quiagen) and phenol chloroform precipitated. The PCIG was linearised performing a double digestion with SmaI and XhoI and dephosphorylated with the use of Shrimp Alkaline Phosphatase (Thermoscientific). Different proportions of linearised PCIG and gel purify and phenol chloroform precipitated insert containing the CDS of the *Sp8* gene (1:0, 1:1, 1:3 and 1:5) were incubated ON at 14ºC for ligation in the presence of polyethilengycol (PEG) and the T4-ligase. The next day, bacteria were transformed and grown as explained previously. Lastly, a couple of colonies containing the target insert as verified by colony PCR screening were grown and plasmidic DNA was purified with the use of Quiaquick gel extraction kit (Quiagen) and finally sequenced.

M13 primers used for colony PCR (5´to 3´orientation):

M13-F: GTAAAACGACGGCCAG

M13-R: CAGGAAACAGCTATGAC

Primers used to amplify *Sp8* from mouse E10.5 RNA samples (5´to 3´orientation):

Sp8-F: GGG AAC GCG AGA AGA ACC

Sp8-R: GCC CAG TCT AGG TAC ACA AGC

### 3.19 TUNEL assay

The ApopTtag Direct Fluorescein In Situ Apoptosis Detection kit (Milipore, S7110) was used to perform terminal deoxynucletidyl transferase mediated deoxyuridinetriphosphate nick end labeling assay (TUNEL) for the analysis of cell death. It was performed following manufacturer recommendations.

The terminal deoxynucleotidyl transferase enzyme (TdT) provided in the kit catalyzes a template-independent addition of fluorescein (FITC) tagged triphosphate nucleotides to the free 3´-OH ends of single stranded or double-stranded DNA. Interestingly, while the low number of free 3´-OH ends present in normal and proliferative nuclei are not stained, the kit allows specific detection of the high concentrated free 3´-OH ends characteristics of apoptotic cells, as a result of DNA fragmentation.

7µm paraffin sections were deparafined, rehydrated and permeabilized. Proteinase K digestion (10ug/ml) was performed for 7min and 30 seconds. Then, samples were rinsed twice in PBS for 5 min and incubated with the Equilibration Buffer provided by the Kit. After 10 seconds approximately, 1h and 30 min incubation in the working strength TdT enzyme was performed. Enzymatic activity was stopped applying the Stop/Wash buffer for 10 min. After washing three times in PBS for 5 min per wash, samples were mounted using Vectashield containing DAPI for nuclear counter stain and were visualized and photographied with the SP-5 laser-scan confocal microscope (Leica Microsystems).

### 3.2O Immunohistochemistry

Laminin-b (Laminin-REF#111575Abcam-) and E-cadherin (Cdh1-REF#600182Byoscience-) were detected by immunohistochemitry (IHC) in paraffin sections, to distinguish between ectodermal and mesodermal compartments of the limb bud. To carry out the double IHC, sections were hydrated and permeabilized with proteinase K and incubated with blocking

serum (Tris 50mM, NaCL 150mM, HCL 0.05N, 1% goat serum, 1% BSA, 0.1% Triton-X) for 1h at RT. Then, samples were incubated with Laminin and Cdh-1 primary Abs (1/300 and 1/200 diluted in blocking serum, respectively) ON at 4ºC. The next day, tissue sections were rinsed twice in PBS for 5 min each and incubated with the fluorescensce secondary Abs. Alexa 488 and TexasRed Ab (Jackson Lab.) (1/2000 and 1/75 in PBS, respectively) for 1h and 30 min. Finally, after three washes of 5 min each in PBS samples were mounted. Vectashield containing DAPI for nuclear counter stain and were visualized and photographied with the SP-5 laser-scan confocal microscope (Leica Microsystems).

# 4. RESULTS

## 4. Results

Several studies have positioned the transcription factors Sp6 and Sp8 downstream of Wnt/β-catenin and upstream *Fgf8* in the limb ectoderm (Talamillo *et al*., 2010; Treichel *et al*., 2003; Bell *et al*., 2003; Kawakami *et al*., 2004). Moreover, the ability of *Sp8* to induce *Fgf8* supports its possible role in *Fgf8* induction (Kawakami *et al*., 2004; Sahara *et al*., 2007). However, single disruption of either *Sp6* or *Sp8* did not result in absence of *Fgf8* induction in the limb ectoderm (Talamillo *et al*., 2010; Treichel *et al*., 2003; Bell *et al*., 2003). *Sp6* and *Sp8* are expressed in the entire prospective limb ectoderm prior to *Fgf8* induction and progressively become confined to the AER as the limb bud emerges (Talamillo *et al*., 2010; Treichel *et al*., 2003; Bell *et al*., 2003). Individual genetic inactivation of *Sp6* results in soft tissue syndactyly of digits 2 and 3 in the forelimb and synostosis of digits 3 and 4 in the hindlimb (Talamillo *et al*., 2010), whereas disruption of *Sp8* results in limb truncation at a variable level but most commonly at the level of the elbow/knee (Treichel *et al*., 2003; Bell *et al*., 2003).

The mild phenotype observed in the *Sp6* mutant may result from an altered formation of the digital plate probably as a consequence of AER maturation defects (Talamillo *et al*., 2010), while the severe limb truncation observed in *Sp8* mutants is due to the premature regression of the AER (Treichel *et al*., 2003; Bell *et al*., 2003). These studies demonstrated that individual inactivation of either *Sp6* or *Sp8* does not interfere with the induction of *Fgf8* in AER cells (Talamillo *et al*., 2010; Treichel *et al*., 2003; Bell *et al*., 2003). Both transcription factor acts downstream of Wnt/ß-catenin signalling and upstream of *Fgf8* in the limb ectoderm (Kawakami *et al*., 2004; Sahara *et al*., 2007; Talamillo *et al*., 2010). This, together with their similar overlapping patterns of expression led us to propose that *Sp6* and *Sp8* could function in a redundant manner mediating the Wnt/ß-catenin dependent induction of *Fgf8*. To test our hypothesis we decided to perform the $Sp6^{-/-};Sp8^{CreERT2/CreERT2}$ double mutant and also the *Sp8* conditional mutant in an *Sp6* null background with the use the *Ap2α-Cre* and the *Msx2-Cre* deleter lines.

## 4.1 Analysis of the expression of *Sp6* in the absence of *Sp8*

In support of a possible functional redundancy between *Sp6* and *Sp8*, it was shown that *Sp8* expression was maintained in the absence of *Sp6* (Talamillo *et al*., 2010). Hence, we decided to analyze if *Sp6* expression was also maintained in mice lacking *Sp8*, with the use of the $Sp8^{CreERT}$ null allele. In the limb, *Sp6* expression is first detected in dorsal and ventral pre-limb ectoderm of both hindlimb and forelimb buds at E9, prior to *Fgf8* induction, and later its expression progressively declines, first from the dorsal and then from the ventral ectoderm to get predominantly confined to the AER (Talamillo *et al*., 2010).

*Sp6* expression in *Sp8* mutant embryos was analyzed at different developmental stages, from E9.5 to E11.5 (Fig. 19). At E9.5 *Sp6* was detected in the mutant limb ectoderm, but at lower levels in comparison to control animals (Fig. 19A, B). At E10.5, *Sp6* expression was still detectable but a considerable decrease was appreciable in comparison to control embryos (Fig. 19.D, E), similarly to the progressively decrease of *Fgf8* expression previously reported for *Sp8* mutants (Treichel *et al*., 2003; Bell *et al*., 2003). At E11.5, residual *Sp6* expression was detected in correlation with the regressing AER (Fig. 19.C, F).

The expression of *Sp6* in *Sp8* mutants and vice versa, together with their overlapping patterns of expression, supports our hypothesis that both factors could function in a redundant manner mediating the Wnt/ß-catenin dependent *Fgf8* induction in the limb ectoderm. Hence, we decided to perform the double *Sp6;Sp8* mutant.

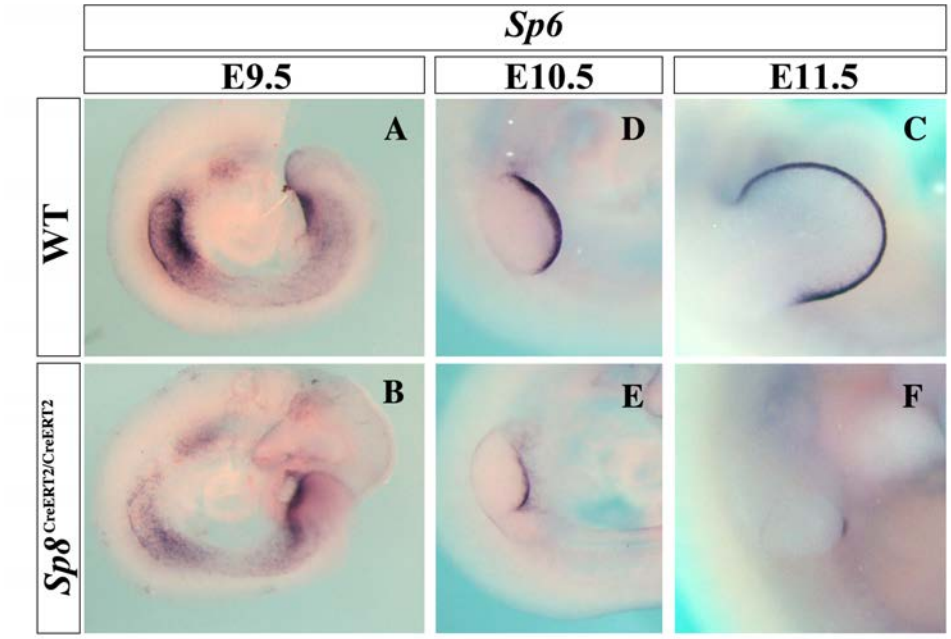


**Figure 19. *Sp6* expression was initiated in *Sp8* mutants but it was not maintained.** Lateral views of control (A,D,C) and *Sp8* mutant embryos (B,E,F) at the stage indicated. Note that *Sp6* expression was initiated in absence of *Sp8* but with a considerable decrease in comparison to control embryo and was progressively lost, in correlation with the regressing AER in *Sp8* mutants.

## 4.2 Limb phenotype of *Sp6;Sp8* compound mutants

To obtain *Sp6;Sp8* dKO, we used the *Sp6*-null (Nakamura *et al*., 2004) and the $Sp8^{CreERT2}$ null alleles. Progeny from crosses between *Sp6;Sp8* double heterozygous mice were analyzed. Double $Sp6^{+/-};Sp8^{+/CreERT2}$ heterozygous mice showed normal limb patterning and skeletogenesis yet displayed subnormal fertility. When performing these crosses, we found a reduced frequency of pregnancies in double heterozygous females. Table 1 shows the Mendelian rates of newborns obtained from crosses between double heterozygous mice. From the 78 recovered, the expected Mendelian rates were obtained for all the genotypes with the exception of double mutants that were represented significantly below the expected 1/16 rate (Table 1).

**Table 1.Expected and obtained Mendelian rates from crosses between double *Sp6*$^{+/-}$;*Sp8*$^{+/CreERT2}$ heterozygous mice.**

| Genotype | Mendelian frequency | Expected | obtained |
|---|---|---|---|
| ***Sp6*$^{+/+}$;*Sp8*$^{+/+}$** | 1/16 | 5 | 6 |
| ***Sp6*$^{+/-}$;*Sp8*$^{+/+}$** | 1/8 | 10 | 14 |
| ***Sp6*$^{+/+}$;*Sp8*$^{+/CreERT2}$** | 1/8 | 10 | 11 |
| ***Sp6*$^{+/-}$;*Sp8*$^{+/CreERT2}$** | 1/4 | 20 | 22 |
| ***Sp6*$^{-/-}$;*Sp8*$^{+/+}$** | 1/16 | 5 | 5 |
| ***Sp6*$^{+/+}$;*Sp8*$^{CreERT2/CreERT2}$** | 1/16 | 5 | 4 |
| ***Sp6*$^{-/-}$;*Sp8*$^{+/CreERT2}$** | 1/8 | 10 | 8 |
| ***Sp6*$^{+/-}$;*Sp8*$^{CreERT2/CreERT2}$** | 1/8 | 10 | 8 |
| ***Sp6-/-;Sp8*$^{CreERT2/CreERT2}$** | 1/16 | 5 | 1 |
| **Total** | | | 78 |

Skeletal preparations of newborns from the whole mutant allelic series were prepared to analyze the limb phenotype. *Sp6* mutant limbs exhibited the previously described phenotype (Talamillo *et al*., 2010). Briefly, limb defects were restricted to the autopods, soft tissue syndactyly of digits 2-3 in forelimb and synostosys of digits 3-4 in hindlimbs (Fig. 20E, F). The penetrance was of 60% with variable expressivity. Interestingly, the phenotype was stronger on the left side with individuals showing only defects in that side. DV defects over the central digits were also present. The hyponychium, the ventral structure of the nail, presented a keratinized morphology typical of the dorsal nail plate conferring a double dorsal phenotype to the distal tips of central digits (Talamillo *et al*., 2010).

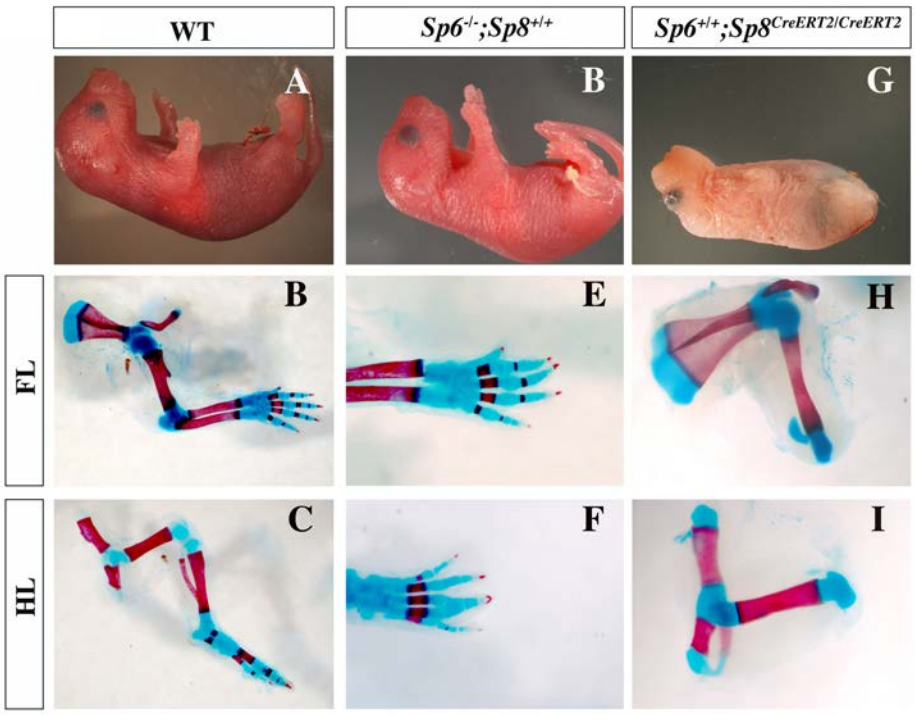


**Figure 20. External morphology and skeletal staining of *Sp6* and *Sp8* mutant newborns**. The genotype is indicated at the top. (A,D,G) Gross morphology of newborn and fore- and hindlimb skeletal staining as indicated. Control embryo (A-C), *Sp6* mutant (D-F) and *Sp8* mutant (G-I). Limb defects in the *Sp6* mutant are restricted to the autopod with the presence of soft tissue syndactyly of digits 2 and 3 in the forelimb and synostosis of digits 3 and 4 in the hindlimb (F). Lack of *Sp8* results in severely truncated limbs at the level of the elbow/knee (H,I).

Mice lacking *Sp8* term to developed and died. This mutants exhibited exencephaly due to defects in neuropore closure and also caudal defects as previously reported (Treichel *et al*., 2003; Bell *et al*., 2003). Elongation of the body along the craneal-caudal axis appeared truncated at the level of the sacral region. Regarding the limb, both the forelimb and the hindlimb exhibited truncations at variable level along the PD axis as previously reported, but most commonly at the level of the elbow/knee (Treichel *et al*., 2003; Bell *et al*., 2003). In our crosses, 5 out of the 8 *Sp8* mutant obtained showed forelimbs truncated at the level of the elbow with either presence (3/8) or absence (2/8) of the olecranon, whereas in the remaining 3 a truncated ulna was developed (Fig. 20H). Half of the hindlimbs analyzed were truncated at the level of the knee lacking all the elements distal to the femur (4/8), whereas in the other half the fibula was developed (4/8) and in one case a truncated tibia was also present (Fig. 20I).

Remarkably, the double mutant specimen obtained showed a tetramelic phenotype (Fig. 21A-C). In this mutant, no skeletal forelimb elements formed distal to the scapula (Fig. 21B). The double mutant also exhibited exencephaly due to a failure in neuropore closure and defects in the caudal region. At caudal level, the lumbar vertebrae appeared highly disorganized and the body was truncated at sacral level (Fig. 21C), consistent with *Sp8* single mutants. However, the caudal defects appreciable in the double mutants were more severe and added the absence of the hip bone.

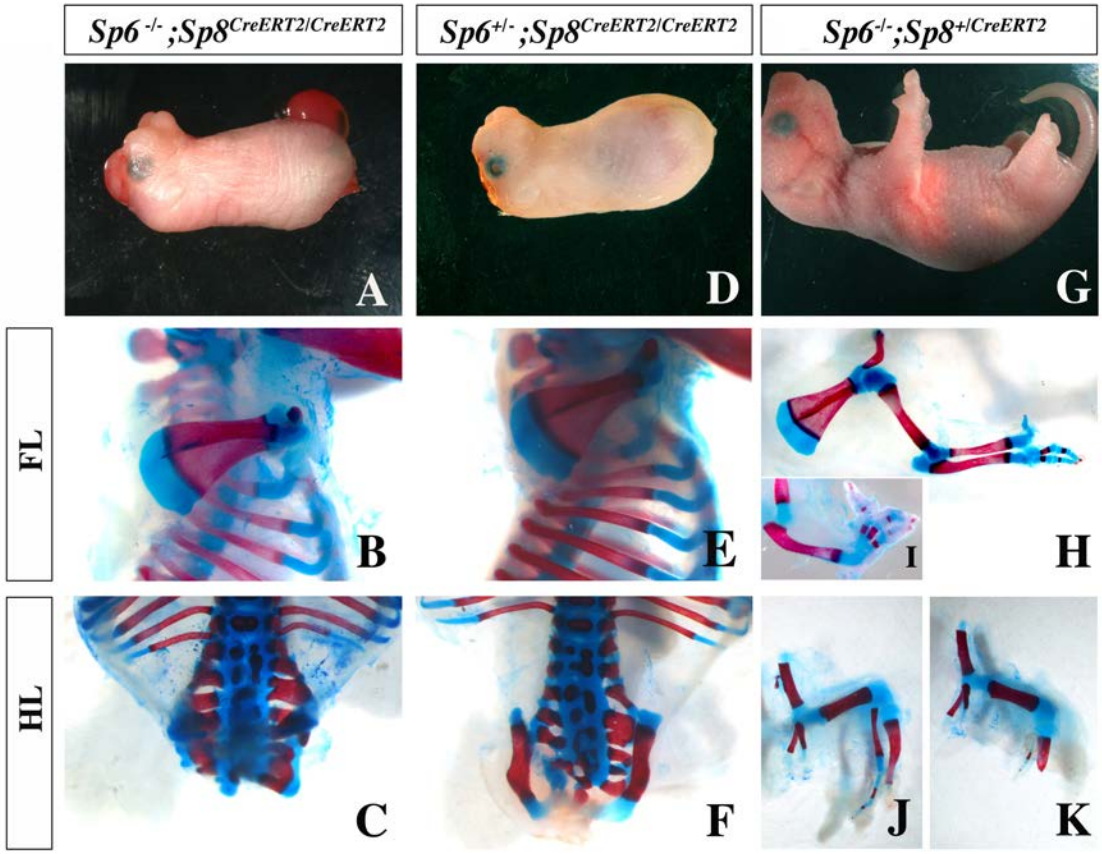


**Figure 21. Effects of reducing the Sp genes on skeletal development.** Gross morphology of newborns (A,D,G) and comparison of skeletal preparations (B,C,E,F,H,I,J,K) of the genotypes indicated. *Sp6*$^{-/-}$;*Sp8*$^{CreERT2/CreERT2}$ mutants lacked all the elements distal to the scapula in the forelimb (B) whereas the body was truncated at the level of the sacrum with the lumbar vertebrae highly disorganized and only a rudimentary cartilage element contributing to the pelvis (C). *Sp6*$^{+/-}$;*Sp8*$^{CreERT2/CreERT2}$ mutants presented the same phenotype to that of *Sp6*$^{-/-}$;*Sp8*$^{CreERT2/CreERT2}$ mutants with the difference that a malformed pelvis lacking the pubis was developed (E,F). *Sp6*$^{-/-}$;*Sp8*$^{+/CreERT2}$ mutants displayed a variable limb phenotype reminiscent of the human Split hand/foot malformation. Forelimbs exhibited severely altered autopods lacking central digits with the remaining posterior ones fused and the radius occasionally missing (H,I). Hindlimbs displayed a misshaped and truncated tibia with either absent or misshaped fibula with a row of skeletal rod (J,K).

All the animals analyzed in which both copies of the *Sp8* gene and one copy of the *Sp6* gene had been removed (8/8) exhibited an amelic phenotype identical to double mutants except the development of a misshaped hip bone lacking the pubis (Fig. 21C,F). As in double mutants, defects in the neuropore closure that resulted in exencephaly were appreciable together with absence of elements distal to the scapula (Fig. 21B) and with the caudal disorganization at the level of the sacral vertebrae (Fig. 21F). The fact that both mutants displayed an indistinguishable limb phenotype raised the question of whether *Sp6* is expressed in $Sp6^{+/-};Sp8^{CreERT2/CreERT2}$.

Skeletal defects in mice in which both copies of the *Sp6* gene and one copy of the *Sp8* gene had been inactivated were restricted to the limbs and were quite variable even in the same animal (Fig. 21G-K). In the forelimbs, the stylopod appeared always normal while the radius was frequently missing and the autopods displayed severely altered and variable phenotypes (Fig. 21H,I). The paw had the "claw-like" appearance reminiscent of the human Split hand/foot malformation (SHFM). In the most severe cases, the anterior or central digits were short or missing and the posterior digits 3-4 or 4-5 were frequently fused (Fig. 21H). In less affected cases 5 digits were distinguishable in spite of the SHFM phenotype. In the hindlimb, the phenotype was constantly more severe (Fig. 21J,K). In the most affected cases, a normal femur developed followed by an incompletely developed tibia and a single thin digit was in a few cases present (Fig. 21K), while in the less severe cases the tibia and the ulna were normally developed exhibiting a single digit (Fig. 21J). Occasionally, distal bifurcation of a digit was observed, in one of the forelimb and one of the hindlimb analyzed. Overall, the phenotype was compatible with the SHFM in humans, characterized by the absence of central digits and fusion of the remaining ones. Of most interest, the digits in both fore and hindlimbs of $Sp6^{-/-};Sp8^{+/CreERT2}$ mutants were bidorsal lacking ventral pads and exhibiting circumferential nails (Fig. 22B). The phenotype was variable within a single animal, each paw showing specific deficiencies. However, a left or right tendency for severity was not identified.

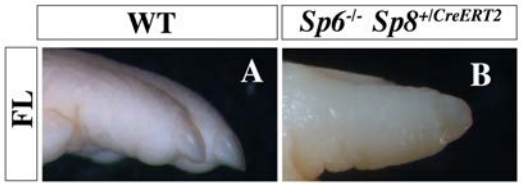


**Figure 22. *Sp6$^{-/-}$;Sp8$^{+/CreERT2}$* exhibited double dorsal digit tips.** Gross morphology of control (A) and *Sp6$^{-/-}$;Sp8$^{+/CreERT2}$* mutant (B) newborns. Note that *Sp6$^{-/-}$;Sp8$^{+/CreERT2}$* digit tips exhibited a double dorsal phenotype with circumferential nails.

The only difference between the double mutant and the *Sp6$^{+/-}$;Sp8$^{CreERT2/CreERT2}$* mutant was at the level of the pelvic hip bone that is more affected in the double *Sp6$^{-/-}$;Sp8$^{CreERT2/CreERT2}$* mutant (Fig. 23B,C) . The pelvic hip bone is formed by the fusion of three distinct skeletal elements the ischium, the ileum and the pubis. The only evidence of the hip bone in the double mutant was a rudimentary and unidentifiable element (Fig. 23B), whereas *Sp6$^{+/-}$;Sp8$^{CreERT2/CreERT2}$* mutants consistently showed a hip bone in which the ischium and the ilium were developed but the pubis was absent (Fig. 23C).

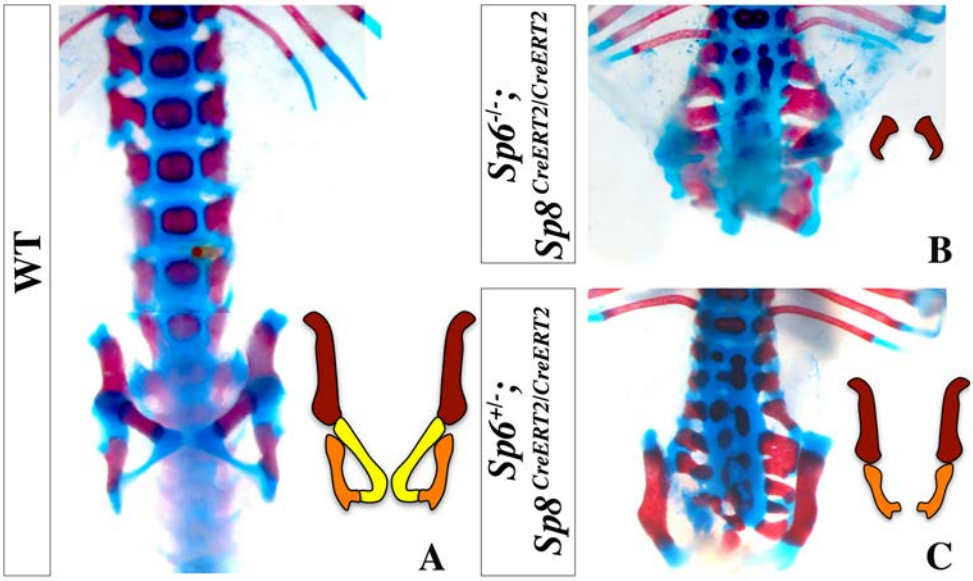


**Figure 23. Pelvic hip bone development in mice lacking Sp genes.** The fusion of three elements, the ileum, the ischium and the pubis, form the hip bone .(A) control. (B) *Sp6$^{-/-}$;Sp8$^{CreERT2/CreERT2}$* mutants showed a caudal truncation of the body at the level of the sacrum with a highly disorganized lumbar vertebrae and a single rudimentary cartilage element contributing to the pelvis. (C) *Sp6$^{+/-}$;Sp8$^{CreERT2/CreERT2}$* mutants presented a similar caudal phenotype to that of *Sp6$^{-/-}$;Sp8$^{CreERT2/CreERT2}$* with the difference that a pelvis lacking the pubis with a misshaped ileum and ischium was developed. Yellow, pubis; orange, ischium and brown ileum.

Our genetic analysis demonstrates that *Sp6* and *Sp8* are together absolutely required for limb development and supports our hypothesis that they perform partially redundant functions in the limb ectoderm, as in their absence no limbs formed. Our study of the whole allelic series also shows that one single functional allele of *Sp6,* in the absence of other *Sp* alleles (*Sp6* and *Sp8*), is unable to support any limb development as the limb phenotype is similar to that of the double mutant. However, one single functional allele of *Sp8,* in the absence of other *Sp* alleles (*Sp6* and *Sp8*), permits a considerably degree of limb development, as the three segments of the limb are developed although digits exhibited a limb phenotype reminiscent of the split hand/malformation in human, where central digits are missing and the remaining posterior ones are fused.

### 4.3 Relative expression levels of *Sp6* and *Sp8* in E10.5 mouse limbs

Since *Sp6* and *Sp8* display similar temporal and spatial patterns of expression in the limb ectoderm, one possible explanation for this functional difference is that *Sp8* has specific functions that *Sp6* cannot accomplish. However, it is also possible that these functional differences rely on differences in their levels of expression. To check this possibility, we quantified the expression levels of *Sp6* and *Sp8* in the limb ectoderm by quantitative PCR analysis at E10.5 in both forelimb and hindlimb buds of wild type embryos.

Our results showed that the level of expression of *Sp8,* at E10.5 in control embryos, was 3-fold times higher than that of *Sp6* in the forelimb and 5-fold times higher in the hindlimb. In addition, the analysis also showed that both *Sp6* and *Sp8* expression occurred at higher levels in the forelimb than in the hindlimb and that this difference was higher for *Sp6.* In the case of *Sp6*, the expression was 4-fold times higher in the forelimb than in the hindlimb, while *Sp8* exhibited a 3-fold increase in the forelimb in comparison to the hindlimb (Fig. 24).

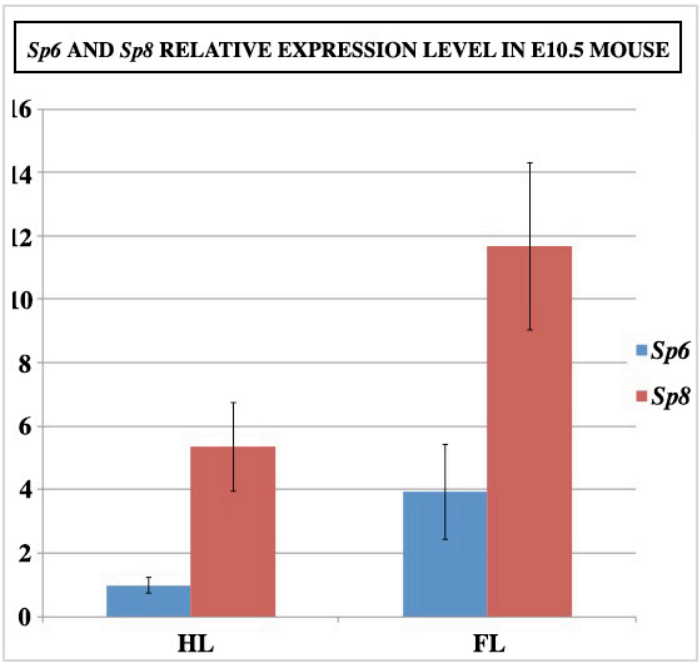


**Figure 24. *Sp8* makes a more substantial contribution to limb development than *Sp6***. Relative expression levels of *Sp6* and *Sp8* in mouse E10.5 limbs from 3 pools of 8 forelimbs or 8 hindlimbs each. *Sp8* showed a 3-fold increase in comparison to *Sp6* in the forelimb and 5-fold in the hindlimb, also showed that *Sp6* and *Sp8* expression levels in the forelimb are higher than in the hindlimb.

Our results suggest that *Sp8* makes a more substantial contribution to limb development than *Sp6* because of a higher level of transcription and provides an explanation for the phenotypical differences when only one copy of them remains.

## 4.4 Selection of a limb ectoderm specific Cre line and monitorization of its activity

Because from the double heterozygous crosses we only got one double mutant, we decided to generate more specimens to the phenotype and evaluate possible genotype variability. To circumvent the issues of the reduced fertility and the low recovery of double mutants, we used an *Sp8* conditional allele to remove it specifically from the limb ectoderm. Amongst the available lines with Cre activity in the limb ectoderm *Msx2-Cre, Brn4-Cre; RAR-Cre; Ap2α-Cre* and

*Mox2-Cre*, we selected the *Ap2α-Cre* line because it has been reported to drive very early Cre function in both fore and hindlimbs, at least prior to *Fgf8* initiation of expression (Boulet *et al*., 2004). Because *Sp8* is already expressed in the pre-limb ectoderm prior to activation of *Fgf8* in the ventral ectoderm (Treichel *et al*., 2003; Bell *et al*., 2003 and authors personal observations), we decided to determine in more detail the activity of the *Ap2α-Cre* transgenic line prior to limb bud emergence using the R26R strain and evaluate its suitability to perform the conditional removal of *Sp8* (Soriano, 1999).

The analysis of *Rosa26$^{+/tg}$;Ap2α-Cre* embryos showed that at E8.5 lacZ staining was widely detected covering practically the whole ectoderm of the embryo, including the pre-limb ectoderm (Fig. 25A, B). Detection across in the pre-limb area was further confirmed in transverse sections within the pre-limb area (Fig. 25C). In addition, transverse sections also revealed the presence of LacZ staining in the dorsal neural tube, with a weaker level of staining in the ventral part of the neural tube (Fig. 25C).

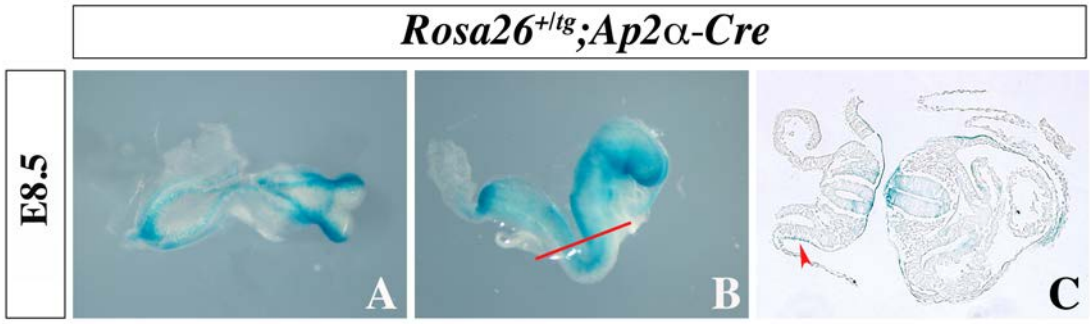


**Figure 25. ROSA26 reporter activity for *Ap2α-Cre* transgenic line in an E8.5 mouse embryo.** Dorsal (A) and lateral (B) views of E8.5 embryo. (C) Transversal section of the same embryo at the level indicated in B. Cre activity is detected in neural tube, with stronger level in the dorsal part and in the entire ectoderm by E8.5, including the pre-limb ectoderm indicated with a red arrow head (C).

The monitorization of the Cre under the *Ap2* promoter indicated that Cre dependent DNA rearrangement in the pre-limb ectoderm occurs at least by E8.5 previous to limb bud appearance, early enough to remove *Sp8* from the limb bud ectoderm before *Fgf8* expression. Thus, we used the *AP2α-Cre* line to

conditionally inactivate a *Sp8* floxed allele in an *Sp6* null background. In addition, the detection of LacZ staining in the neural tube indicates that the defects in the closure of the neural tube characteristic of *Sp8* mutants will persist when using this Cre line, due to the overlapping patterns of expression of the Cre, under the *Ap2* promoter, and *Sp8* in this region.

## 4.5 Conditional inactivation of *Sp8* with the *Ap2α-Cre* line in an *Sp6* null background: Morphological characterization of the compound mutants by skeletal staining

Newborn skeletal phenotypes from the whole allelic series obtained with the use of the *Ap2α-Cre* line were similar to those obtained from croses between $Sp6^{+/-};Sp8^{+/CreERT2}$ double heterozygous mice. As previously mentioned in materials and methods (3.2 Mouse mating strategies ), the *Ap2α-Cre* line is active in the germ line. The activation of the Cre in the germ line lead to the removal of the floxed alleles flanking the *Sp8* gene, leading to the generation of deleted alleles (D). Therefore, all the *Sp8* mutants obtained from this crosses bears a floxed allele, but also a deleted allele for *Sp8* ($Sp8^{f/D}$).

With these crosses we recovered 2 newborns that lacked both *Sp6* and *Sp8* in the limb, and that showed in tetramelic phenotype similar to that of $Sp6^{-/-};Sp8^{CreERT2/CreERT2}$ (Fig. 26A-C). In addition 5 conditional mutants for *Sp8* bearing a single functional allele of *Sp6* that displayed a similar phenotype to the $Sp6^{+/-};Sp8^{CreERT2/CreERT2}$ mutants were recovered (Fig. 26D-F). The conditional phenotype was not restricted to the limb confirming a wide overlaping between the expression of *Ap2* and *Sp8* in the neural tube, leading to defects in the neural tube closure. However, the general phenotype was slightly improved, due to a less severe caudal regresion present in double conditional mutants in comparison to the ubiquitous mutants (Fig. 26C).

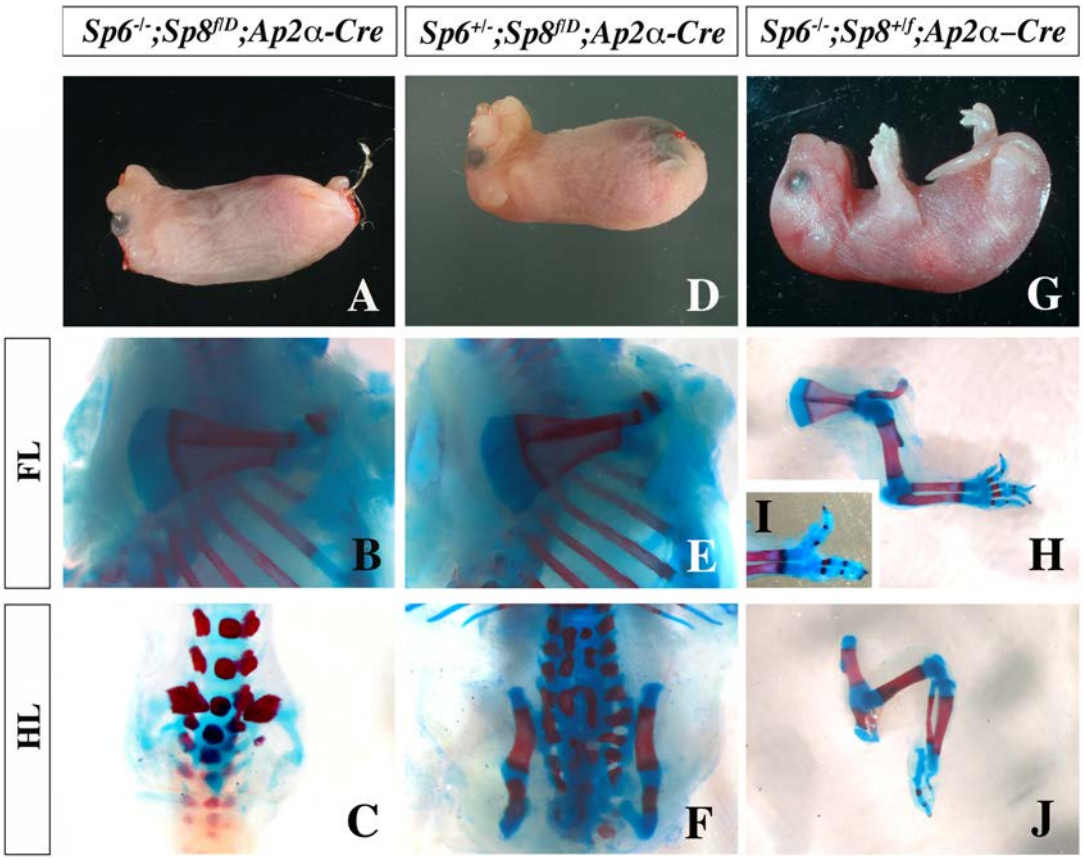


**Figure 26. *Ap2α-Cre* dependent removal of the *Sp8* floxed allele in an *Sp6* null background mimicked the phenotype obtained from ubiquitous mutants.** Gross morphology of newborns (A,D,G) and of skeletal preparations (B,C,E,F,H,I,J) of the genotypes indicated. *Sp6$^{-/-}$;Sp8$^{f/D}$;Ap2α-Cre* mutants lacked all the elements distal to the scapula in the forelimb (B) whereas only a rudimentary cartilage element formed the pelvis (C). *Sp6$^{+/-}$;Sp8$^{f/D}$;Ap2α-Cre* mutants exhibited the same phenotype to that of *;Sp6$^{-/-}$;Sp8$^{CreERT2/CreERT2}$* mutants with the difference that the body was truncated at the level of the sacrum with the lumbar vertebrae highly disorganized and a malformed pelvis lacking the pubis was developed (E,F). *Sp6$^{-/-}$;Sp8$^{+/f}$;Ap2α-Cre* mutants showed a SHFM like phenotype with a highly variable phenotype. Forelimbs displayed severely altered autopods lacking central digits with the posterior ones fused and the radius occasionally missing (H,I). Hindlimbs displayed a misshaped and truncated tibia with either absent or misshaped fibula with a row of skeletal rods (J).

Mutants for *Sp6* in which one copy of *Sp8* was conditionally removed with the *Ap2α-Cre* line (n=7), exhibited the same range of phenotypes described for *Sp6$^{-/-}$;Sp8$^{+/CreERT2}$* ubiquitous mutants (Fig. 26 G-J). The defects were restricted to the limbs. The forelimbs exhibited a weaker phenotype in comparison to the hindlimbs with defects restricted to the zeugopod and the autopod, which was quite variable even in the same animal. The styolpod was perfectly developed and the zeugopod when affected was mainly due to defects in the radius. The autopods displayed severely affected phenotypes with the "claw-like"

appearance typical of SHFM in which anterior or central digits were short or missing and posterior digits 3-4 or 4-5 were frequently fused (Fig. 26H-I). The hindlimbs displayed a more severe phenotype. The stylopod was correctly developed, whereas defects in the zeugopod were variable. The tibia was always present but sometimes truncated and the fibula, when present, was truncated and frequently only showed one or two thin and unidentifiable digits attached to it (Fig.26J). This phenotype was compatible with the SHFM in humans mentioned above. In addition, as it was the case in previous *Sp6*$^{-/-}$;*Sp8*$^{+/CreERT2}$ mutant, digits in both fore and hindlimbs were bidorsal lacking ventral pads and exhibiting circumferential nails. Finally, due to the activation of the Cre in the germ line mutants for *Sp6* bearing a deleted allele of *Sp8* were also obtained (*Sp6*$^{-/-}$*;Sp8*$^{+/D}$*;Ap2αCre)*. This mutants displayed a similar phenotype to that of *Sp6*$^{-/-}$*;Sp8*$^{+/CreERT2}$ obtained from crosses between *Sp6*$^{+/-}$*;Sp8*$^{+/CreERT2}$ double heterozygous mice.

Therefore, we confirmed that *Ap2α-Cre* dependent removal occurs in the limb ectoderm early enough to remove *Sp8* and mimicked the ubiquitous removal. These results, further supported our hypothesis that both factors are together absolutely required for limb development and perform redundant functions in the limb ectoderm. In addition, confirms that a single functional allele of *Sp6* in the absence of *Sp8* is irrelevant to support any limb development due to the phenotypical similarity with the double *Sp6;Sp8* mutants. However, one single functional allele of *Sp8*, in the absence of *Sp6*, permits a considerably degree of limb development as digits form although with an ectrodactyly phenotype.

## 4.6 Conditional inactivation of *Sp8* with the *Msx2-Cre* line in an *Sp6* null background: Morphological characterization of the compound mutants series by skeletal staining

Amongst the Cre lines available we decided to use the *Msx2-Cre* deleter line to conditionally remove *Sp8* from an *Sp6* null background with the aim to distinguish between the requirement of *Sp8* in the induction and the

maintenance of the AER. The use *Msx2-Cre* line enables us to distinguish between the requirement of this Sp factors in AER induction and maintenance, because Cre recombinase under the *Msx2* AER specific enhancer is active at 19 somites, 12 hours prior to AER induction in the hindlimb ectoderm, while in the forelimb *Msx2-Cre* is active at 21 somites, in the AER and the ventral limb ectoderm, just after AER induction (Sun *et al.,* 2002; Barrow *et al.,* 2003).

As expected the hindlimbs exhibited a stronger phenotype in comparison to the forelimbs in all the specimens analyzed, due to an earlier onset of Cre activity. Conditional removal of *Sp8* in the absence of *Sp6* (*Sp6*$^{-/-}$;*Sp8*$^{f/D}$;*Msx2-Cre*) resulted in truncated forelimbs at the level of the elbow with the olecranon present, total absence of hindlimbs and a pelvic girdle that lacked the pubis (Fig. 27A-C).

Conditional mutants for *Sp8* bearing a single functional allele of *Sp6* (*Sp6*$^{+/-}$;*Sp8*$^{f/D}$;*Msx2-Cre*) exhibited a considerable degree of variability even in the same animals with a stronger hindlimb phenotype in comparison to the forelimb (Fig. 27D-G). The forelimbs were truncated at the level of the wrist. The humerus was perfectly developed and the zeugopod showed a truncated radius in half of the limbs analyzed (5/10), while in the other half the radius and the ulna were correctly developed. Regarding the autopod, this was practically missing except in 4 cases in which carpal elements were also developed and a cartilaginous element that resembled a digit was developed (Fig. 27E). Half of the hindlimb lacked all the elements distal to the femur (5 /10) (Fig. 27G). 3 out of 10 mutant hindlimbs exhibited an unidentifiable element distal to the femur, while in 2 out of 10 hindlimbs analyzed the fibula was developed with even smaller unidentifiable element distal to it (Fig. 27F).

*Sp6* mutants in which one copy of *Sp8* was conditionally removed with the *Msx2-Cre* (*Sp6*$^{-/-}$;*Sp8*$^{f/+}$;*Msx2-Cre*) exhibited a SHFM phenotype as the previously described ones bearing a single functional allele of *Sp8* with the use of the *Ap2α-Cre* line or the ones obtained from crosses between double *Sp6*$^{+/-}$;*Sp8*$^{+/CreERT2}$ heterozygous mice (Fig. 27H-K). In addition, germ line activation of the Cre under the *Msx2* AER specific enhancer, as in the case of the *Ap2αCre* line, led the

to ubiquitous removal of the floxed allele generating individuals bearing null alleles (D) for *Sp8*. As expected, the *Sp6*$^{-/-}$;*Sp8*$^{+/D}$ mutant obtained in these crosses exhibited also the SHFM phenotype as the ones obtained in previous ubiquitous and conditional approaches with the *Ap2αCre* .

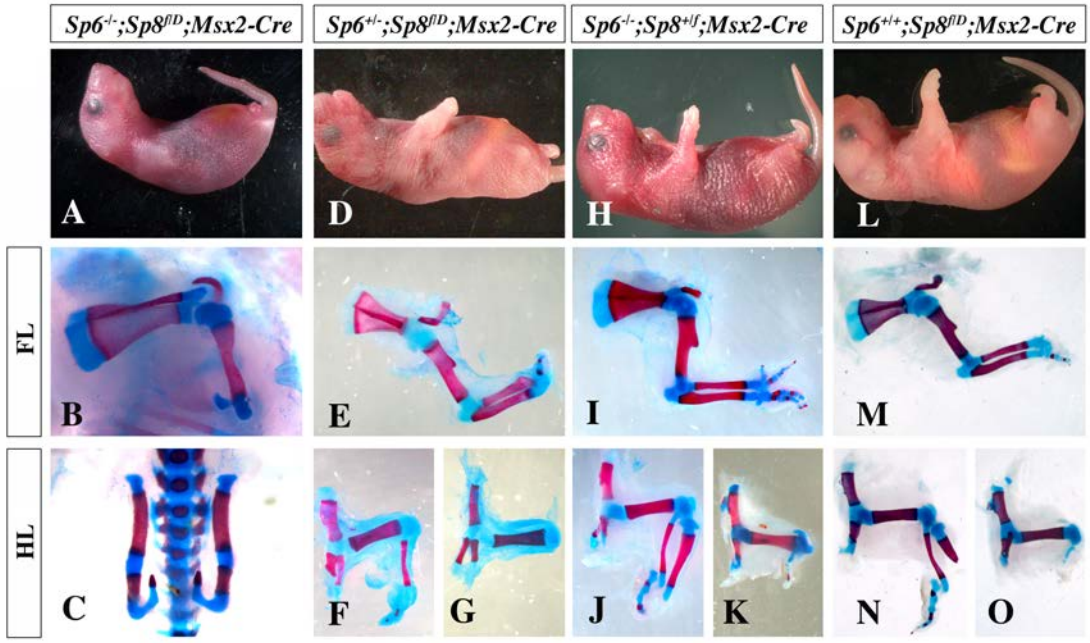


**Figure 27. *Msx2-Cre* dependent removal of the *Sp8* floxed allele in an *Sp6* null background.** Gross morphology of newborns (A,D,H,L) and comparison of skeletal preparations (B,C,E,F,G,I,J,K,M,N,O) of the genotypes indicated. *Sp6*$^{-/-}$;*Sp8*$^{f/D}$;*Msx2α-Cre* mutant forelimbs lacked all the elements distal to the elbow (B) and resulted in a pelvic girdle that lacked the pubis with total absence of the hindlimbs (C). *Sp6*$^{+/-}$;*Sp8*$^{f/D}$;*Msx2α-Cre* forelimbs displayed a variable degree of truncations at the wrist level associated to an incomplete digit with the radius present but often truncated (E), whereas in the hindlimbs the femur appeared associated either to an unidentifiable element or the fibula associated to a single digit (F,G). *Sp6*$^{-/-}$;*Sp8*$^{+/f}$;*Msx2α-Cre* mutants forelimbs displayed severely altered autopods lacking central digits with the posterior ones fused and the radius occasionally missing (I). Hindlimbs displayed a misshaped and truncated tibia with either absent or misshaped fibula with a single digit (J,K). *Sp6*$^{+/+}$;*Sp8*$^{f/D}$;*Msx2α-Cre* exhibited forelimb defects restricted to the autopod with only the most posterior digit present (M), while the hindlimbs showed a single digit (N) or in the most affected a cartilaginous element attached to the femur was developed (O).

The phenotype of the *Sp6* mutants was identical as previously described (Talamillo *et al.*, 2010). Conditional mutants for *Sp8* with the use of the *Msx2-Cre* deleter line exhibited a limb phenotype milder than that of the ubiquitous mutant (Bell *et al.*, 2003; Treichel *et al.*, 2003)(Fig. 27L). Forelimbs defects were restricted to the autopod in which anterior digits were missing and only digit 5

or digit 4 and 5 were developed (Fig. 27M). In hindlimbs, the stylopod was always developed. In half of them the zeugopod was absent and exhibited an unidentifiable cartilaginous element distal to the femur, while in the other half a fibula and a truncated tibia associated to a digit were developed (Fig. 27N, O).

In sum, the phenotypes obtained with the *Msx2-Cre* line implies that both transcription factors are not only required prior to AER induction but also later in development to ensure proper PD limb patterning. The range of phenotypes obtained from different combinations of conditional and ubiquitous approaches support a model in which *Sp6* and *Sp8* are functionally equivalents during limb development, with *Sp8* making a more substantial contribution than *Sp6*, probably due to a higher level of expression. Our results also suggest that a threshold of Sp dosage may be required and that below that threshold limbs are not formed.

## 4.7 Molecular and morphological characterization of *Sp6;Sp8* double mutant limb buds

Gene expression analysis together with morphological characterization of mutant limb buds were performed in embryos obtained from crosses between $Sp6^{+/-};Sp8^{+/CreERT2}$ double heterozygous mice, because the fraction of double mutant recovered at E9.5 (Table 2) and E10.5 (Table3) was according to the expected 1/16 Mendelian frequency. At E9.5, according to the expected Mendelian rate 6 double $Sp6^{-/-};Sp8^{CreERT2/CreERT2}$ mutant embryos were obtained from a total of 95 embryos recovered (Table2), while at E10.5 from 153 embryos recovered 9 double $Sp6^{-/-};Sp8^{CreERT2/CreERT2}$ mutants were obtained from the 10 expected (Table3). That indicates that the double mutant is lethal after E10.5.

**Table 2 Expected and obtained Mendelian rates at E9.5 from crosses between double *Sp6$^{+/-}$;Sp8$^{+/CreERT2}$* heterozygous mice.**

| Genotype | Probability | Expected | Obtained |
|---|---|---|---|
| *Sp6$^{+/+}$;Sp8$^{+/+}$* | 1/16 | 6 | 4 |
| *Sp6$^{+/-}$;Sp8$^{+/+}$* | 1/8 | 12 | 10 |
| *Sp6$^{+/+}$;Sp8$^{+/CreERT2}$* | 1/8 | 12 | 16 |
| *Sp6$^{+/-}$;Sp8$^{+/CreERT2}$* | 1/4 | 24 | 29 |
| *Sp6$^{-/-}$;Sp8$^{+/+}$* | 1/16 | 6 | 6 |
| *Sp6$^{+/+}$;Sp8$^{CreERT2/CreERT2}$* | 1/16 | 6 | 4 |
| *Sp6$^{-/-}$;Sp8$^{+/CreERT2}$* | 1/8 | 12 | 11 |
| *Sp6$^{+/-}$;Sp8$^{CreERT2/CreERT2}$* | 1/8 | 12 | 9 |
| *Sp6$^{-/-}$;Sp8$^{CreERT2/CreERT2}$* | 1/16 | 6 | 6 |
| **Total** | | | 95 |

**Table 3 Expected and obtained Mendelian rates at E10.5 from crosses between double *Sp6$^{+/-}$;Sp8$^{+/CreERT2}$* heterozygous mice.**

| Genotype | Probability | Expected | Obtained |
|---|---|---|---|
| *Sp6$^{+/+}$;Sp8$^{+/+}$* | 1/16 | 10 | 11 |
| *Sp6$^{+/-}$;Sp8$^{+/+}$* | 1/8 | 19 | 19 |
| *Sp6$^{+/+}$;Sp8$^{+/CreERT2}$* | 1/8 | 19 | 19 |
| *Sp6$^{+/-}$;Sp8$^{+/CreERT2}$* | 1/4 | 38 | 36 |
| *Sp6$^{-/-}$;Sp8$^{+/+}$* | 1/16 | 10 | 6 |
| *Sp6$^{+/+}$;Sp8$^{CreERT2/CreERT2}$* | 1/16 | 10 | 12 |
| *Sp6$^{-/-}$;Sp8$^{+/CreERT2}$* | 1/8 | 19 | 18 |
| *Sp6$^{+/-}$;Sp8$^{CreERT2/CreERT2}$* | 1/8 | 19 | 23 |
| *Sp6$^{-/-}$;Sp8$^{CreERT2/CreERT2}$* | 1/16 | 10 | 9 |
| **Total** | | | 153 |

### 4.7.1 Molecular characterization of *Sp6$^{-/-}$;Sp8$^{CreERT2/CreERT2}$* double mutant AER

Since genetic removal of either Wnt/ß-catenin or AER-Fgfs resulted in amelic phenotypes (Barrow *et al*., 2003; Soshnikova *et al*., 2003; Sun *et al*., 2002; Boulet *et al*., 2004) identical to *Sp6$^{-/-}$;Sp8$^{CreERT2/CreERT2}$* or *Sp6$^{+/-}$;Sp8$^{CreERT2/CreERT2}$* and also because *Sp6* and *Sp8* have been suggested to be involved in the Wnt/ß-catenin induction of *Fgf8* in the limb ectoderm (Kawakami *et al*., 2004; Sahara *et al*., 2007; Talamillo *et al*., 2010; Lin *et al.,* 2013), it seems reasonable to assume that the amelic phenotype of double mutants may rely on a failure to induce *Fgf8* expression in the limb ectoderm (Sun *et al.,* 2002; Boulet *et al.,* 2004). Therefore we examined embryonic limbs at the stages when the limb bud initiates and the AER is formed. In the control limb buds, *Fgf8* is first detected in the ventral limb ectoderm at E9.5 and become progressively confined to the distal AER as it matures (Martin, 1998; Loomis; *et al.*, 1998; Bell *et al.*, 1998). *Bmp4* follows the same dynamics to that of *Fgf8*, with the difference that *Bmp4* is also expressed in the limb mesoderm prior to and during limb bud development (Ahn *et al.,* 2001; Selever *et al.,* 2004).

Induction of *Fgf8* expression has been reported to occur normally in mice lacking *Sp6*, however these limbs exhibited an expanded domain of *Fgf8* expression along the DV axis of the limb that developed into a double ridge phenotype in both hindlimbs and forelimbs (Talamillo *et al.*, 2010). In absence of *Sp8*, *Fgf8* and *Bmp4* are correctly induced but are lost at E10.5 when the AER prematurely regresses (Bell *et al.,* 2003; Treichel *et al.,* 2003). Therefore, we analyzed their expression at E9.5 (22-26 somites) and found that *Sp6$^{-/-}$;Sp8$^{CreERT2/CreERT2}$* and *Sp6$^{+/-}$;Sp8$^{CreERT2/CreERT2}$* compound mutants failed to express *Fgf8* in the limb ectoderm. Because both genotypes always showed the same expression patterns for all the genes analyzed in all the stages, in the figures only the results of the *Sp6$^{-/-}$;Sp8$^{CreERT2/CreERT2}$* mutant are shown.

Expression of *Fgf8* was never detected from E9.5 to E11.5 in forelimbs of both *Sp6$^{-/-}$;Sp8$^{CreERT2/CreERT2}$* and *Sp6$^{+/-}$;Sp8$^{CreERT2/CreERT2}$* mutants (Fig. 29A, B, G, H, M, N), indicating that *Sp6* and *Sp8* are required for the induction of *Fgf8* in the limb

ectoderm. In contrast, *Bmp4* expression was found to be normal in both the limb ectoderm and limb mesoderm at E9.5 (Fig. 29D). In addition, expression of *Msx2* a bonafide target of Bmp signalling, confirmed the presence of Bmp signalling in the limb ectoderm at E9.5 (Fig. 29F). From E10.5 on, *Bmp4* and *Msx2* were not detected in the limb ectoderm confirming the absence of Bmp signaling in the limb ectoderm, while both were detected in the limb mesoderm (Fig. 29L,J). At E11.5 when the limb practically regressed, *Bmp4* expression was detected in the limb bud mesoderm but not in the ectoderm (Fig. 29O).

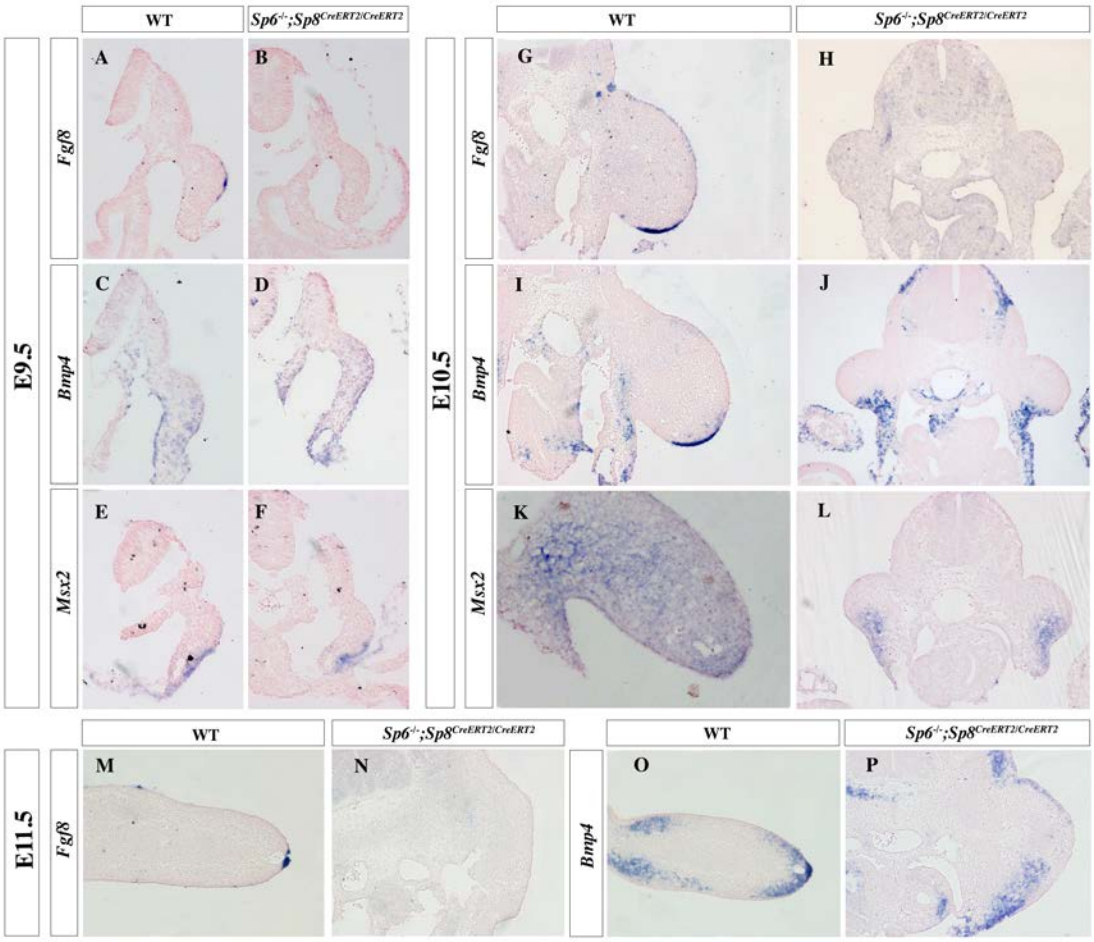


**Figure 29. Gene expression analysis in *Sp6*$^{-/-}$*;Sp8*$^{CreERT2/CreERT2}$ double mutant AER.** In situ hybridization in transverse section of control (A,C,E,G,I,K,M,O) and *Sp6*$^{-/-}$*;Sp8*$^{CreERT2/CreERT2}$ double mutant (B,D,F,H,J,L,N,P) forelimbs at the stages indicated. *Fgf8* expression was not detected in mutant limb ectoderm at any of the stages analyzed (B,H,N), while *Bmp4* was detected in the limb ectoderm and mesoderm at E9.5 (D) but was lost from the limb ectoderm at E10.5 (J) and E11.5 embryos (P). Expression of *Msx2*, a bonafide target of BMP signalling, was detected in E9.5 (F) and E10.5 (L) mutant limbs. Note that initial budding occurs in *Sp6*$^{-/-}$*;Sp8*$^{CreERT2/CreERT2}$ double mutant (B,D,F,H,J,L) and that the bud has practically regressed by E11.5 (O,P).

In sum, our results are consistent with *Sp6* and *Sp8* acting downstream of Wnt/ß-catenin in the limb ectoderm required for *Fgf8* induction. In addition, the fact that single disruption of either *Sp6* or *Sp8* leads to *Fgf8* induction in the limb ectoderm, while *Fgf8* is never detected in either double mutants or when only one functional allele of *Sp6* remains, demonstrated that both transcription factors are conjointly absolutely required and act in a redundant manner in the induction of *Fgf8*. However, in the absence of *Sp6* and *Sp8*, *Bmp4* is initially expressed in the limb ectoderm by E9.5, implying that neither *Sp6* nor *Sp8* are mediating the induction of *Bmp4* in the AER.

It is important to note that, disregarding the absence of *Fgf8* expression, both *Sp6*$^{-/-}$;*Sp8*$^{CreERT2/CreERT2}$ and *Sp6*$^{+/-}$;*Sp8*$^{CreERT2/CreERT2}$ mutants initiated limb bud development and formed a small bulge. These emergent limb buds regressed and became not visible between E10.5 and E11. The current view considers that *Fgf10* signalling from the limb mesoderm through its receptor *Fgfr2b* induces the expression of a Wnt ligand in the limb ectoderm, *Wnt3a* in chick and *Wnt3 i*n mouse, leading to Wnt/ß-catenin dependent induction of *Fgf8* in the precursor cells of the AER (Kengaku *et al.,* 1998; Barrow *et al.,* 2003; Soshnikova *et al.,* 2003). In turns, *Fgf8* signalling from the ectoderm is then required to maintain *Fgf10* expression in the limb mesoderm, establishing a positive regulatory feedback loop between *Fgf8* expressed in the ectoderm and *Fgf10* in the mesoderm that is absolutely required for PD outgrowth and patterning of the limb (Kawakami *et al*., 2001). Therefore, we decided to analyze the expression of *Fgf10* in the limb mesoderm of *Sp6*$^{-/-}$;*Sp8*$^{CreERT2/CreERT2}$ mutants.

Accordingly, in *Sp6*$^{-/-}$;*Sp8*$^{CreERT2/CreERT2}$ double mutant limb buds *Fgf10* expression in the limb mesenchyme was normally detected at E9.5 in comparison to control embryos (Fig. 30A,B). However, at E10.5 *Fgf10* expression was not maintained in the limb mesoderm (Fig. 30D). Thus, lack of *Sp6* and *Sp8* resulted in absence of *Fgf8* induction in the AER leading to the failure in *Fgf10* maintenance in the limb mesenchyme.

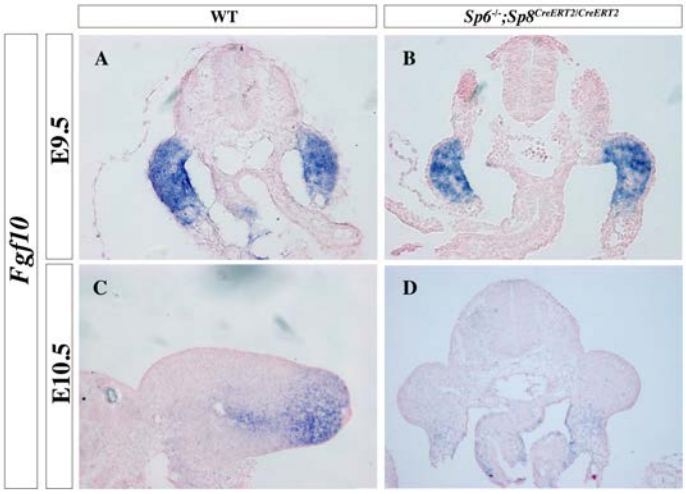


**Figure 30. Lack of *Sp6* and *Sp8* resulted in loss of *Fgf10* maintenance in the limb mesoderm.** In situ hybridization in transverse sections of control (A,C) and *Sp6*$^{-/-}$;*Sp8*$^{CreERT2/CreERT2}$ mutant (B,D) forelimb buds at the stages indicated. *Fgf10* expression was detected at E9.5 (C) in mutant embryos, but was not maintained by E10.5 (D).

Briefly, our results are consistent with Sp6/8 acting as mediators of the Wnt/β-catenin dependent induction of *Fgf8*. We have demonstrated that *Sp6* and *Sp8* are absolutely required and act in a redundant manner in the induction of *Fgf8* in the limb ectoderm. In addition, our results fits with the existence of a regulatory loop between *Fgf10* in the mesoderm and *Fgf8* in the limb ectoderm that predicts that the failure of *Fgf8* induction in the limb ectoderm will result in the downregulation of *Fgf10* expression in the limb mesoderm leading to an amelic phenotype, as occurred in *Sp6*$^{-/-}$;*Sp8*$^{CreERT2/CreERT2}$ and *Sp6*$^{+/-}$;*Sp8*$^{CreERT2/CreERT2}$. Finally, we have also demonstrated that initial *Bmp4* and *Msx2* expression are detected in absence of *Sp6* and *Sp8* as occurs with several AER markers in the double *Fgf8/4* (Sun *et al*., 2002). In contrast, these AER markers are not expressed in mice in which Wnt/β-catenin has been disrupted (Barrow *et al.,* 2003; Soshnikova *et al.,* 2003). Therefore, we provide further evidence supporting that there is not a simple linear relationship between Wnt/β-catenin in the limb ectoderm and *Fgf8* in the AER.

### 4.7.2 Cell death in the developing limb bud in absence of *Sp6* and *Sp8*

At E9.5 an initial budding was evident in *Sp6*$^{-/-}$;*Sp8*$^{CreERT2/CreERT2}$ mutant embryos but later on this budding regressed resulting in an amelic phenotype as a consequence of a failure in *Fgf8* induction, reminiscent of that of *Limbless* chicken mutant. *Limbless* is characterized by the development of a limb bud that undergoes extensive apoptosis and regresses leading to an amelic phenotype, as a consequence of the inability to induce an AER (Fallon *et al*., 1983; Carrington and Fallon, 1988). Moreover, surgical removal of the AER in chick, leads to increased cell death of the distal mesoderm (Rowe *et al*., 1982; Dudley *et al*., 2002) while genetic attenuation of Fgf signalling from the AER results in proximal cell death both in the mesoderm and ectoderm that account for the smaller size and regression of the limb buds under those circumstances (Sun *et al*., 2002; Boulet *et al*., 2004). With the aim to determine the cell death repercussion due to the removal of *Sp6* and *Sp8*, we analyzed cell death by TUNEL assay in *Sp6*$^{-/-}$;*Sp8*$^{CreERT2/CreERT2}$ double mutant limb buds.

At E9.5 no cell death was detected neither in the control embryo nor in the double mutant forelimbs. However, by E10.5 the entire limb bud undergoes massive apoptosis in the *Sp6*$^{-/-}$;*Sp8*$^{CreERT2/CreERT2}$ double mutant, while in comparison yo wild type animals (Fig. 31A,B). Apoptotic cells were detected in both ectodermal and mesodermal compartment. Cell death was extended all over the mesodermal compartment of the limb bud, while in the ectodermal compartment apoptotic cells were more prominent in the proximo-dorsal and in the distal-ventral ectoderm.

Our results demonstrated that in the absence of both *Sp6* and *Sp8* the limb bud undergoes extensive apoptosis. The massive cell death in *Sp6*$^{-/-}$;*Sp8*$^{CreERT2/CreERT2}$ double mutant limb buds, can account for the regression of the limb bud leading to the amelic phenotype as reported for the chicken mutant limbless (Fallon *et al*., 1983; Carrington and Fallon, 1988). According to this, *Sp6* and *Sp8* are required to ensure the integrity of the limb bud, in order to avoid cell death in the developing limb.

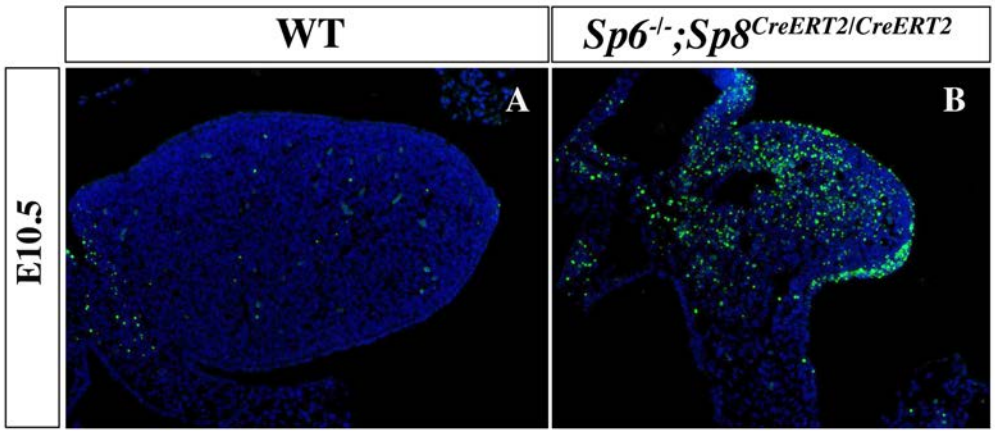


**Figure 31. Cell death repercussion in *Sp6*$^{-/-}$;*Sp8*$^{CreERT2/CreERT2}$ mutant limb buds.** Transverse sections of control (A) and *Sp6*$^{-/-}$;*Sp8*$^{CreERT2/CreERT2}$ (B) mutant forelimb buds at E10.5. On each panel, the nucleus is counter stained with DAPI (Blue) and apoptotic cells (Green) are shown. No cell death was detected in control embryo (A). Extensive apoptosis was detected in both the ectoderm and the mesoderm of double mutant limb buds (B).

### 4.7.3 Morphological characterization of *Sp6*$^{-/-}$;*Sp8*$^{CreERT2/CreERT2}$ double mutant AER

Conditional removal of *Fgf8* and *Fgf4* from the AER stunts limb development due to the absence of Fgf signalling from the AER, while a morphological AER is still formed (Sun *et al*., 2002; Boulet *et al*., 2004). However, disruption of Wnt/β-catenin signalling in the limb ectoderm resulted in absence of a morphologycal AER, implying that the relation between Wnt/β-catenin and Fgf in the limb ectoderm is not linear (Sun *et al*., 2002; Barrow *et al.,* 2003; Soshnikova *et al.,* 2003). Therefore, we analyzed in more detail the thickening present in the ventral limb ectoderm of *Sp6*$^{-/-}$;*Sp8*$^{CreERT2/CreERT2}$ double mutants, evident in TUNEL assays due to the massive cell death in this area.

In mice, at E10.5 morphogenetic movements confined the AER cells induced in the ventral limb ectoderm to the distal tip of the limb bud at the DV interface and adopts a polystratified organization (Meyer *et al.,* 1997; Bell *et al.,* 1998) (Fig. 32 A,B). In transverse semithin sections of *Sp6*$^{-/-}$;*Sp8*$^{CreERT2/CreERT2}$ mutant forelimbs at E10.5 a thickening was detected in the ventral limb ectoderm of *Sp6*$^{-/-}$;*Sp8*$^{CreERT2/CreERT2}$ double mutants with the appearence of an inmature AER, sometimes protruding into the mesoderm (Fig. 32C,D).

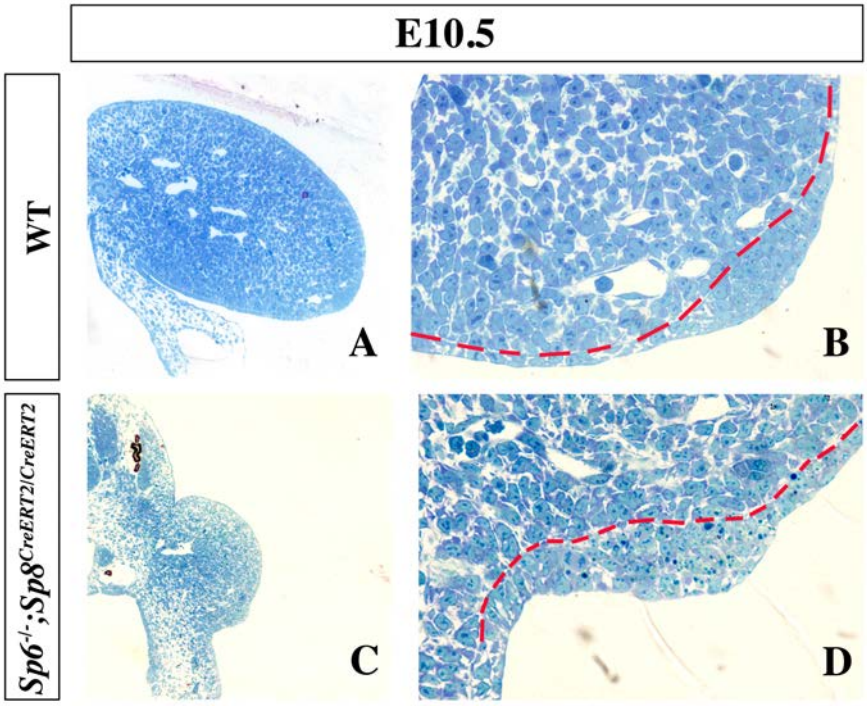


**Figure 32. AER morphology of *Sp6*$^{-/-}$;*Sp8*$^{CreERT2/CreERT2}$ double mutants limb buds.** Semithin sections of control (A,B) and mutant(C,D) forelimb buds at E10.5. (A) Control E10.5 limb and (B) higher magnification of A. (C) Mutant limb bud and (D) higher magnification of C, where a slight thickening in the ventral ectoderm is appreciable. Note that basement membrane is marked with a red dashed line in B and D.

To analyze in more detail the thickening present in the ventral limb ectoderm of *Sp6*$^{-/-}$;*Sp8*$^{CreERT2/CreERT2}$ mutants limb buds, we decided to analyze the presence of ectodermal markers by immunhistochemistry. The analysis of laminin, marker of the basement membrane, and E-cadherin (Cdh1), a transmembrane protein specific of ectodermal cells (Fig. 33A), led us to verified the contribution of ectodermal cells to the thickening present in the ventral ectoderm of *Sp6*$^{-/-}$;*Sp8*$^{CreERT2/CreERT2}$ mutant limb buds.

At E10.5 Cdh1 was specifically detected in the forelimb ectoderm of control embryos and in the AER, while laminin was detected in the basement membrane immediately under the ectoderm (Fig. 33A). In *Sp6*$^{-/-}$;*Sp8*$^{CreERT2/CreERT2}$ double mutant limb buds Cdh1 was detected in the limb ectoderm and also in the ventral ectodermal thickening. In addition, laminin was detected below the limb ectoderm and also below the ventral thickening implying that the ventral ectodermal thickening was of ectodermal origin (Fig 33B).

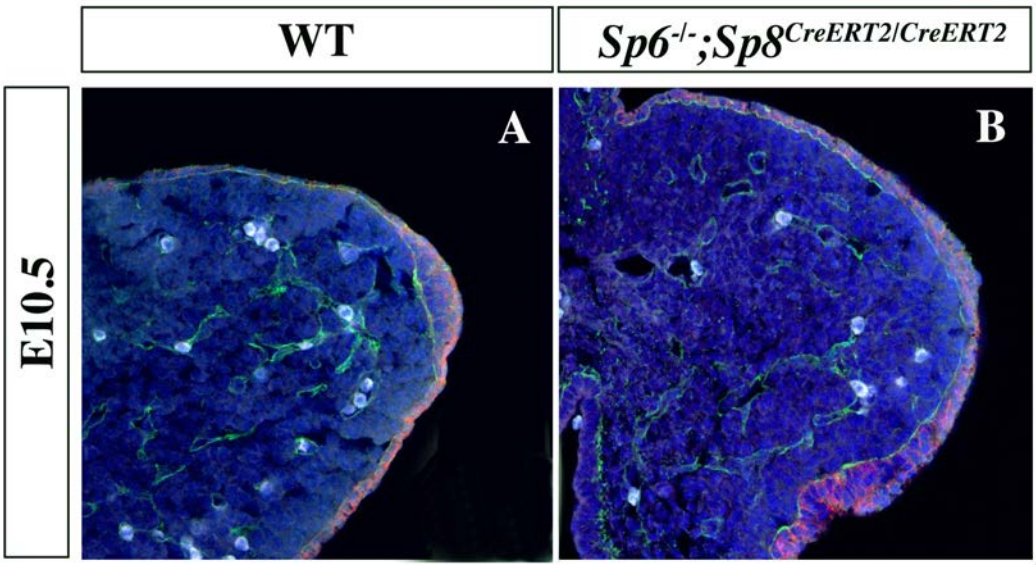


**Figure 33. Ectodermal cells contribute to the ventral thickening present in *Sp6*$^{-/-}$*;Sp8*$^{CreERT2/CreERT2}$ double mutant limb buds.** Immunolabeling of E10.5 control (A) and *Sp6*$^{-/-}$*;Sp8*$^{CreERT2/CreERT2}$ double mutant (B) forelimb buds. Laminin-b was detected below the limb ectoderm of control embryos, positive for E-cadherin. Contribution of ectodermal cells to the ventral limb thickening was confirmed due to presence of Cdh1 in the ventral thickening and also because this thickening was above the basement membrane as assess by laminin immunostaining. Nucleus are counter stained with DAPI (Blue), Laminin-b (laminin;Green), and E-cadherin (Cdh1; Red).

In sum, the presence of ectodermal markers in the ventral thickening present in *Sp6*$^{-/-}$*;Sp8*$^{CreERT2/CreERT2}$ mutant limb buds demonstrated that ectodermal cells are accumulated in the ventral limb ectoderm. Thus, in the absence of both *Sp6* and *Sp8* AER morphogenesis is initiated, but the process is arrested and cells are not pulled to the distal tip of the limb and get accumulated in the ventral limb ectoderm.

### 4.7.4 Dorso-Ventral pattern establishment in *Sp6*$^{-/-}$*;Sp8*$^{CreERT2/CreERT2}$ mutant limb buds

Lack of *Fgf8* expression and subsequent absence of AER development in the chick mutant *limbless* has been reported to occur associated to a failure in DV pattern establishment due to the absence of *En1* expression in the ventral limb ectoderm and ectopic expression of *Wnt7a* in the ventral ectoderm (Ros *et al.*, 1996; Grieshammer *et al.*, 1996; Noramly *et al.*, 1996). Moreover, the ventrally

extended AER developed in *En1* mutant mice suggested it requirement for proper positioning of the AER in the limb DV boundary (Cygan *et al*., 1997; Loomis *et al*., 1996; Loomis *et al*., 1998). Additionally, mice lacking *ß-catenin* exhibited a double-dorsal limb phenotype due to lack of *En1* expression in the ventral ectoderm and ectopic *Wnt7a* expression (Soshnikova *et al*., 2003). Therefore, once determined that both *Sp6* and *Sp8* are absolutely required for *Fgf8* induction in the limb ectoderm together with morphological analysis that confirmed that ventral ectodermal cells of double $Sp6^{-/-};Sp8^{CreERT2/CreERT2}$ mutants initiated AER morphogenesis, but are not pulled to the distal tip and get accumulated in the ventral ectoderm, we proceeded to analyze DV pattern establishment in the absence of both *Sp6* and *Sp8,* through the analysis of the expression of the DV markers *En1* and *Wnt7a* (Riddle *et al*., 1995; Parr and McMahon, 1995; Loomis *et al*., 1996; Cygan *et al*., 1997; Loomis *et al*., 1998; Ahn *et al*., 2001).

Previous analysis of *Sp6* and *Sp8* single mutants revealed that DV pattern establishment was correctly initiated in both mutant limbs (Talamillo *et al.,* 2010; Bell *et al.,* 2003; Treichel *et al.,* 2003). Limbs in which *Sp6* was disrupted *Lmx1b* expression remained restricted to dorsal mesoderm but by E14.5 occasional patches of expression were detected in the ventral distal mesoderm of either digit 3, 4 or 5, without ectopic expression of *Wnt7a*. Authors argued that double dorsal digit developed in central digits of *Sp6* mutants were independent of *Lmx1b* expression in the ventral mesoderm, because *Lmx1b* ectopic expression was detect also in digit 5, but this digit did not exhibited a bidorsal phenotype (Talamillo *et al.,* 2010). In contrast, in mouse lacking *Sp8* DV patterning is correctly initiated at E9.5 as assessed by *En1* and *Lmx1b* expression, in the ventral ectoderm and the dorsal mesoderm, respectively. However, by E10.5 when limb development stunted, *En1* expression was lost (Bell *et al.,* 2003; Treichel *et al.,* 2003).

The analysis of the expression of DV markers in double mutant forelimbs was performed from E9.5 to E11.5 (Fig. 34). In control embryos, *Wnt7a* is first detected in the dorsal limb ectoderm at E9.5 (Fig. 34A) and at E10.5 it is expressed all over the dorsal ectoderm up to the dorsal boundary of the AER

(Fig. 34E). *En1* expression is first detected at E9.5 in the ventral limb ectoderm (Fig. 34C) and at E10.5 it is expressed all over the ventral ectoderm including the ventral half of the AER (Fig. 34G).

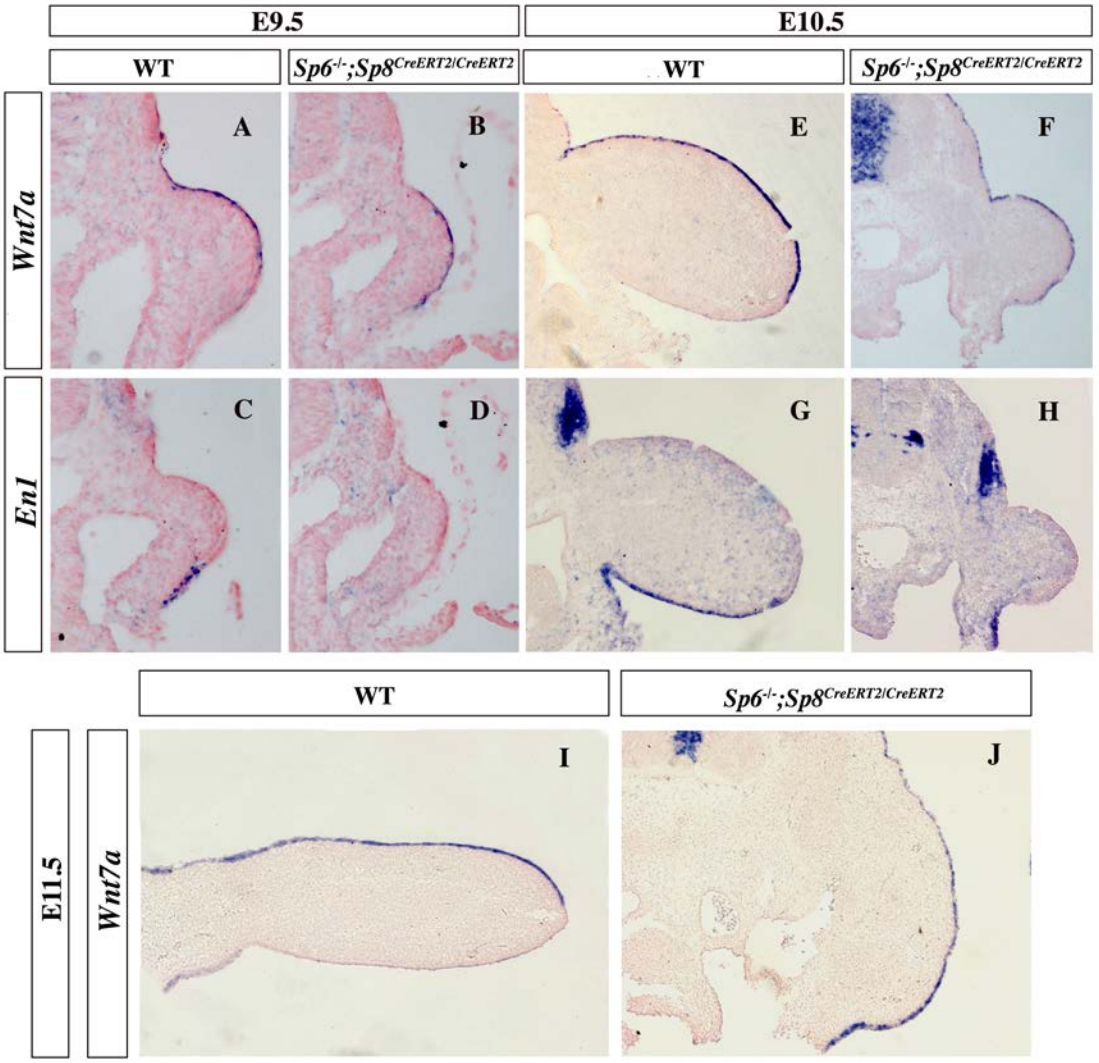


**Figure 34. Analysis of DV markers in *Sp6$^{-/-}$;Sp8$^{CreERT2/CreERT2}$* double mutants forelimb buds.** In situ hybridization for the DV markers *Wnt7a* (A,B,E,F,I,J) and *En1* (C,D,G,H) in transverse section of control (A,C,E,G,I) and *Sp6$^{-/-}$;Sp8$^{CreERT2/CreERT2}$* double mutant (B,D,F,H,J) forelimbs at the stages indicated. *En1* expression was not detected in the ventral ectoderm (D,H) and *Wnt7a* expression was extended into the ventral ectoderm of *Sp6$^{-/-}$;Sp8$^{CreERT2/CreERT2}$* from E9.5 to E11.5 (B,F,J).

The analysis of the DV markers *Wnt7a* and *En1* in double *Sp6$^{-/-}$;Sp8$^{CreERT2/CreERT2}$* mutant forelimbs revealed the absence of DV pattern establishment with limb buds exhibiting a double dorsal phenotype. *Wnt7a* expression was initially extended into the ventral limb ectoderm at E9.5 (Fig.

34B) and its expression persisted over the dorsal and ventral ectoderm of mutant limb buds at E10.5 and E11.5 (Fig. 34,F,J), while *En1* was never detected in the limb ventral ectoderm neither at E9.5 nor E10.5 (Fig, 34D,H), but it was detected in the flank ectoderm ventral to the limb bud by E10.5 (Fig. 34H).

Our results demonstrated that DV pattern is not established in the absence of *Sp6* and *Sp8. En1* expression is not detected in the ventral limb ectoderm and *Wnt7a* expression is detected extending all over the limb ventral ectoderm, leading to the development of double dorsal limb buds. In addition, besides normal expression of *Bmp4,* in both the ectoderm and the mesoderm of *Sp6*$^{-/-}$*;Sp8*$^{CreERT2/CreERT2}$ mutant limb buds, *En1* is not expressed in the absence of *Sp6* and *Sp8*, implying their requirement for proper ventral limb pattern establishment.

## 4.8 Molecular characterization of *Sp6*$^{-/-}$*;Sp8*$^{+/CreERT2}$ mutant limb buds

### 4.8.1 Gene expression analysis of the *Sp6*$^{-/-}$*;Sp8*$^{+/CreERT2}$ mutant AER

The ectrodactylous limb phenotype of the *Sp6*$^{-/-}$*;Sp8*$^{+/CreERT2}$ mutant resembles the human malformation SHFM that is characterized by the absence of central digits and fusion of the remaining ones as a possible consequence of a failure in the maintenance of the medial region of the AER that lacks *Fgf8* expression (Temtamy and McKusick 1978; Sifakis *et al*., 2001). Therefore, we checked for *Fgf8* expression in *Sp6*$^{-/-}$*;Sp8*$^{+/CreERT2}$ mutant limbs to determine if the failure in *Fgf8* expression in the central region of the AER could account for the limb phenotype of *Sp6*$^{-/-}$*;Sp8*$^{+/CreERT2}$ mutants.

In *Sp6*$^{-/-}$*;Sp8*$^{+/CreERT2}$ mutant limbs, *Fgf8* expression was detected at E9.5 in the limb ectoderm in a more restricted manner in comparison to control limbs (Fig. 35A,B). At E10.5, *Fgf8* expression was confined to the distal tip of the limb in control embryos (Fig. 35E,I,J). However, consecutive transverse sections throughout *Sp6*$^{-/-}$*;Sp8*$^{+/CreERT2}$ mutant limbs revealed an irregular *Fgf8* expression along the limb AP axis (Fig. 35F,F´) that was further confirmed by whole mount in situ hybridization. Discontinuous *Fgf8* expression was detected in the AER

together with a patchy pattern of *Fgf8* expression in the ventral limb ectoderm of *Sp6$^{-/-}$;Sp8$^{+/CreERT2}$* mutants, that corresponded to an inmature AER (Fig. 35K,L). *Bmp4* expression in the AER followed the same dynamics and showed the same irregular expression patterns of *Fgf8* at E9.5 and E10.5 in *Sp6$^{-/-}$;Sp8$^{+/CreERT2}$* mutant limbs, as demonstrated in transverse sections (Fig. 35D, H, H´) and whole mount in situ hybridization (Fig. 35M,N).

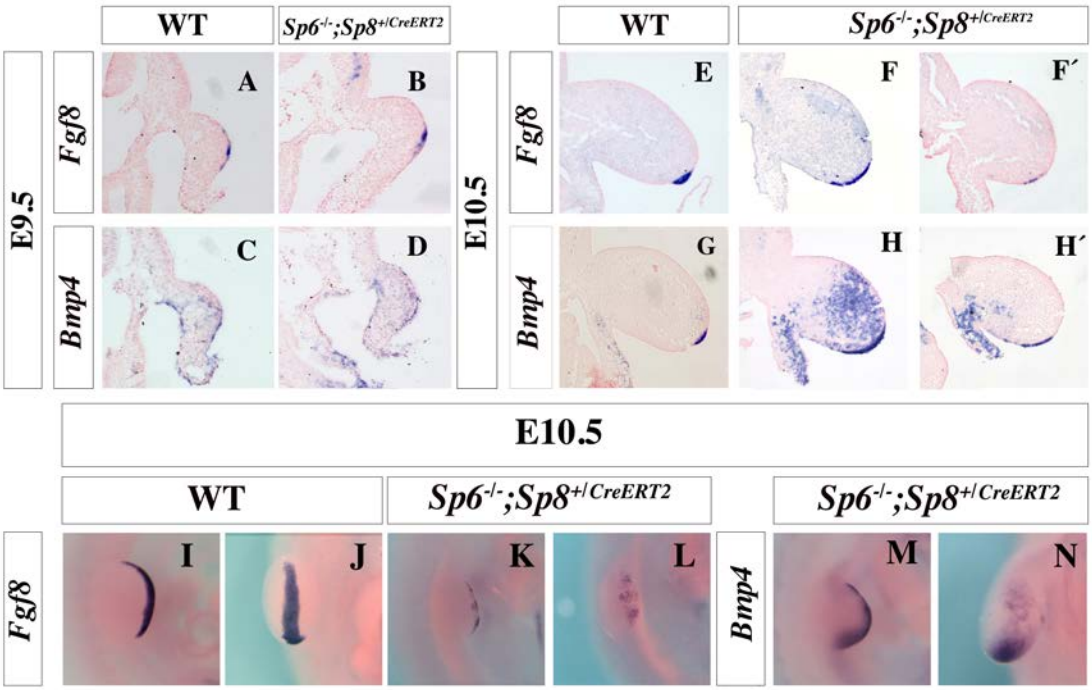


**Figure 35 Gene expression analysis throughout *Sp6$^{-/-}$;Sp8$^{+/CreERT2}$* mutant AER.** *Fgf8* (A,B,E,F,FF´) and *Bmp4* (C,D,G,H,H´) expression in transverse sections of control (A,C,E,G) and *Sp6$^{-/-}$;Sp8$^{+/CreERT2}$* (B,D,F,F´,H,H´) mutant forelimbs buds at the stage indicated and dorsal (I,K,M) and distal views (J,L,N) of control (J,K) and *Sp6$^{-/-}$;Sp8$^{+/CreERT2}$* mutant (K,L,M,N) E10.5 forelimbs hybridized for *Fgf8* (I,J,K,L) and *Bmp4* (M,N). *Fgf8* expression showed irregular activation of AER cells in *Sp6$^{-/-}$;Sp8$^{+/CreERT2}$* mutant ventral forelimb ectoderm. By E10.5 the AER remained flat displaying gaps of *Fgf8* (F,F´,K.L) and *Bmp4* (H,H´,M,N) expression as shown in transverse sections (F,F´,H,H´) and whole mount in situ hybridization (K,L,M,N) of E10.5 forelimb buds. Note that F,F´and H,H´are consecutive section of the same limb.

In order to confirm the presence of an immature AER in *Sp6$^{-/-}$;Sp8$^{+/CreERT}$* mutants, we decided to perform a double Laminin;Cdh1 immunolabeling in *Sp6$^{-/-}$;Sp8$^{+/CreERT}$* mutants limbs buds at E10.5. In wild type animals, laminin was expressed in the basement membrane below the ectoderm, while in the ectoderm Cdh1 was specifically expressed in the limb ectoderm (Fig. 36 A,B). As

shown in *Sp6*$^{-/-}$;*Sp8*$^{+/CreERT}$ mutant limb sections, the AER was not confined to the DV boundary of the limb and did not exhibited the polystratified organization appreciable in control embryos. The ventral ectoderm was slightly thicker than the dorsal ectoderm as shown by laminin and Cdh1 immunolabeling (Fig. 36A,B), consistent with ventrally expanded expression of *Fgf8* and *Bmp4* in the limb ectoderm of *Sp6*$^{-/-}$;*Sp8*$^{+/CreERT}$ mutant. Therefore, we confirmed the presence of a slightly thicker ventral than dorsal ectoderm that corresponded to an inmature AER morphology .

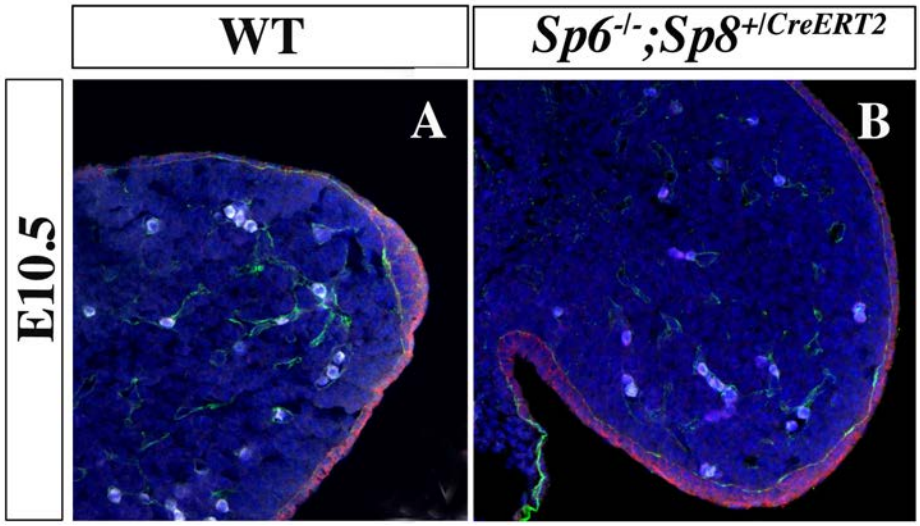


**Figure 36. *Sp6*$^{-/-}$;*Sp8*$^{+/CreERT2}$ mutant limb bud.** Transverse limb buds sections counter stained with DAPI (Blue) showing inmunostaining for Laminin (Green) and E-cadherin (Cdh1) (Red) within control (A) and *Sp6*$^{-/-}$;*Sp8*$^{+/CreERT}$ (B) mutant limb buds. *Sp6*$^{-/-}$;*Sp8*$^{+/CreERT2}$ mutants displayed an immature and flatten AER.

From these results we conclude that a single functional allele of *Sp8* in the absence of *Sp6* is not sufficient to achieve normal AER morphology and leads to irregular activation of *Fgf8.* As the limb develops the irregular activation of *Fgf8* results in gaps of *Fgf8* expression along the AP length of the AER that could account for the absence of central digits.

### 4.8.2 *Sp6* and *Sp8* and the Tp63 network leading to SHFM

In humans, six different loci have been associated to SHFM. This syndrome is characterized by absence of central digits and fusion of the remaining ones, possibly due to a failure in the maintenance of the medial region of the AER that lacks *Fgf8* expression (Temtamy and McKusick 1978; Sifakis *et al*., 2001). The similar limb phenotype between the distinct forms of SHFM underlies the possible existence of a regulatory cascade involving the disease genes. *Dlx5*/*Dlx6* and *Tp63* are the only genes that have been unequivocally shown to be involved in SHFM type I and SHFM type IV, respectively (Mills *et al*., 1999; Yang *et al*., 1999; Robledo *et al.,* 2002; Merlo *et al*., 2002). It has been demonstrated that both phenotypes arise due to the disruption of the same regulatory cascade, in which *Tp63* acts upstream of the *Dlx* genes for proper expression of *Fgf8* in the AER (Lo Iacono *et al*., 2008).

Since the limb phenotype of $Sp6^{-/-};Sp8^{+/CreERT}$ mutants is similar to the human SHFM, we proceed to analyze the expression of *Tp63* and *Dlx5/6* in $Sp6^{-/-};Sp8^{+/CreERT}$ and $Sp6^{-/-};Sp8^{CreERT/CreERT}$ mutant limbs, in order to determine if the Sp transcription factors were components of the *Tp63* network leading to SHFM .

*Tp63* is a key regulator of epidermis morphogenesis and it is expressed in the epithelial surface of the embryo, including the limb ectoderm. Later on, at E10.5, it is highly expressed within the AER (Yang *et al*., 1999; Mills *et al*., 1999). At E10.5, *Tp63* expression was detected in the entire ectoderm and the AER of control embryos (Fig. 37A), while *Dlx5* expression, a direct target of *Tp63* (Lo Iacono *et al*., 2008), was restricted to the AER and *Dlx6* (not shown) (Fig. 37D). *Tp63* expression was detected in the entire limb ectoderm of both $Sp6^{-/-};Sp8^{+/CreERT}$ (Fig. 37B) and $Sp6^{-/-};Sp8^{CreERT2/CreERT}$ mutant limb buds (Fig. 37C,C´), while a slight downregulation of *Dlx5* expression was appreciable in the inmature and flatten AER of $Sp6^{-/-};Sp8^{+/CreERT}$ (Fig. 36E) and also in $Sp6^{-/-};Sp8^{CreERT2/CreERT}$ mutant limb buds (Fig. 37F,F) .

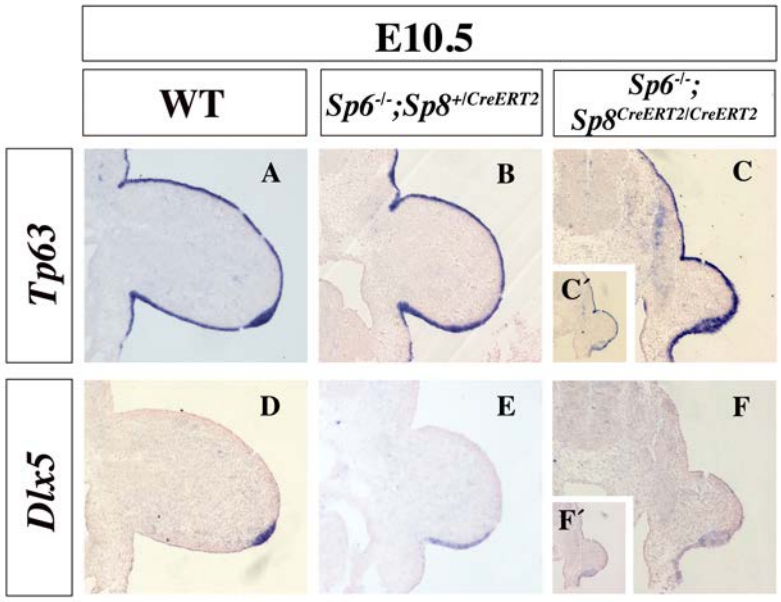


**Figure 37. Analysis of the expression of *Tp63* and *Dlx5* in *Sp6$^{-/-}$;Sp8$^{-/CreERT2}$* and *Sp6$^{-/-}$;Sp8$^{CreERT2/CreERT2}$* mutant forelimb buds.** Transverse limb sections showing the expression of *Tp63* (A,B,C,C´) and *Dlx5* (D,E,F,F´) genes in control (A,D), *Sp6$^{-/-}$;Sp8$^{+/CreERT2}$* (B,E) and *Sp6$^{-/-}$;Sp8$^{CreERT2/CreERT2}$* (C,C´,F,´F´) mutant limb buds at E10.5. *Tp63* was detected in both *Sp6$^{-/-}$;Sp8$^{CreERT2/CreERT2}$* (B) and *Sp6$^{-/-}$;Sp8$^{+/CreERT2}$* (C,C´) mutants while *Dlx5* (E, F; F´) was slightly downregulated in both mutants.

The expression of *Tp63* and the *Dlx* genes in *Sp6$^{-/-}$;Sp8$^{+/CreERT}$* mutant limb buds lead us to demonstrate that if the Sp transcription factors are components of the Tp63 network they act downstream of the *Dlx* genes.

### 4.8.3. Dorso-Ventral pattern establishment in *Sp6$^{-/-}$;Sp8$^{+/CreERT2}$* mutant limb buds

*Sp6$^{-/-}$;Sp8$^{+/CreERT2}$* newborns displayed double dorsal digit tips. As we have demonstrated in absence of both *Sp6* and *Sp8* or when a single functional allele of *Sp6* remains in absence of *Sp8* DV pattern is not established. In addition, as absence of *En1* has been related to AER maturation defects (Loomis *et al*., 1996; Cygan *et al*., 1997; Loomis *et al*., 1998), we proceed to analyze DV pattern establishment in *Sp6$^{-/-}$;Sp8$^{+/CreERT}$* mutant limb buds, looking for the expression of *Wnt7a* and *En1*.

At E10.5, *Wnt7a* expression is restricted to the dorsal limb ectoderm and reaches the dorsal AER border in control embryos (Fig. 38A). In *Sp6*$^{-/-}$;*Sp8*$^{+/CreERT}$ mutant limb buds, *Wnt7a* expression was extremely variable even within a single limb. Expression of *Wnt7a* at a variable ventral extent within a same limb was appreciated as shown by consecutive transverse limb section of E10.5 *Sp6*$^{-/-}$;*Sp8*$^{+/CreERT}$ mutants (Fig. 38B,B´). Consistent with this, *En1* appeared downregulated in the ventral limb ectoderm of *Sp6*$^{-/-}$;*Sp8*$^{+/CreERT}$ mutants, in comparison to wild type animals (Fig. 38C,D,D´). Interestingly, *En1* downregulation exhibited a clear correlation with the variable ventral ectopic expression of *Wnt7a*, correlation easily appreciated when consecutive limb section were hybridized for *Wnt7a* and *En1* (Fig. 38B, B´,D,D´).

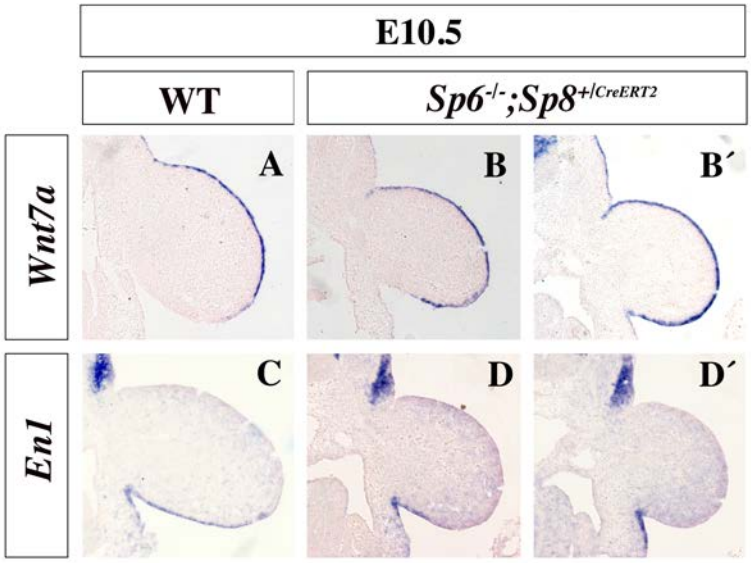


**Figure 38. Analysis of DV markers expression in *Sp6*$^{-/-}$;*Sp8*$^{+/CreERT2}$ mutant forelimb buds.** Expression of *Wnt7a* (A,B,B´) and *En1* (C,D,D´) in control (A,C) and mutant (B,B´,D,D´) forelimb transverse sections at E10.5. DV establishment was disrupted in *Sp6*$^{-/-}$;*Sp8*$^{+/CreERT2}$ mutant embryos. *Wnt7a* expression was extended into the ventral limb ectoderm (B,B´) in correlation to *En1* expression downregulation (D,D´), appreciable in limb consecutive sections bud (B,B´,D,D´).

In sum, our results demonstrate that when only one functional allele of *Sp8* remains, in the absence of other *Sp* alleles (*Sp6* and *Sp8*), DV pattern establishment is disrupted. Besides normal expression of *Bmp4* irregular

activation of *En1* in the ventral limb ectoderm was detected, in strong correlation to ventral ectopic expression of *Wnt7a,* leading to the development of double dorsal limb buds that could account for the double dorsal digit tips developed in *Sp6*$^{-/-}$;*Sp8*$^{+/CreERT}$ mutant.

## 4.9 Temporally controlled deletion of genes specifically expressed in the limb bud ectoderm with the *Sp8*$^{CreERT2}$ line

Several Cre lines have been described for the conditional removal of genes expressed in the limb ectoderm. These include the *Msx2-Cre* (Lewandosky *et al.,* 2000), the *Brn4-Cre* (Ahn *et al.,* 2001), the *Ap2α-Cre* (Boulet *et al.,* 2004) and the *Mox2-Cre* (Delgado *et al.,* 2008) lines of which any of them is inducible. The *Sp8* null allele we have used in this work bears the inducible CreERT2 fusion protein that drives the expression of the Cre in the limb ectoderm under the *Sp8* locus. This line is characterized by a modification of the Cre that contains a G400V/M543A/L544A triple mutation in the Estrogen Receptor ligand-binding domain (ER-LBD) that makes it more sensitive to Tamoxifen (Tam) than the mutant ER LBD with a single G521R substitution. We decided to evaluate the activity of this line, using the *ROSA26* reporter strain (R26R; Soriano, 1999), as a possible ectodermal-specific inducible deleter line. With this purpose we analyzed *Rosa26*$^{+/tg}$;*Sp8*$^{+/CreERT2}$ embryos after administration of Tam.

Since it has been previously shown that Cre-mediated recombination is evident by 8h and complete by 12h after a single-dose tamoxifen intraperitoneal injection (Chen *et al.,* 2008), we decided to analyze LacZ expression in E9.5 embryos that had received a single dose of Tam at E8.5. As expected, our results showed that the Cre recombinase was active in the sites of *Sp8* expression replicating the pattern of expression described for *Sp8*. Maximum staining was observed in the neural tube, somites and trunk ectoderm. In particular, Cre activity was observed through the dorsal and ventral limb bud ectoderm although in a mosaic fashion (Fig. 39).

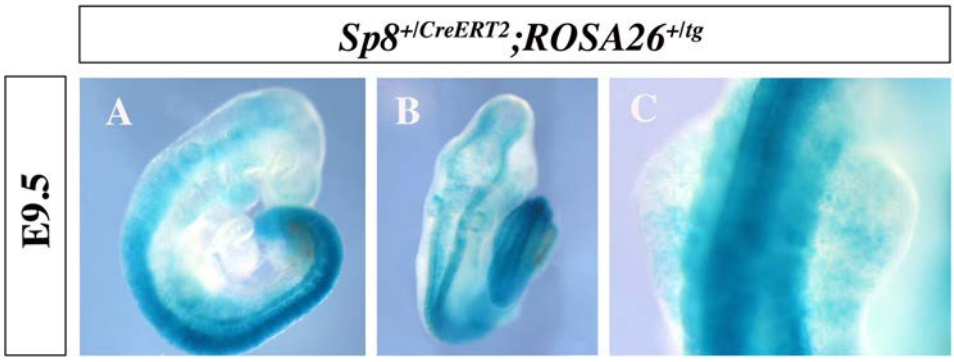


**Figure 39. Monitorization of the Cre activity under the *Sp8* locus.** Whole mount LacZ staining of *Sp8*$^{+/CreERT2}$;*ROSA26*$^{+/tg}$ E9.75 embryo. (A) Lateral view, (B) dorsal view and (C) forelimb buds. After tamoxifen administration the embryo showed strong LacZ expression in the neural tube, the somites, in the forelimb ectoderm and practically all the caudal region of the embryo including hindlimbs.

In sum, the CreERT2 in the *Sp8* locus drives Cre activity in both hindlimb and forelimb ectoderm early enough to remove genes from the limb ectoderm at early stages. However, gene deletion is not restricted to the limbs as shown by strong LacZ staining in the other domains of *Sp8* expression.

### 4.10 *β-catenin* Gain of function with the *Sp8*$^{CreERT2}$ line

*Sp6* expression in the limb ectoderm has been shown to be under the control of Wnt/β-catenin signalling (Talamilo *et al.,* 2010). However, this analysis has not been performed for *Sp8* although experiments in chick have suggested that it is also under Wnt/β-catenin control (Kawakami *et al*., 2004). Therefore, we decided to analyze the expression of *Sp8* in mutants with GOF of *β-catenin* with the help of the inducible *Sp8*$^{CreERT2}$ line we have just characterized.

For this experiment pregnant females from *Sp8*$^{+/CreERT2}$ and *Catn-b*$^{lox(ex3)}$ crosses were given Tam via intragastric gavage every 24h for 3 consecutive days from E7.5 to E9.5. This procedure was followed to make the recombination event occur in all cells and the embryos were recovered by cesarean section at E10.5.

*β-catenin* GOF mutants with the *Sp8*$^{CreERT2}$ line exhibited ectopic *Sp8* expression in both dorsal and ventral forelimb ectoderm as assessed by whole mount in situ hybridization of E10.5 *Catn-b*$^{+/lox(ex3)}$;*Sp8*$^{CreERT2/+}$ mutant embryos, confirming that in the mouse *Sp8* acts downstream of Wnt/β-catenin (Fig. 40 D, E). In addition, in correlation to *Sp8* expression, *Fgf8* was also found to be ectopically expressed in *Catn-b*$^{+/lox(ex3)}$;*Sp8*$^{CreERT2/+}$ mutant embryos (Fig. 40F ).

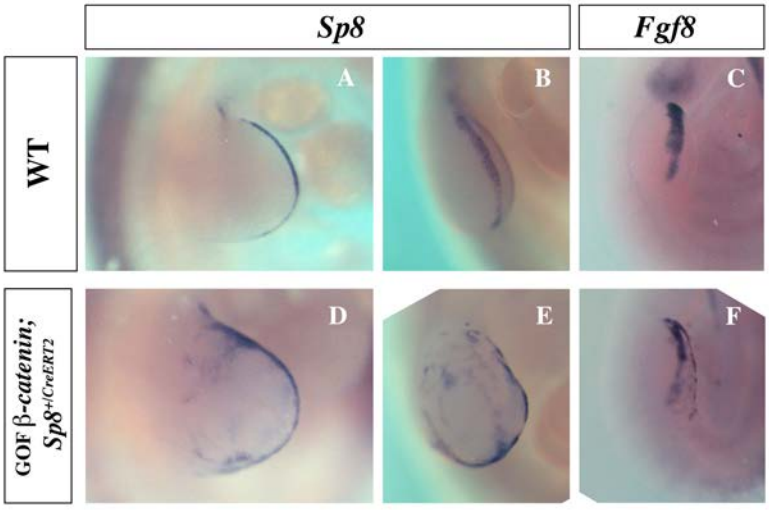


**Figure 40. Gain of function mutation of *β-catenin* with the *Sp8*$^{CreERT2}$ led to ectopic expression of *Sp8* and *Fgf8* in the limb ectoderm.** Whole mount in situ hybridization within control (A, B, C) and GOF β-*catenin;Sp8*$^{+/CreERT2}$ (D, E, F) mutant limb at E10.5 showing the ectopic expression of both *Sp8* (D, E) and *Fgf8* (F). Note that A and D are dorsal views of the limb while B,C,E and F are distal views of the limb bud.

To further analyze the *ß-catenin* GOF phenotype with the *Sp8*$^{CreERT2}$ line, we decided to perform transverse sections within mutant limb buds at E10.5 to analyze in more detail the ectopic expression of *Fgf8* and *Sp8*. In addition, we decided to check *Bmp4* and *En1* expression in *Catn-b*$^{+/lox(ex3)}$;*Sp8*$^{CreERT2/+}$ embryos, because it has been reported that Bmp signalling pathway lies downstream of Wnt signalling for DV pattern establishment in the limb ectoderm (Soshnikova *et al.*, 2003; Barrow *et al.,* 2003). By E10.5, *Fgf8* and *Bmp4* expression is confined to the distal tip of the developing limb of control embryos (Fig. 41A), while *Sp8* at this stage is predominantly expressed in the AER and in a less abundant manner in the ventral limb ectoderm (Bell *et al*., 2003; Treichel *et*

*al*., 2003). However, expression of *Fgf8* and *Bmp4* were ectopically detected in both ventral and dorsal limb ectoderm of E10.5 *Catn-b*$^{+/lox(ex3)}$;*Sp8*$^{CreERT2/+}$ limb transverse sections (Fig. 41B, E) as it was for *Sp8* (Fig. 41C). Nevertheless, *En1*, the most downstream effector for DV limb patterning downstream of the Bmp signalling pathway that it is expressed in the ventral limb ectoderm and the ventral half of the AER at E10.5 (Fig. 41 F), was completely downregulated and was only detected in the most proximo-ventral ectoderm of *Catn-b*$^{+/lox(ex3)}$;*Sp8*$^{CreERT2/+}$ limb buds (Fig. 41G).

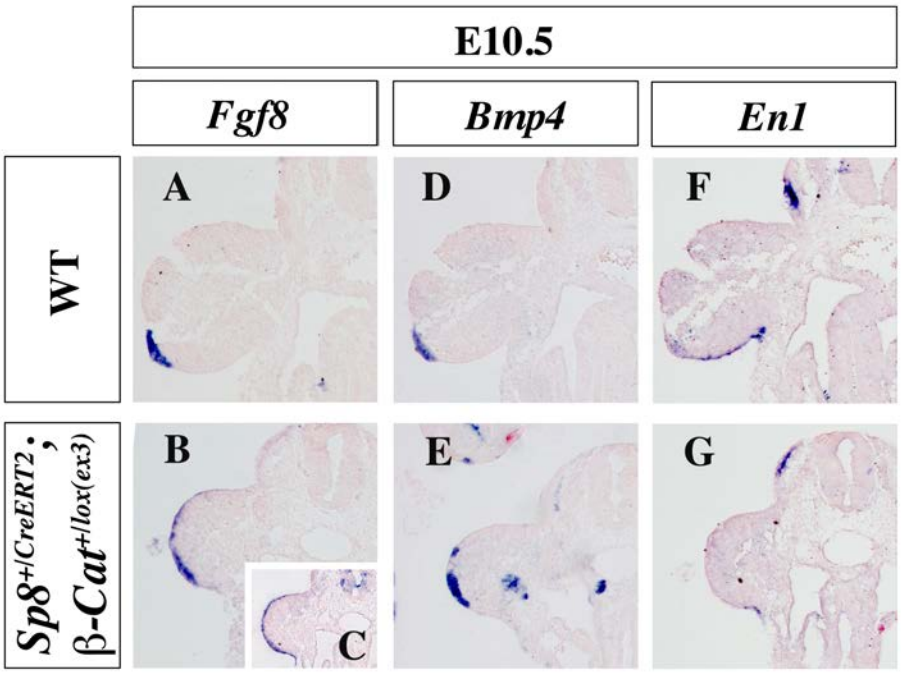


**Figure 41. Gene expression analysis in *Sp8*$^{CreERT2}$ mediated *β-catenin* gain of function limb buds.** *Fgf8* (A,B), *Sp8* (C), *Bmp4* (D,E) and *En1* (F,G) expression in transverse sections within control (A,D,F) and *Catn-b*$^{+/lox(ex3)}$;*Sp8*$^{CreERT2/+}$ (B,C,E,G) mutant limb buds. Gain of function mutation of *β-catenin* resulted in ectopic expression of *Fgf8* (B), *Sp8* (C) and *Bmp4* (E) in the dorsal and ventral embryos, while *En1* expression from the ventral limb ectoderm was lost (G).

Briefly, our experiments are consistent with previous results that demonstrate or even suggested that Wnt signalling lies upstream of both *Sp8* and *Fgf8* expression in the limb ectoderm (Bell *et al*., 2003; Treichel *et al*., 2003; Barrow et al 2003; Soshnikova *et al*., 2003 Kawakami *et al*., 2004; Sahara *et al*.,

2007; Lu *et al*., 2008; Talamillo *et al*., 2010; Lin *et al.,* 2013). In addition, we have demonstrated that *Sp8* and *Fgf8* expression patterns are identical upon $Sp8^{CreERT2}$ mediated *β-catenin* GOF. These results fit with *Sp8* acting upstream of *Fgf8* in the limb ectoderm, in a *Wnt*/*β-catenin* dependent manner (Lin *et al.,* 2013). Finally, we confirmed the ability of *Wnt*/*β-catenin* to upregulated Bmp signalling in the limb ectoderm as assessed by the ectopic expression of *Bmp4* (Barrow *et al.,* 2003; Soshnikova *et al.*, 2003), while unexpectedly *En1* expression was downregulated in the ventral limb ectoderm (Soshnikova *et al.*, 2003). Thus, it is possible that the GOF of *β-catenin* did not rescue the DV phenotype, because there was not enough space in the ventral ectoderm for *En1,* due to the expanded expression of *Fgf8*.

# 5.DISCUSSION

# 5. Discussion

The use of conditional and knock out approaches allows us to determine the requirement and redundancy of both Sp6 and Sp8 transcription factors in limb development. In the total absence of *Sp6* and *Sp8* or even when only a single functional allele of *Sp6* remains, in the absence of *Sp8*, no limbs formed leading to a tetramelic phenotype. In addition, the disruption of one of the *Sp8* alleles in the absence of *Sp6* resulted in a phenotype reminiscent of the Split hand/foot malformation in humans. The analysis of the compound mutants demonstrates that both transcription factors are conjointly required in a dose dependent manner and that *Sp8* makes a more substantial contribution to limb outgrowth than *Sp6*, probably, due to a higher level of expression.

We have also demonstrated that both transcription factors, *Sp6* and *Sp8*, are required and act in a redundant manner mediating the induction of *Fgf8* in the AER. In addition they are required to ensure proper AER morphology, as in their total absence no morphological AER is observed. Of most interest, besides Bmp expression and signalling in the limb ectoderm at early stages, as assess by the expression of *Bmp4* and *Msx2*, *En1* expression is not detected in the ventral limb ectoderm and double dorsal limb are developed.

## 5.1 *Sp6* and *Sp8* are conjointly required in a redundant and dose dependent manner for limb development

The limb as other organs is generated as a result of complex interactions amongst different signalling pathways that orchestrate several processes such as specification, differentiation, proliferation or apoptosis. These complex interactions between different signaling pathways lead to the generation of intricate networks that specifically pattern the different organs. The generation during the last decades of different mice harboring multiple mutations of genes belonging to the same family that exhibited similar patterns of expression, highlighted the robustness of the networks provided by these genes acting in a redundant manner (Sun *et al.,* 2000; Boulet *et al.,* 2004, Mariani *et al*., 2008; Sheth *et al.,* 2013).

In the case of the Fgf, Bmp or Hox families, it is well documented that the members of these families play redundant roles during limb development and that the overall final dosage, rather than particular dosage, is the most important parameter for morphogenesis (Sun *et al.,* 2000; Boulet *et al.,* 2004, Mariani *et al*., 2008; Sheth *et al.,* 2013). In this study, through the generation of *Sp6;Sp8* double knock out and *Sp8* conditional mutant in absence of *Sp6,* we provide further evidence for the roles of Sp6 and Sp8 transcription factors during limb development. Single gene-targeting analysis related their role with AER maintenance or maturation rather than induction (Treichel *et al*., 2003; Bell *et al*., 2003; Talamillo *et al*., 2010).

The analysis of the *Sp6;Sp8* double mutants performed in this study demonstrated that these transcription factors are together absolutely required for limb development. In contrast to single gene-inactivation studies, *Sp6;Sp8* double mutants or even mutants bearing a single functional allele of *Sp6* in the absence of other Sp alleles (*Sp6* or *Sp8*) no limbs formed. In addition, knock out approaches together with conditional approaches allowed us to determine not only that both transcription factors act in a redundant manner during limb development, but also in a dose dependent manner. Despite the variability associated to each genotype, when predominant phenotypes were considered, the phenotypes displayed a strong correlation between the increase in severity and the decrease in the level of Sp6 and/or Sp8 gene products, with *Sp8* making a more substantial contribution to limb outgrowth than *Sp6*, probably, due to a higher level of expression. Regarding the forelimb, progressive decrease of *Sp6* and/or *Sp8* gene products resulted in an increasing severity of the limb phenotype leading first to soft tissue syndactyly of digit 2-3 in *Sp6* KO mutant animals, then Split hand/foot malformation when only a single functional allele of *Sp8* remains, then limb truncations in the absence of both *Sp8* alleles and finally amelic phenotypes in the absence of both, *Sp6* and *Sp8*, or even when only a functional allele of *Sp6* remains (Fig. 42).

The increase in severity observed in the compound mutants as the level of Sp6/Sp8 gene-products decreased showed the requirement of a minimum threshold level of Sp6/Sp8 gene-product for limb development. Lack of limbs

when a single functional allele of *Sp6* still remains, in the absence of other Sp alleles (*Sp6* and *Sp8*), indicate that the level of *Sp6* expression provide by a single functional allele of *Sp6* was not sufficient to support limb development These level of expression provided by a single functional allele is below a minimum critical threshold required for limb development. In addition, the more severe limb phenotype of the *Sp8* mutant in comparison to mutants bearing a single functional allele of *Sp8*, in the absence of other Sp alleles (*Sp6* and *Sp8*), implies that the gene dose provided by two alleles of *Sp6* is below the dose provided by a single allele of *Sp8*. Moreover, when compared with the phenotype of the *Sp8* conditional mutant with the use of the *Msx2-Cre* demonstrates that the dose provided by two alleles of *Sp6* is even below a transient expression of single *Sp8* allele (Fig. 42). Thus, the limb phenotypes of compound mutants supports a major contribution of *Sp8* to limb development in comparison to *Sp6,* probably due to higher level of expression.

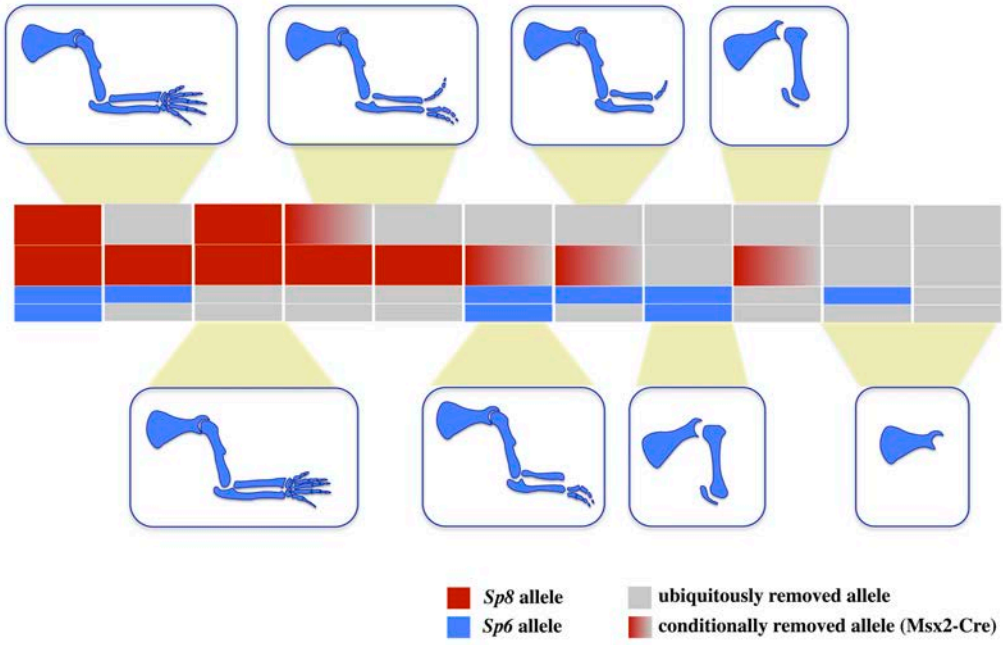


**Figure 42. Scheme illustrating the dose dependent requirement of *Sp6* and *Sp8* transcription factors for proper limb development.** Progressive decrease of *Sp6* and/or *Sp8* gene products resulted in an increasing severity of the limb phenotype leading first to soft tissue syndactyly of digit 2-3 in *Sp6* KO mutant animals, then Split hand/foot malformation when only a single functional allele of *Sp8* remained, then limb truncations in the absence of both *Sp8* alleles and finally amelic phenotypes the in absence of both, *Sp6* and *Sp8*, or even when only a functional allele of *Sp6* remained.

*Sp9,* another member of the Sp family of transcription factors that is also expressed in the limb ectoderm, has been proposed to act in a redundant manner with *Sp8* during limb development (Kawakami *et al*., 2004). However, our results show that in the absence of both *Sp6* and *Sp8, Sp9* during limb development is irrelevant as shown by the total absence of limbs in the *Sp6; Sp8* double mutant.

### 5.2 *Sp6* and *Sp8* are required for *Fgf8* induction in the AER

The predominant phenotypes obtained by progressive removal of the *Sp6* and *Sp8* alleles are consistent with defects involving AER development. Truncated limbs developed in the absence of *Sp8* result from a premature regression of the AER, while irregular induction of *Fgf8* leading to defects in AER maturation are responsible for the SHFM phenotype developed in mutants bearing a single functional allele of *Sp8,* in the absence of other Sp alleles (*Sp6* and *Sp8*). Finally the total absence of *Sp6* and *Sp8* or even when a single functional allele of *Sp6* remains in the absence of the other Sp alleles (*Sp6* and *Sp8*) lead to amelic phenotypes due to a failure in *Fgf8* induction in the AER.

The induction of the AER relies on intricate interactions between different signalling pathways that lead to the induction of *Fgf8* in the limb ectoderm (Barrow *et al.,* 2003; Soshnikova *et al.,* 2003). Big efforts have been made to unveil the mechanisms responsible for *Fgf8* induction, but while some aspects have been unraveled and different signalling pathways have been involved, the crosstalk between them is not fully understood. At least three signalling inputs have been demonstrated to be critical for *Fgf8* induction in the limb ectoderm. One is the requirement of Fgf10 signalling from the mesoderm through it receptor *Fgfr2*, expressed in the limb ectoderm (Ohuchi *et al.,* 1997; Min *et al*., 1998; Sekine *et al*., 1999; Xu *et al.,* 1998; Arman *et al*., 1999; Yu *et al*., 2008; Lu *et al*., 2008). The second is a Wnt/β-catenin activity preferentially signalling into the ventral limb ectoderm where AER precursor cells are induced (Barrow *et al*., 2003; Soshnikova *et al*., 2003). Finally, the third involves Bmp signalling in the limb ectoderm, through it receptor *BmprIa* (Ahn *et al.,* 2001; Pizette *et al*., 2001; Soshnikova *et al*., 2003; Pajni-Underwood *et al*., 2007). The disruption of any of

the mentioned signalling pathways leads to amelic phenotypes due to the inability to induce *Fgf8* expression in the limb ectoderm.

*Fgf10* signalling from the mesoderm through its *Fgfr2* is responsible for *Fgf8* induction, in a Wnt/β-catenin dependent manner, through the induction of *Wnt3a* and *Wnt3* in chick and mouse limb ectoderm, respectively. Once *Fgf8* is induced, its signalling to the mesoderm is required to maintain *Fg10* expression in the mesoderm and a feedback regulatory loop is established. Thus, both *Fgf10* and Wnt/β-catenin are not only required for the induction of *Fgf8,* also for its maintenance (Kawakami *et al*., 2001). Regarding Bmp signaling but disruption of the *BmprIa* abolished AER induction without interfering with *Fgf10* induction in the limb mesoderm (Ahn *et al.,* 2001; Pajni-Underwood *et al.,* 2007; Soshnikova *et al*., 2003). However, whether Bmp signalling lies upstream or downstream to Wnt/β-catenin signalling remains quite controversial. Nevertheless, genetic evidence favors a model in which Wnt /β-catenin signalling is require downstream of Bmp signalling for *Fgf8* induction in the AER (Barrow *et al.,* 2003*;* Soshnikova *et al*., 2003).

We have demonstrated here that the combined absence of *Sp6* and *Sp8*, results in absence of limbs due to the striking inability to induce *Fgf8* expression in the AER, while normal expression of *Fgf10* in the limb mesoderm and also Bmp in both the limb ectoderm and mesoderm is achieved at early stages of limb development, when the AER is induced. Because both transcription factors are expressed in a temporal and spatial manner compatible with the induction of *Fgf8* (Bell *et al*., 2003; Treichel *et al*., 2003; Talamillo *et al*., 2010), together with compelling evidence positioning them downstream of Wnt/β-catenin signalling in the limb ectoderm (Bell *et al*., 2003; Treichel *et al*., 2003; Kawakami *et al*., 2004; Talamillo *et al*., 2010) and the binding ability of *Sp8* to the *Fgf8* promoter (Sahara *et al*., 2007), our results are consistent with a model in which *Sp6* and *Sp8* are necessary mediators responsible for Wnt/β-catenin dependent induction of *Fgf8* (Fig. 43), acting downstream of *Fgf10* and Bmp signalling in AER induction. In addition, the phenotypes obtained and the gene expression analysis performed suggest that both factors act in a redundant and dose dependent manner in the induction of *Fgf8*. However, although they are functionally

redundant they do not contribute in the same manner in *Fgf8* induction. When a single functional allele of *Sp6* remains, in the absence of other Sp alleles (*Sp6* and *Sp8*), *Fgf8* is not induced implying that a minimum threshold of Sp dose that is not reached in this mutants is required to ensure the induction of *Fgf8*. In contrast, the dose provided by a single functional allele of *Sp8,* in the absence of other Sp alleles, is just above this minimum threshold level required for the induction and maintenance of *Fg8* leading to the development of all three proximo-distal skeletal elements, although a SHFM phenotype is achieved.

Of most interest, disruption of either Wnt/β-catenin or the major contributors of the Fgf dose provided by the AER, *Fgf8* and *Fgf4*, resulted in amelic phenotypes similar to the total absence of *Sp6* and *Sp8* (Sun *et al*., 2002; Boulet *et al*., 2004). However, while the disruption of Wnt/β-catenin in the limb ectoderm prevents *Fgf8* induction and also AER morphogenesis (Barrow *et al.*, 2003; Soshnikova *et al*., 2003), a morphological normal or even hyperplastic AER is still formed in the double *Fgf4*;*Fgf8* conditional mutant implying that there is not a simple linear relationship between Wnt/β-catenin signalling and Fgf in the limb ectoderm (Sun *et al*., 2002; Boulet *et al*., 2004). Thus, the absence of *Fgf8* induction together with the ventral ectodermal thickening present in double mutants lacking both *Sp6* and *Sp8*, implies that AER morphogenesis has been initiated but the process is arrested and cells are not confined to DV boundary. Hence, our results favors a model in which Wnt/β-catenin accomplish additional functions during AER development apart from the induction of *Fgf8*, related with AER morphogenesis as has been previously suggested (Barrow *et al*., 2003). We have provided further evidence that support that the role of Wnt/β-catenin in the limb ectoderm is not exclusive to the Wnt/β-catenin-Sp6/Sp8-Fgf regulatory loop. In addition, the early expression of the AER markers *Msx2* and *Bmp4* in the absence of *Sp6* and *Sp8* (also expressed in the double *Fgf4;Fgf8)* that are lost when Wnt/β-catenin signalling is disrupted (Sun *et al*., 2002; Barrow *et al*., 2003; Soshnikova *et al*., 2003), demonstrated that Wnt/β-catenin signalling is required for their induction independents of the Sp6/8 transcription factors.

Based on *Sp8* conditional GOF function approaches, it has been recently reported that *Sp8* partially mediates the Wnt/β-catenin dependent induction of

*Fgf8*, function that we have demonstrated here that is fully accomplished by *Sp6* and *Sp8*. Considering the dose dependent effect of the Sp factors, the inability to rescue the loss of Wnt/β-catenin with forced overexpression of *Sp8* under the *Rosa26* locus, may rely on the inability to reach the minimum threshold of Sp level required for the induction of *Fgf8*. In support of this notion, it has been argued that the incomplete rescue of Wnt/β-catenin LOF after overexpression of *Fgf8* under the *Rosa26* locus could be due to the weaker expression level of *Fgf8* from this locus compared to it endogenous level of expression (Lin *et al*., 2013).

### 5.3 Role of *Sp6* and *Sp8* in Dorso-Ventral pattern establishment

The AER is a highly dynamic and transitory structure subject to morphogenetic movements during its development. In mouse, the pre-AER cells are induced in the ventral limb ectoderm by the time limb ectoderm is polarized (Kimmel *et al*., 2000). As the limb bud grows, morphogenetic movements confine the pre-AER cells to the DV boundary of the limb, that separates *En1* expressing and non-expressing cells. The fact that AER induction and DV pattern establishment occurs concomitantly together with the positioning of the mature AER at the DV interface, reflects a link between these two processes.

Several experiments in chick as well as gene-targeting analysis in mice together with spontaneous mutations in chick suggested that the establishment of a DV boundary is an indispensable pre-requisite for AER induction. Grafting experiments in chick in which confrontation of ventral and dorsal ectoderm led to the development of ectopic AERs at the junction of the manipulated ventral and dorsal ectoderms (Laufer *et al*., 1997; Tanaka *et al*., 1997), together with Fgf-soaked bead induced ectopic limb buds developing at the right DV boundary disregarding the position of the bead supported this linkage (Altabef and Tickle, 2002). In addition, overexpression experiments in chick suggested that a boundary of *En1* expressing and non-expressing cells was an indispensable pre-requisite for AER induction (Pizette *et al.,* 2001). Consistent with this, the inability to induce an AER in the chick mutant *limbless* associates on the absence of *En1* expression in the ventral limb ectoderm and the subsequent extended

expression of *Wnt7a* in the ventral ectoderm (Fallon, 1983; Carringthon and Fallon, 1988; Ros *et al*., 1996; Grieshammer *et al*., 1996; Noramly *et al*., 1996).

In contrast, the chick mutant *eudiplopodia* is characterized by the development of an ectopic AER in the dorsal ectoderm leading to digits with a double dorsal phenotype (Goetinck, 1964). In addition, experiments in chick in which prospective limb mesoderm was grafted between two rows of somites led to the development of ectopic double dorsal limbs due to the dorsalizing effects of signals emanating from the somites, are against the requirement of *En1* expressing and non-expressing boundary for AER formation (Michaud *et a*l., 1997). Moreover, *En1* mutant mice and also the double mutant *En1;Wnt7a* that failed to express *En1* in the ventral ectoderm developed an AER and in the case of the double mutant was morphologically normal (Cygan *et al*., 1997; Loomis *et al*., 1996; Loomis *et al*., 1998; Parr and McMahon, 1995). Based on the ventrally extended AER of *En1* mutants, it is currently accepted that the role of *En1* is also involved with AER maturation (Loomis *et al*., 1996; Loomis *et al*., 1998). Therefore, the requirement of a DV pattern for the induction of the AER remains controversial.

We have demonstrated that a progressive decrease in the *Sp6*/*Sp8* dose lead to DV pattern establishment defects. As shown in the total absence of *Sp6* and *Sp8* or even when a single functional allele of *Sp6* remains in the absence of other Sp alleles (*Sp6* and *Sp8*), the limb buds emerges but rapidly regresses. Gene expression analysis of these limb buds showed that *En1* was absent from the ventral limb ectoderm leading to ectopic expression of *Wnt7a* in the ventral limb ectoderm what confers a double dorsal phenotype to the emerging limb bud. Interestingly, lack of *En1* induction in the ventral ectoderm in the absence of *Sp6* and *Sp8* occurs disregarding normal expression of Bmp ligands and signalling as confirmed by normal expression of *Msx2*, indicating the involvement of *Sp6* and *Sp8* in the induction of *En1* in the limb ventral ectoderm. Since the ability of members of the Sp family to interact with other transcription factor has been demonstrated, including SMADs, we hypothesize that *Sp6*/*Sp8* could be required for the induction of *En1* acting downstream of Bmp signalling, through the

cooperation with SMADs (Fig. 43)(Pardali *et al.,* 2000; Sakaguchi *et al.,* 2005; Kim *et al.,* 2006).

On the other hand, when a single functional allele of *Sp8* remains in the absence of other Sp alleles (*Sp6* and *Sp8*), irregular activation of *Fgf8* is achieved and as the AER develops maturation defects with gaps of *Fgf8* expression along its AP axis are developed together with expression of *Fgf8* in the ventral limb ectoderm. These AER defects could account for the SHFM phenotype in these mutants. Remarkably, ventrally abnormal extended expression of *Wnt7a* at variable degree was always in correlation with the restriction of *En1* to a more proximal domain. This defect in DV pattern establishment can explain the double dorsal digits of mutants bearing a single functional allele of *Sp8* in the absence of the other Sp alleles (*Sp6* and *Sp8*). Therefore, it is consistent with previous reports indicating the continuous requirement of Wnt/β-catenin for the correct DV pattern establishment (Barrow *et al*., 2003). The ventrally extended *AER* is also consistent with phenotypes in which AER maturation defects arise due to lack of *En1* expression in the limb ectoderm (Loomis *et al*., 1998).

Finally, the limb phenotype of the *Sp6*;*Sp8* double mutant resembles that of the chicken mutant *limbless*. *Limbless* is a Mendelian autosomal recessive mutation in chick affecting the ectodermal component of the limb that is characterized by the total absence of limbs (Prahlad *et al*., 1979). However, in contrast to double *Sp6;Sp8* mutants *limbless* defects are restricted to the limbs (Carrington and Fallon, 1984b; Lanser and Fallon, 1984). In *limbless* mutants, the limb bud is initiated but at early stages (20 HH) the mesoderm undergoes cell-death as a consequence of the inability of these mutants to activate *Fgf8* expression in the limb ectoderm and the limb bud consequently regresses (Fallon *et al*., 1983; Ros *et al*., 1996). In addition, *limbless* limb buds lacks *En1* expression in the ventral ectoderm with the subsequent *Wnt7a* expression in both dorsal and ventral ectoderm, leading to the development of bidorsal limb buds. Interestingly, the genetic cause of the chicken *limbless* mutation has not been identified yet. Therefore, the similarity between *limbless* and *Sp6*;*Sp8* double mutants limb phenotype, together with the fact that *Sp6* seems to be absent in the chick, lead us to consider the possibility that *Sp8* could be the

candidate gene responsible of the *limbless* phenotype, as has been previously proposed (Robb *et al.,* 2011). However, as *limbless* defects are restricted to the limbs and mutants do not exhibit any neural defect as occurs in *Sp8* mutants, if *Sp8* is the responsible gene for the *limbless* mutation in chick, this mutation needs to be in a limb specific regulatory element rather than in the gene. Nevertheless, another possibility could be that a possible redundancy between *Sp8* and *Sp9* in chick could account for the differences between *limbless* and the double *Sp6;Sp8* mutant. However, the absence of a morphological AER in *limbless* does not support *Sp8* as responsible gene.

### 5.4 *Sp6*/*Sp8* and Split hand/foot malformation

SHFM is a genetically heterogeneous congenital human malformation characterized a central cleft in upper and lower limbs where central digits may be absent and the remaining posterior digits appear normally fused (Temtamy and McKusick, 1978; Sifakis *et al*., 2001). The phenotype is highly variable even within the same individual and ranges from mild central syndactyly to severe loss of elements with oligodactyly and it may include defects in the zeugopod. The incidence of SHFM is about 1:18,000 live births and can appear as an isolated entity or as part of a syndrome. In human, at least 6 loci have been associated to this SHFM phenotype (Scherer *et al*. 1994; Johnson *et al.,* 1995; Mills *et al*., 1999; Yang *et al*., 1999; Lo Iacono *et al*., 2008). It is currently accepted that these limb defects are the result of a failure in the maintenance of the central region of the AER that losses *Fgf8* expression. We have demonstrated that the dose provided by a single functional allele of *Sp8* in the absence of other *Sp* alleles (*Sp6* or *Sp8*) is just above the minimum threshold of the Sp dose required for *Fgf8* induction leading to its irregular activation that results in the formation of an irregular AER presenting gaps along its AP length. We show that these irregularities in the AER from early stages also result in SHFM phenotype.

Although 6 loci has been associated to the different types of SHFM, only *Tp63* (SHFM type IV) and *Dlx5* and *Dlx6* (SHFM type I) have been unequivocally involved in this malformation. Both of them have been shown to be components of the same regulatory network. Regarding the epistatic relation between *Tp63* and *Dlx* genes in this network, it has been shown that *Tp63* lies upstream of *Dlx* genes and it is required for its expression (Lo Iacono *et al*., 2008; Kouwenhoven *et al*., 2010). Since similar phenotypes are frequently caused by disruption of components of a regulatory network, we have considered the possibility that *Sp6* and *Sp8* genes might be part of the *Tp63* network. Indeed, the phenotypes of our mutants are identical, including the dorso-ventral component to those recently reported in a new identified mutation in *Dlx5* (Shamseldin *et al*., 2012). However, the fact that *Tp63* and *Dlx5* and *Dlx6* are expressed virtually normal in *Sp6/Sp8* mutants indicate that, if *Sp6/Sp8* transcription factors would act downstream of *Tp63*-Dlx factors if they are in the same network.

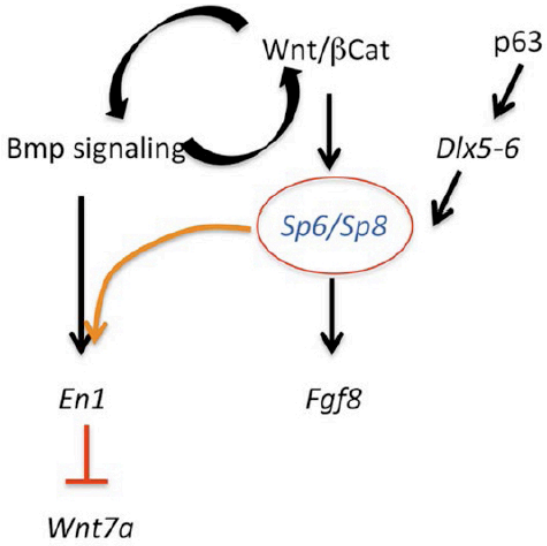


**Figure 43. Schematic representation of the major signalling pathways leading to *Fgf8* induction and DV pattern establishment and the relative position of *Sp6* and *Sp8*.** *Sp6* and *Sp8* act in a redundant manner in the Wnt/β-catenin dependent induction of *Fgf8* in the limb ectoderm. In addition both transcription factors are required for the induction of *En1* in the ventral limb ectoderm maybe through cooperation with the Bmp signalling pathway. Finally if *Sp6* and *Sp8* are involved in the *Tp63* network leading to SHFM they must act downstream the Dlx genes. Arrows indicated induction and bars repression.

Briefly, we provide strong evidence that support the functional redundancy and a dose dependent requirement of *Sp6* and *Sp8* in both AER induction and DV pattern establishment. We demonstrate that they are required and act in a redundant and dose dependent manner downstream of Wnt/β-catenin in the induction of *Fgf8* in the limb ectoderm, as *Fgf8* is not induced in the absence of both transcription factors and limbs are not formed. In addition, both transcription factors are also required for the induction of *En1* in the ventral limb ectoderm and subsequent ventral identity specification. Since, Sp1 is known to interact with Smad, the Bmp signalling transducers, it is possible that cooperation between Sp6/8 and Smad are required for the induction of *En1*. Therefore, we propose a model in which *Sp6* and *Sp8* are absolutely required for *Fgf8* induction and DV pattern establishment.

# 6.CONCLUSIONS

## 6. Conclusions

**1-** *Sp6* and *Sp8* are conjointly required for limb development as in the complete absence of both transcription factors, no limbs form. The progressive reduction in the dose of Sp6 and Sp8 gene products leads first to split hand/foot malformation, then oligodactyly, then truncation and finally amelia. Furthermore, the digits that form with reduced *Sp6*/*Sp8* gene dosage exhibit bi-dorsal features.

**2-** In the absence of others Sp alleles (either *Sp6* or *Sp8*), a single functional allele of *Sp6* is not sufficient to support any limb development, while a single functional allele of *Sp8* permits development of all three proximo-distal segments, although exhibits an split hand/foot malformation phenotype. This functional difference likely relies on the much higher level of expression of *Sp8* in the limb ectoderm, compared to *Sp6* .

**3-** The molecular characterization of the mutant limb buds shows that, when the dosage of *Sp6/Sp8* is significantly reduced, *Fgf8* and *En1* are not activated although initiation of AER morphology occurs.

**4-** The limb phenotype of the embryos that develop with a single copy of S*p*8 mimicked the human split hand/foot malformation. The cause of the phenotype is an irregular *Fgf8* activation associated with a constant abnormal extension of *Wnt7a* in the ventral ectoderm in correlation with a corresponding restriction of *En1*. *Tp63*, *Dlx5* and *Dlx6* are normally expressed in these limbs indicating that if *Sp6*/*Sp8* are components of the *Tp63* network, they act downstream of *Dlx5* and *Dlx6*.

**5-** Our results are consistent with *Sp6* and *Sp8* being functionally equivalent and working in concert during limb development as necessary mediators of the Wnt/β-catenin induction of *Fgf8* and also as cooperators of the Bmp signalling in the induction of *En1*.

# 7.CONCLUSIONES

## 7. Conclusiones

**1-** *Sp6* y *Sp8* son conjuntamente requeridos para el desarrollo de la extremidad, dado que en la completa ausencia de ambos factores de transcripción las extremidades no se desarrollan. La reducción progresiva en la dosis de *Sp6* y *Sp8* da lugar primero a malformaciones de mano hendida/pie hendido, luego oligodactilia, después truncamientos y finalmente amelia. Además, los dedos que se forman con dosis reducidas de *Sp6*/*Sp8* muestran características bi-dorsales.

**2-** En ausencia de otros alelos de Sp (tanto *Sp6* como *Sp8*), un solo alelo funcional de *Sp6* no es suficiente para el desarrollo de la extremidad, mientras que un solo alelo de *Sp8* permite el desarrollo de los tres segmentos próximo-distales, aunque presentando un fenotipo de de mano hendida. Esta diferencia funcional probablemente reside en un mayor nivel de expresión de *Sp8* en el ectodermo de la extremidad, en comparación con *Sp6*.

**3-** La caracterización molecular de los esbozos de extremidad de los mutantes muestra que, cuando la dosis de Sp6/Sp8 se reduce significativamente, *Fgf8* y *En1* no se activadan a pesar de que se produce la inducción de una AER morfológica.

**4-** El fenotipo de la extremidad de los embriones que se desarrollan con una única copia de *Sp8* reproducen la malformación en humanos de mano hendida. La causa del fenotipo es una activación irregular de *Fgf8* asociada a una anormal y constante extensión de *Wnt7a* en el ectodermo ventral, en correlación con la correspondiente restricción de *En1*. La normal expresión de *Tp63*, *Dlx5* y *Dlx6* en estas extremidades indica que si *Sp6*/*Sp8* son componentes de la vía de *Tp63*, éstos estarían actuando por debajo de *Dlx5* y *Dlx6*.

**5-** Nuestros resultados muestran que *Sp6* y *Sp8* son funcionalmente equivalentes y actúan de manera conjunta durante el desarrollo de la extremidad. Estos resultados apoyan un modelo en el que *Sp6* y *Sp8* estarían actuando como mediadores necesarios para la inducción de *Fgf8* mediada por Wnt/β-Catenin, además de cooperar con la vía de señalización de Bmp para la inducción de *En1*.

# 8.REFERENCES

## 8. References

**Agarwal, P., Wylie, J. N., Galceran, J., Arkhitko, O., Li, C., Deng, C., Grosschedl, R. and Bruneau, B. G.** (2003). Tbx5 is essential for forelimb bud initiation following patterning of the limb field in the mouse embryo. *Development* **130**, 623-33.

**Ahmad, M., Abbas, H., Haque, S. and Flatz, G.** (1987). X-chromosomally inherited split-hand/split-foot anomaly in a Pakistani kindred. *Hum Genet* **75**, 169-73.

**Ahn, D. G., Kourakis, M. J., Rohde, L. A., Silver, L. M. and Ho, R. K.** (2002). T-box gene tbx5 is essential for formation of the pectoral limb bud. *Nature* **417**, 754-8.

**Ahn, K., Mishina, Y., Hanks, M. C., Behringer, R. R. and Crenshaw, E. B., 3rd.** (2001). BMPR-IA signaling is required for the formation of the apical ectodermal ridge and dorsal-ventral patterning of the limb. *Development* **128**, 4449-61.

**Akam, M., Averof, M., Castelli-Gair, J., Dawes, R., Falciani, F. and Ferrier, D.** (1994). The evolving role of Hox genes in arthropods. *Dev Suppl*, 209-15.

**Akita, K.** (1996). The effect of the ectoderm on the dorsoventral pattern of epidermis, muscles and joints in the developing chick leg: a new model. *Anat Embryol (Berl)* **193**, 377-86.

**Altabef, M., Clarke, J. D. and Tickle, C.** (1997). Dorso-ventral ectodermal compartments and origin of apical ectodermal ridge in developing chick limb. *Development* **124**, 4547-56.

**Altabef, M. and Tickle, C.** (2002). Initiation of dorso-ventral axis during chick limb development. *Mech Dev* **116**, 19-27.

**Arman, E., Haffner-Krausz, R., Gorivodsky, M. and Lonai, P.** (1999). Fgfr2 is required for limb outgrowth and lung-branching morphogenesis. *Proc Natl Acad Sci U S A* **96**, 11895-9.

**Attisano, L. and Wrana, J. L.** (1998). Mads and Smads in TGF beta signalling. *Curr Opin Cell Biol* **10**, 188-94.

**Bandyopadhyay, A., Tsuji, K., Cox, K., Harfe, B. D., Rosen, V. and Tabin, C. J.** (2006). Genetic Analysis of the Roles of BMP2, BMP4, and BMP7 in Limb Patterning and Skeletogenesis. *PLoS Genet* **2**, e216.

**Barrow, J. R., Thomas, K. R., Boussadia-Zahui, O., Moore, R., Kemler, R., Capecchi, M. R. and McMahon, A. P.** (2003). Ectodermal Wnt3/beta-catenin signaling is required for the establishment and maintenance of the apical ectodermal ridge. *Genes Dev* **17**, 394-409.

**Behrens, J., von Kries, J. P., Kuhl, M., Bruhn, L., Wedlich, D., Grosschedl, R. and Birchmeier, W.** (1996). Functional interaction of beta-catenin with the transcription factor LEF-1. *Nature* **382**, 638-42.

**Bell, S. M., Schreiner, C. M. and Scott, W. J.** (1998). The loss of ventral ectoderm identity correlates with the inability to form an AER in the legless hindlimb bud. *Mech Dev* **74**, 41-50.

**Bell, S. M., Schreiner, C. M., Waclaw, R. R., Campbell, K., Potter, S. S. and Scott, W. J.** (2003). Sp8 is crucial for limb outgrowth and neuropore closure. *Proc Natl Acad Sci U S A* **100**, 12195-200.

**Boulet, A. M., Moon, A. M., Arenkiel, B. R. and Capecchi, M. R.** (2004). The roles of Fgf4 and Fgf8 in limb bud initiation and outgrowth. *Dev Biol* **273**, 361-72.

**Bouwman, P., Gollner, H., Elsasser, H. P., Eckhoff, G., Karis, A., Grosveld, F., Philipsen, S. and Suske, G.** (2000). Transcription factor Sp3 is essential for post-natal survival and late tooth development. *EMBO J* **19**, 655-61.

**Brook, W. J., Diaz-Benjumea, F. J. and Cohen, S. M.** (1996). Organizing spatial pattern in limb development. *Annu Rev Cell Dev Biol* **12**, 161-80.

**Burke, A. C., Nelson, C. E., Morgan, B. A. and Tabin, C.** (1995). Hox genes and the evolution of vertebrate axial morphology. *Development* **121**, 333-46.

**Callejo, A., Culi, J. and Guerrero, I.** (2008). Patched, the receptor of Hedgehog, is a lipoprotein receptor. *Proc Natl Acad Sci U S A* **105**, 912-7.

**Carrington, J. L. and Fallon, J. F.** (1988). Initial limb budding is independent of apical ectodermal ridge activity; evidence from a limbless mutant. *Development* **104**, 361-7.

**Cohn, M. J. and Bright, P. E.** (1999). Molecular control of vertebrate limb development, evolution and congenital malformations. *Cell Tissue Res* **296**, 3-17.

**Cohn, M. J., Izpisua-Belmonte, J. C., Abud, H., Heath, J. K. and Tickle, C.** (1995). Fibroblast growth factors induce additional limb development from the flank of chick embryos. *Cell* **80**, 739-46.

**Cohn, M. J., Patel, K., Krumlauf, R., Wilkinson, D. G., Clarke, J. D. and Tickle, C.** (1997). Hox9 genes and vertebrate limb specification. *Nature* **387**, 97-101.

**Cohn, M. J. and Tickle, C.** (1999). Developmental basis of limblessness and axial patterning in snakes. *Nature* **399**, 474-9.

**Cooper, K. L., Hu, J. K., ten Berge, D., Fernandez-Teran, M., Ros, M. A. and Tabin, C. J.** (2011). Initiation of proximal-distal patterning in the vertebrate limb by signals and growth. *Science* **332**, 1083-6.

**Crackower, M. A., Scherer, S. W., Rommens, J. M., Hui, C. C., Poorkaj, P., Soder, S., Cobben, J. M., Hudgins, L., Evans, J. P. and Tsui, L. C.** (1996). Characterization of the split hand/split foot malformation locus SHFM1 at 7q21.3-q22.1 and analysis of a candidate gene for its expression during limb development. *Hum Mol Genet* **5**, 571-9.

**Crossley, P. H. and Martin, G. R.** (1995). The mouse Fgf8 gene encodes a family of polypeptides and is expressed in regions that direct outgrowth and patterning in the developing embryo. *Development* **121**, 439-51.

**Crossley, P. H., Minowada, G., MacArthur, C. A. and Martin, G. R.** (1996). Roles for FGF8 in the induction, initiation, and maintenance of chick limb development. *Cell* **84**, 127-36.

**Cunningham, T. J., Zhao, X., Sandell, L. L., Evans, S. M., Trainor, P. A. and Duester, G.** (2013). Antagonism between retinoic acid and fibroblast growth factor signaling during limb development. *Cell Rep* **3**, 1503-11.

**Cygan, J. A., Johnson, R. L. and McMahon, A. P.** (1997). Novel regulatory interactions revealed by studies of murine limb pattern in Wnt-7a and En-1 mutants. *Development* **124**, 5021-32.

**Chevallier, A., Kieny, M. and Mauger, A.** (1977). Limb-somite relationship: origin of the limb musculature. *J Embryol Exp Morphol* **41**, 245-58.

**Chiang, C., Litingtung, Y., Harris, M. P., Simandl, B. K., Li, Y., Beachy, P. A. and Fallon, J. F.** (2001). Manifestation of the limb prepattern: limb development in the absence of sonic hedgehog function. *Dev Biol* **236**, 421-35.

**Chiang, C., Litingtung, Y., Lee, E., Young, K. E., Corden, J. L., Westphal, H. and Beachy, P. A.** (1996). Cyclopia and defective axial patterning in mice lacking Sonic hedgehog gene function. *Nature* **383**, 407-13.

**Choi, K. S., Lee, C., Maatouk, D. M. and Harfe, B. D.** (2012). Bmp2, Bmp4 and Bmp7 are co-required in the mouse AER for normal digit patterning but not limb outgrowth. *PLoS One* **7**, e37826.

**Christ, B., Jacob, H. J. and Jacob, M.** (1977). Experimental analysis of the origin of the wing musculature in avian embryos. *Anat Embryol (Berl)* **150**, 171-86.

**Datta, S. R., Brunet, A. and Greenberg, M. E.** (1999). Cellular survival: a play in three Akts. *Genes Dev* **13**, 2905-27.

**Davis, A. P., Witte, D. P., Hsieh-Li, H. M., Potter, S. S. and Capecchi, M. R.** (1995). Absence of radius and ulna in mice lacking hoxa-11 and hoxd-11. *Nature* **375**, 791-5.

**Davis, C. A., Holmyard, D. P., Millen, K. J. and Joyner, A. L.** (1991). Examining pattern formation in mouse, chicken and frog embryos with an En-specific antiserum. *Development* **111**, 287-98.

**de Mollerat, X. J., Everman, D. B., Morgan, C. T., Clarkson, K. B., Rogers, R. C., Colby, R. S., Aylsworth, A. S., Graham, J. M., Jr., Stevenson, R. E. and Schwartz, C. E.** (2003). P63 mutations are not a major cause of non-syndromic split hand/foot malformation. *J Med Genet* **40**, 55-61.

**Dealy, C. N., Roth, A., Ferrari, D., Brown, A. M. and Kosher, R. A.** (1993). Wnt-5a and Wnt-7a are expressed in the developing chick limb bud in a manner suggesting roles in pattern formation along the proximodistal and dorsoventral axes. *Mech Dev* **43**, 175-86.

**Delgado I, Domínguez-Frutos E, Schimmang T, Ros MA** (2008) The incomplete inactivation of Fgf8 in the limb ectoderm affects the morphogenesis of the anterior autopod through BMP-mediated cell death. Dev. Dyn.**237**(3):649-58

**Derynck, R., Zhang, Y. and Feng, X. H.** (1998). Smads: transcriptional activators. of TGF-beta responses. *Cell* **95**, 737-40.

**Deschamps, J.** (2007). Ancestral and recently recruited global control of the Hox genes in development. *Curr Opin Genet Dev* **17**, 422-7.

**Diaz-Benjumea, F. J. and Cohen, S. M.** (1993). Interaction between dorsal and ventral cells in the imaginal disc directs wing development in Drosophila. *Cell* **75**, 741-52.

**Duboc, V. and Logan, M. P.** (2011). Pitx1 is necessary for normal initiation of hindlimb outgrowth through regulation of Tbx4 expression and shapes hindlimb morphologies via targeted growth control. *Development* **138**, 5301-9.

**Duboule, D. and Dolle, P.** (1989). The structural and functional organization of the murine HOX gene family resembles that of Drosophila homeotic genes. *EMBO J* **8**, 1497-505.

**Duboule, D. and Morata, G.** (1994). Colinearity and functional hierarchy among genes of the homeotic complexes. *Trends Genet* **10**, 358-64.

**Dudley, A. T., Lyons, K. M. and Robertson, E. J.** (1995). A requirement for bone morphogenetic protein-7 during development of the mammalian kidney and eye. *Genes Dev* **9**, 2795-807.

**Dudley, A. T., Ros, M. A. and Tabin, C. J.** (2002). A re-examination of proximodistal patterning during vertebrate limb development. *Nature* **418**, 539-44.

**Duijf, P. H., van Bokhoven, H. and Brunner, H. G.** (2003). Pathogenesis of split-hand/split-foot malformation. *Hum Mol Genet* **12 Spec No 1**, R51-60.

**Dunn, N. R., Winnier, G. E., Hargett, L. K., Schrick, J. J., Fogo, A. B. and Hogan, B. L.** (1997). Haploinsufficient phenotypes in Bmp4 heterozygous null mice and modification by mutations in Gli3 and Alx4. *Dev Biol* **188**, 235-47.

**Dynan, W. S. and Tjian, R.** (1983). The promoter-specific transcription factor Sp1 binds to upstream sequences in the SV40 early promoter. *Cell* **35**, 79-87.

**Eastman, Q. and Grosschedl, R.** (1999). Regulation of LEF-1/TCF transcription factors by Wnt and other signals. *Curr Opin Cell Biol* **11**, 233-40.

**Estella, C. and Mann, R. S.** (2010). Non-redundant selector and growth-promoting functions of two sister genes, buttonhead and Sp1, in Drosophila leg development. *PLoS Genet* **6**, e1001001.

**Estella, C., Rieckhof, G., Calleja, M. and Morata, G.** (2003). The role of buttonhead and Sp1 in the development of the ventral imaginal discs of Drosophila. *Development* **130**, 5929-41.

**Faiyaz ul Haque, M., Uhlhaas, S., Knapp, M., Schuler, H., Friedl, W., Ahmad, M. and Propping, P.** (1993). Mapping of the gene for X-chromosomal split-hand/split-foot anomaly to Xq26-q26.1. *Hum Genet* **91**, 17-9.

**Fallon, J. F., Lopez, A., Ros, M. A., Savage, M. P., Olwin, B. B. and Simandl, B. K.** (1994). FGF-2: apical ectodermal ridge growth signal for chick limb development. *Science* **264**, 104-7.

**Fernandez-Teran, M. and Ros, M. A.** (2008). The Apical Ectodermal Ridge: morphological aspects and signaling pathways. *Int J Dev Biol* **52**, 857-71.

**Fromental-Ramain, C., Warot, X., Lakkaraju, S., Favier, B., Haack, H., Birling, C., Dierich, A., Doll e, P. and Chambon, P.** (1996). Specific and redundant functions of the paralogous Hoxa-9 and Hoxd-9 genes in forelimb and axial skeleton patterning. *Development* **122**, 461-72.

**Galceran, J., Farinas, I., Depew, M. J., Clevers, H. and Grosschedl, R.** (1999). Wnt3a-/--like phenotype and limb deficiency in Lef1(-/-)Tcf1(-/-) mice. *Genes Dev* **13**, 709-17.

**Ganan, Y., Macias, D., Duterque-Coquillaud, M., Ros, M. A. and Hurle, J. M.** (1996). Role of TGF beta s and BMPs as signals controlling the position of the digits and the areas of interdigital cell death in the developing chick limb autopod. *Development* **122**, 2349-57.

**Gardner, C. A. and Barald, K. F.** (1992). Expression patterns of engrailed-like proteins in the chick embryo. *Dev Dyn* **193**, 370-88.

**Garrity, D. M., Childs, S. and Fishman, M. C.** (2002). The heartstrings mutation in zebrafish causes heart/fin Tbx5 deficiency syndrome. *Development* **129**, 4635-45.

**Gaunt, S. J.** (1988). Mouse homeobox gene transcripts occupy different but overlapping domains in embryonic germ layers and organs: a comparison of Hox-3.1 and Hox-1.5. *Development* **103**, 135-44.

**Geduspan, J. S. and MacCabe, J. A.** (1989). Transfer of dorsoventral information from mesoderm to ectoderm at the onset of limb development. *Anat Rec* **224**, 79-87.

**Gibson-Brown, J. J., Agulnik, S. I., Chapman, D. L., Alexiou, M., Garvey, N., Silver, L. M. and Papaioannou, V. E.** (1996). Evidence of a role for T-box

genes in the evolution of limb morphogenesis and the specification of forelimb/hindlimb identity. *Mech Dev* **56**, 93-101.

**Gibson-Brown, J. J., Agulnik, S. I., Silver, L. M., Niswander, L. and Papaioannou, V. E.** (1998). Involvement of T-box genes Tbx2-Tbx5 in vertebrate limb specification and development. *Development* **125**, 2499-509.

**Goetinck, P. F.** (1964). Studies on Limb Morphogenesis. Ii. Experiments with the Polydactylous Mutant Eudiplopodia. *Dev Biol* **10**, 71-91.

**Gollner, H., Dani, C., Phillips, B., Philipsen, S. and Suske, G.** (2001). Impaired ossification in mice lacking the transcription factor Sp3. *Mech Dev* **106**, 77-83.

**Greco, T. L., Takada, S., Newhouse, M. M., McMahon, J. A., McMahon, A. P. and Camper, S. A.** (1996). Analysis of the vestigial tail mutation demonstrates that Wnt-3a gene dosage regulates mouse axial development. *Genes Dev* **10**, 313-24.

**Grieshammer, U., Minowada, G., Pisenti, J. M., Abbott, U. K. and Martin, G. R.** (1996). The chick limbless mutation causes abnormalities in limb bud dorsal-ventral patterning: implications for the mechanism of apical ridge formation. *Development* **122**, 3851-61.

**Gritli-Linde, A., Lewis, P., McMahon, A. P. and Linde, A.** (2001). The whereabouts of a morphogen: direct evidence for short- and graded long-range activity of hedgehog signaling peptides. *Dev Biol* **236**, 364-86.

**Guo, Q., Loomis, C. and Joyner, A. L.** (2003). Fate map of mouse ventral limb ectoderm and the apical ectodermal ridge. *Dev Biol* **264**, 166-78.

**Halford, M. M., Armes, J., Buchert, M., Meskenaite, V., Grail, D., Hibbs, M. L., Wilks, A. F., Farlie, P. G., Newgreen, D. F., Hovens, C. M. et al.** (2000). Ryk-deficient mice exhibit craniofacial defects associated with perturbed Eph receptor crosstalk. *Nat Genet* **25**, 414-8.

**Hamburger, V.** (1938) "Morphogenetic and axial cell differentiation of transplanted limb primordia of 2-day chick embryos" *J. Exp. Zool.*77:379-400

**Hamburger, V. and Hamilton, H. L.** (1951). A series of normal stages in the development of the chick embryo. *Journal of Morphology* **88**, 49-92.

**Harada, N., Tamai, Y., Ishikawa, T., Sauer, B., Takaku, K., Oshima, M. and Taketo, M. M.** (1999). Intestinal polyposis in mice with a dominant stable mutation of the beta-catenin gene. *EMBO J* **18**, 5931-42.

**Harfe, B. D., Scherz, P. J., Nissim, S., Tian, H., McMahon, A. P. and Tabin, C. J.** (2004). Evidence for an expansion-based temporal Shh gradient in specifying vertebrate digit identities. *Cell* **118**, 517-28.

**Harrison, S. M., Houzelstein, D., Dunwoodie, S. L. and Beddington, R. S.** (2000). Sp5, a new member of the Sp1 family, is dynamically expressed during development and genetically interacts with Brachyury. *Dev Biol* **227**, 358-72.

**Hasson, P., Del Buono, J. and Logan, M. P.** (2007). Tbx5 is dispensable for forelimb outgrowth. *Development* **134**, 85-92.

**Heikinheimo, M., Lawshe, A., Shackleford, G. M., Wilson, D. B. and MacArthur, C. A.** (1994). Fgf-8 expression in the post-gastrulation mouse suggests roles in the development of the face, limbs and central nervous system. *Mech Dev* **48**, 129-38.

**Heldin, C. H., Miyazono, K. and ten Dijke, P.** (1997). TGF-beta signalling from cell membrane to nucleus through SMAD proteins. *Nature* **390**, 465-71.

**Helms, J. A., Kim, C. H., Eichele, G. and Thaller, C.** (1996). Retinoic acid signaling is required during early chick limb development. *Development* **122**, pp. 1385–1394.

**Hertveldt, V., Louryan, S., van Reeth, T., Dreze, P., van Vooren, P., Szpirer, J. and Szpirer, C.** (2008). The development of several organs and appendages is impaired in mice lacking Sp6. *Dev Dyn* **237**, 883-92.

**Hofmann, C., Luo, G., Balling, R. and Karsenty, G.** (1996). Analysis of limb patterning in BMP-7-deficient mice. *Dev Genet* **19**, 43-50.

**Hoodless, P. A., Haerry, T., Abdollah, S., Stapleton, M., O'Connor, M. B., Attisano, L. and Wrana, J. L.** (1996). MADR1, a MAD-related protein that functions in BMP2 signaling pathways. *Cell* **85**, 489-500.

**Hou, J. Z., Kan, M. K., McKeehan, K., McBride, G., Adams, P. and McKeehan, W. L.** (1991). Fibroblast growth factor receptors from liver vary in three structural domains. *Science* **251**, 665-8.

**Huelsken, J. and Birchmeier, W.** (2001). New aspects of Wnt signaling pathways in higher vertebrates. *Curr Opin Genet Dev* **11**, 547-53.

**Hui, C. C. and Joyner, A. L.** (1993). A mouse model of greig cephalopolysyndactyly syndrome: the extra-toesJ mutation contains an intragenic deletion of the Gli3 gene. *Nat Genet* **3**, 241-6.

**Isaac, A., Rodriguez-Esteban, C., Ryan, A., Altabef, M., Tsukui, T., Patel, K., Tickle, C. and Izpisua-Belmonte, J. C.** (1998). Tbx genes and limb identity in chick embryo development. *Development* **125**, 1867-75.

**Johnson, K. R., Lane, P. W., Ward-Bailey, P. and Davisson, M. T.** (1995). Mapping the mouse dactylaplasia mutation, Dac, and a gene that controls its expression, mdac. *Genomics* **29**, 457-64.

**Johnson, R. L. and Tabin, C. J.** (1997). Molecular models for vertebrate limb development. *Cell* **90**, 979-90.

**Kadonaga, J. T., Carner, K. R., Masiarz, F. R. and Tjian, R.** (1987). Isolation of cDNA encoding transcription factor Sp1 and functional analysis of the DNA binding domain. *Cell* **51**, 1079-90.

**Kawakami, Y., Capdevila, J., Buscher, D., Itoh, T., Rodriguez Esteban, C. and Izpisua Belmonte, J. C.** (2001). WNT signals control FGF-dependent limb initiation and AER induction in the chick embryo. *Cell* **104**, 891-900.

**Kawakami, Y., Esteban, C. R., Matsui, T., Rodriguez-Leon, J., Kato, S. and Izpisua Belmonte, J. C.** (2004). Sp8 and Sp9, two closely related buttonhead-like transcription factors, regulate Fgf8 expression and limb outgrowth in vertebrate embryos. *Development* **131**, 4763-74.

**Kawakami, Y., Ishikawa, T., Shimabara, M., Tanda, N., Enomoto-Iwamoto, M., Iwamoto, M., Kuwana, T., Ueki, A., Noji, S. and Nohno, T.** (1996). BMP signaling during bone pattern determination in the developing limb. *Development* **122**, 3557-66.

**Kawakami, Y., Marti, M., Kawakami, H., Itou, J., Quach, T., Johnson, A., Sahara, S., O'Leary, D. D., Nakagawa, Y., Lewandoski, M. et al.** (2011). Islet1-mediated activation of the beta-catenin pathway is necessary for hindlimb initiation in mice. *Development* **138**, 4465-73.

**Kengaku, M., Capdevila, J., Rodriguez-Esteban, C., De La Pena, J., Johnson, R. L., Izpisua Belmonte, J. C. and Tabin, C. J.** (1998). Distinct WNT pathways regulating AER formation and dorsoventral polarity in the chick limb bud. *Science* **280**, 1274-7.

**Kessel, M. and Gruss, P.** (1990). Murine developmental control genes. *Science* **249**, 374-9.

**Khokha, M. K., Hsu, D., Brunet, L. J., Dionne, M. S. and Harland, R. M.** (2003). Gremlin is the BMP antagonist required for maintenance of Shh and Fgf signals during limb patterning. *Nat Genet* **34**, 303-7.

**Kieny, M., Mauger, A. and Thevenet, A.** (1971). [Influence of the axial nervous system on the morphogenesis of the limbs in the chick embryo]. *C R Acad Sci Hebd Seances Acad Sci D* **272**, 121-4.

**Kim, Y. K., Bae, G. U., Kang, J. K., Park, J. W., Lee, E. K., Lee, H. Y., Choi, W. S., Lee, H. W. and Han, J. W.** (2006). Cooperation of H2O2-mediated ERK activation with Smad pathway in TGF-beta1 induction of p21WAF1/Cip1. *Cell Signal* **18**, 236-43.

**Kimmel, R. A., Turnbull, D. H., Blanquet, V., Wurst, W., Loomis, C. A. and Joyner, A. L.** (2000). Two lineage boundaries coordinate vertebrate apical ectodermal ridge formation. *Genes Dev* **14**, 1377-89.

**Kingsley, D. M.** (1994). The TGF-beta superfamily: new members, new receptors, and new genetic tests of function in different organisms. *Genes Dev* **8**, 133-46.

**Koenig, B. B., Cook, J. S., Wolsing, D. H., Ting, J., Tiesman, J. P., Correa, P. E., Olson, C. A., Pecquet, A. L., Ventura, F., Grant, R. A. et al.** (1994). Characterization and cloning of a receptor for BMP-2 and BMP-4 from NIH 3T3 cells. *Mol Cell Biol* **14**, 5961-74.

**Kondo, T. and Duboule, D.** (1999). Breaking colinearity in the mouse HoxD complex. *Cell* **97**, 407-17.

**Korinek, V., Barker, N., Morin, P. J., van Wichen, D., de Weger, R., Kinzler, K. W., Vogelstein, B. and Clevers, H.** (1997). Constitutive transcriptional activation by a beta-catenin-Tcf complex in APC-/- colon carcinoma. *Science* **275**, 1784-7.

**Kouwenhoven, E. N., van Heeringen, S. J., Tena, J. J., Oti, M., Dutilh, B. E., Alonso, M. E., de la Calle-Mustienes, E., Smeenk, L., Rinne, T., Parsaulian, L. et al.** (2010). Genome-wide profiling of p63 DNA-binding sites identifies an element that regulates gene expression during limb development in the 7q21 SHFM1 locus. *PLoS Genet* **6**, e1001065.

**Kraus, P., Fraidenraich, D. and Loomis, C. A.** (2001). Some distal limb structures develop in mice lacking Sonic hedgehog signaling. *Mech Dev* **100**, 45-58.

**Kraus, P. and Lufkin, T.** (2006). Dlx homeobox gene control of mammalian limb and craniofacial development. *Am J Med Genet A* **140**, 1366-74.

**Krumlauf, R.** (1992). Evolution of the vertebrate Hox homeobox genes. *Bioessays* **14**, 245-52.

**Krumlauf, R.** (1994). Hox genes in vertebrate development. *Cell* **78**, 191-201.

**Lallemand, Y., Nicola, M. A., Ramos, C., Bach, A., Clement, C. S. and Robert, B.** (2005). Analysis of Msx1; Msx2 double mutants reveals multiple roles for Msx genes in limb development. *Development* **132**, 3003-14.

**Lanctot, C., Moreau, A., Chamberland, M., Tremblay, M. L. and Drouin, J.** (1999). Hindlimb patterning and mandible development require the Ptx1 gene. *Development* **126**, 1805-10.

**Laufer, E., Dahn, R., Orozco, O. E., Yeo, C. Y., Pisenti, J., Henrique, D., Abbott, U. K., Fallon, J. F. and Tabin, C.** (1997). Expression of Radical fringe in limb-bud ectoderm regulates apical ectodermal ridge formation. *Nature* **386**, 366-73.

**Laufer, E., Nelson, C. E., Johnson, R. L., Morgan, B. A. and Tabin, C.** (1994). Sonic hedgehog and Fgf-4 act through a signaling cascade and feedback loop to integrate growth and patterning of the developing limb bud. *Cell* **79**, 993-1003.

**Lewandoski, M., Sun, X. and Martin, G. R.** (2000). Fgf8 signalling from the AER is essential for normal limb development. *Nat Genet* **26**, 460-3.

**Lin, C., Yin, Y., Bell, S. M., Veith, G. M., Chen, H., Huh, S. H., Ornitz, D. M. and Ma, L.** (2013). Delineating a conserved genetic cassette promoting outgrowth of body appendages. *PLoS Genet* **9**, e1003231.

**Lin, X.** (2004). Functions of heparan sulfate proteoglycans in cell signaling during development. *Development* **131**, 6009-21.

**Litingtung, Y., Dahn, R. D., Li, Y., Fallon, J. F. and Chiang, C.** (2002). Shh and Gli3 are dispensable for limb skeleton formation but regulate digit number and identity. *Nature* **418**, 979-83.

**Liu, Y., Liu, C., Yamada, Y. and Fan, C. M.** (2002). Growth arrest specific gene 1 acts as a region-specific mediator of the Fgf10/Fgf8 regulatory loop in the limb. *Development* **129**, 5289-300.

**Livak, K. J. and Schmittgen, T. D.** (2001). Analysis of relative gene expression data using real-time quantitative PCR and the 2(-Delta Delta C(T)) Method. *Methods* **25**, 402-8.

**Lo Iacono, N., Mantero, S., Chiarelli, A., Garcia, E., Mills, A. A., Morasso, M. I., Costanzo, A., Levi, G., Guerrini, L. and Merlo, G. R.** (2008). Regulation of Dlx5 and Dlx6 gene expression by p63 is involved in EEC and SHFM congenital limb defects. *Development* **135**, 1377-88.

**Logan, C., Hornbruch, A., Campbell, I. and Lumsden, A.** (1997). The role of Engrailed in establishing the dorsoventral axis of the chick limb. *Development* **124**, 2317-24.

**Logan, M., Martin, J. F., Nagy, A., Lobe, C., Olson, E. N. and Tabin, C. J.** (2002). Expression of Cre Recombinase in the developing mouse limb bud driven by a Prxl enhancer. *Genesis* **33**, 77-80.

**Logan, M., Simon, H. G. and Tabin, C.** (1998). Differential regulation of T-box and homeobox transcription factors suggests roles in controlling chick limb-type identity. *Development* **125**, 2825-35.

**Logan, M. and Tabin, C. J.** (1999). Role of Pitx1 upstream of Tbx4 in specification of hindlimb identity. *Science* **283**, 1736-9.

**Loomis, C. A., Harris, E., Michaud, J., Wurst, W., Hanks, M. and Joyner, A. L.** (1996). The mouse Engrailed-1 gene and ventral limb patterning. *Nature* **382**, 360-3.

**Loomis, C. A., Kimmel, R. A., Tong, C. X., Michaud, J. and Joyner, A. L.** (1998). Analysis of the genetic pathway leading to formation of ectopic apical ectodermal ridges in mouse Engrailed-1 mutant limbs. *Development* **125**, 1137-48.

**Lopez-Martinez, A., Chang, D. T., Chiang, C., Porter, J. A., Ros, M. A., Simandl, B. K., Beachy, P. A. and Fallon, J. F.** (1995). Limb-patterning activity and restricted posterior localization of the amino-terminal product of Sonic hedgehog cleavage. *Curr Biol* **5**, 791-6.

**Lu, P., Yu, Y., Perdue, Y. and Werb, Z.** (2008). The apical ectodermal ridge is a timer for generating distal limb progenitors. *Development* **135**, 1395-405.

**Luo, G., Hofmann, C., Bronckers, A. L., Sohocki, M., Bradley, A. and Karsenty, G.** (1995). BMP-7 is an inducer of nephrogenesis, and is also required for eye development and skeletal patterning. *Genes Dev* **9**, 2808-20.

**Maatouk, D. M., Choi, K., Bouldin, C. M. and Harfe, B. D.** (2009). In the limb AER Bmp2 and Bmp4 are required for dorsal-ventral patterning and interdigital cell death but not limb outgrowth. *Dev Biol* **doi: 10.1016/j.ydbio.2009.01.004**.

**Macatee, T. L., Hammond, B. P., Arenkiel, B. R., Francis, L., Frank, D. U. and Moon, A. M.** (2003). Ablation of specific expression domains reveals discrete functions of ectoderm- and endoderm-derived FGF8 during cardiovascular and pharyngeal development. *Development* **130**, 6361-74.

**MacCabe, J. A., Errick, J. and Saunders, J. W., Jr.** (1974). Ectodermal control of the dorsoventral axis in the leg bud of the chick embryo. *Dev Biol* **39**, 69-82.

**Mahmood, R., Bresnick, J., Hornbruch, A., Mahony, C., Morton, N., Colquhoun, K., Martin, P., Lumsden, A., Dickson, C. and Mason, I.** (1995). A role for FGF-8 in the initiation and maintenance of vertebrate limb bud outgrowth. *Curr Biol* **5**, 797-806.

**Mariani, F. V., Ahn, C. P. and Martin, G. R.** (2008). Genetic evidence that FGFs have an instructive role in limb proximal-distal patterning. *Nature* **453**, 401-5.

**Mariani, F. V. and Martin, G. R.** (2003). Deciphering skeletal patterning: clues from the limb. *Nature* **423**, 319-25.

**Marin, M., Karis, A., Visser, P., Grosveld, F. and Philipsen, S.** (1997). Transcription factor Sp1 is essential for early embryonic development but dispensable for cell growth and differentiation. *Cell* **89**, 619-28.

**Martin, G. R.** (1998). The roles of FGFs in the early development of vertebrate limbs. *Genes Dev* **12**, 1571-86.

**Massague, J.** (1998). TGF-beta signal transduction. *Annu Rev Biochem* **67**, 753-91.

**Megason, S. G. and McMahon, A. P.** (2002). A mitogen gradient of dorsal midline Wnts organizes growth in the CNS. *Development* **129**, 2087-98.

**Merlo, G. R., Paleari, L., Mantero, S., Genova, F., Beverdam, A., Palmisano, G. L., Barbieri, O. and Levi, G.** (2002). Mouse model of split hand/foot malformation type I. *Genesis* **33**, 97-101.

**Meyer, R. A., Cohen, M. F., Recalde, S., Zakany, J., Bell, S. M., Scott, W. J., Jr. and Lo, C. W.** (1997). Developmental regulation and asymmetric expression of the gene encoding Cx43 gap junctions in the mouse limb bud. *Dev Genet* **21**, 290-300.

**Michaud, J. L., Lapointe, F. and Le Douarin, N. M.** (1997). The dorsoventral polarity of the presumptive limb is determined by signals produced by the somites and by the lateral somatopleure. *Development* **124**, 1453-63.

**Mills, A. A., Zheng, B., Wang, X. J., Vogel, H., Roop, D. R. and Bradley, A.** (1999). p63 is a p53 homologue required for limb and epidermal morphogenesis. *Nature* **398**, 708-13.

**Min, H., Danilenko, D. M., Scully, S. A., Bolon, B., Ring, B. D., Tarpley, J. E., DeRose, M. and Simonet, W. S.** (1998). Fgf-10 is required for both limb and lung development and exhibits striking functional similarity to Drosophila branchless. *Genes Dev* **12**, 3156-61.

**Minguillon, C., Del Buono, J. and Logan, M. P.** (2005). Tbx5 and Tbx4 are not sufficient to determine limb-specific morphologies but have common roles in initiating limb outgrowth. *Dev Cell* **8**, 75-84.

**Minguillon, C., Gibson-Brown, J. J. and Logan, M. P.** (2009). Tbx4/5 gene duplication and the origin of vertebrate paired appendages. *Proc Natl Acad Sci U S A* **106**, 21726-30.

**Minguillon, C., Nishimoto, S., Wood, S., Vendrell, E., Gibson-Brown, J. J. and Logan, M. P.** (2012). Hox genes regulate the onset of Tbx5 expression in the forelimb. *Development* **139**, 3180-8.

**Mishina, Y., Suzuki, A., Ueno, N. and Behringer, R. R.** (1995). Bmpr encodes a type I bone morphogenetic protein receptor that is essential for gastrulation during mouse embryogenesis. *Genes Dev* **9**, 3027-37.

**Mo, R., Freer, A. M., Zinyk, D. L., Crackower, M. A., Michaud, J., Heng, H. H., Chik, K. W., Shi, X. M., Tsui, L. C., Cheng, S. H. et al.** (1997). Specific and redundant functions of Gli2 and Gli3 zinc finger genes in skeletal patterning and development. *Development* **124**, 113-23.

**Mohammadi, M., Honegger, A. M., Rotin, D., Fischer, R., Bellot, F., Li, W., Dionne, C. A., Jaye, M., Rubinstein, M. and Schlessinger, J.** (1991). A tyrosine-phosphorylated carboxy-terminal peptide of the fibroblast growth factor receptor (Flg) is a binding site for the SH2 domain of phospholipase C-gamma 1. *Mol Cell Biol* **11**, 5068-78.

**Moon, A. M. and Capecchi, M. R.** (2000). Fgf8 is required for outgrowth and patterning of the limbs. *Nat Genet* **26**, 455-9.

**Naiche, L. A. and Papaioannou, V. E.** (2003). Loss of Tbx4 blocks hindlimb development and affects vascularization and fusion of the allantois. *Development* **130**, 2681-93.

**Naiche, L. A. and Papaioannou, V. E.** (2007). Tbx4 is not required for hindlimb identity or post-bud hindlimb outgrowth. *Development* **134**, 93-103.

**Nakamura, T., Unda, F., de-Vega, S., Vilaxa, A., Fukumoto, S., Yamada, K. M. and Yamada, Y.** (2004). The Kruppel-like factor epiprofin is expressed by

epithelium of developing teeth, hair follicles, and limb buds and promotes cell proliferation. *J Biol Chem* **279**, 626-34.

**Nakashima, K., Zhou, X., Kunkel, G., Zhang, Z., Deng, J. M., Behringer, R. R. and de Crombrugghe, B.** (2002). The novel zinc finger-containing transcription factor osterix is required for osteoblast differentiation and bone formation. *Cell* **108**, 17-29.

**Nelson, C. E., Morgan, B. A., Burke, A. C., Laufer, E., DiMambro, E., Murtaugh, L. C., Gonzales, E., Tessarollo, L., Parada, L. F. and Tabin, C.** (1996). Analysis of Hox gene expression in the chick limb bud. *Development* **122**, 1449-66.

**Ng, J. K., Kawakami, Y., Buscher, D., Raya, A., Itoh, T., Koth, C. M., Rodriguez Esteban, C., Rodriguez-Leon, J., Garrity, D. M., Fishman, M. C. et al.** (2002). The limb identity gene Tbx5 promotes limb initiation by interacting with Wnt2b and Fgf10. *Development* **129**, 5161-70.

**Nguyen-Tran, V. T., Kubalak, S. W., Minamisawa, S., Fiset, C., Wollert, K. C., Brown, A. B., Ruiz-Lozano, P., Barrere-Lemaire, S., Kondo, R., Norman, L. W. et al.** (2000). A novel genetic pathway for sudden cardiac death via defects in the transition between ventricular and conduction system cell lineages. *Cell* **102**, 671-82.

**Niederreither, K., Vermot, J., Schuhbaur, B., Chambon, P. and Dolle, P.** (2002). Embryonic retinoic acid synthesis is required for forelimb growth and anteroposterior patterning in the mouse. *Development* **129**, 3563-74.

**Niederreither, K., Ward, S. J., Dolle, P. and Chambon, P.** (1996). Morphological and molecular characterization of retinoic acid-induced limb duplications in mice. *Dev Biol* **176**, 185-98.

**Niemann, S., Zhao, C., Pascu, F., Stahl, U., Aulepp, U., Niswander, L., Weber, J. L. and Muller, U.** (2004). Homozygous WNT3 mutation causes tetra-amelia in a large consanguineous family. *Am J Hum Genet* **74**, 558-63.

**Niswander, L.** (2003). Pattern formation: old models out on a limb. *Nat Rev Genet* **4**, 133-43.

**Niswander, L., Jeffrey, S., Martin, G. R. and Tickle, C.** (1994). A positive feedback loop coordinates growth and patterning in the vertebrate limb. *Nature* **371**, 609-12.

**Niswander, L., Tickle, C., Vogel, A., Booth, I. and Martin, G. R.** (1993). FGF-4 replaces the apical ectodermal ridge and directs outgrowth and patterning of the limb. *Cell* **75**, 579-87.

**Noramly, S., Pisenti, J., Abbott, U. and Morgan, B.** (1996). Gene expression in the limbless mutant: polarized gene expression in the absence of Shh and an AER. *Dev Biol* **179**, 339-46.

**Ohuchi, H., Nakagawa, T., Yamamoto, A., Araga, A., Ohata, T., Ishimaru, Y., Yoshioka, H., Kuwana, T., Nohno, T., Yamasaki, M. et al.** (1997). The

mesenchymal factor, FGF10, initiates and maintains the outgrowth of the chick limb bud through interaction with FGF8, an apical ectodermal factor. *Development* **124**, 2235-44.

**Ohuchi, H., Takeuchi, J., Yoshioka, H., Ishimaru, Y., Ogura, K., Takahashi, N., Ogura, T. and Noji, S.** (1998). Correlation of wing-leg identity in ectopic FGF-induced chimeric limbs with the differential expression of chick Tbx5 and Tbx4. *Development* **125**, 51-60.

**Ohuchi, H., Yoshioka, H., Tanaka, A., Kawakami, Y., Nohno, T. and Noji, S.** (1994). Involvement of androgen-induced growth factor (FGF-8) gene in mouse embryogenesis and morphogenesis. *Biochem Biophys Res Commun* **204**, 882-8.

**Oliver, G., De Robertis, E. M., Wolpert, L. and Tickle, C.** (1990). Expression of a homeobox gene in the chick wing bud following application of retinoic acid and grafts of polarizing region tissue. *EMBO J.* **9**, 3093-99.

**Ornitz, D. M.** (2000). FGFs, heparan sulfate and FGFRs: complex interactions essential for development. *Bioessays* **22**, 108-12.

**Ornitz, D. M. and Marie, P. J.** (2002). FGF signaling pathways in endochondral and intramembranous bone development and human genetic disease. *Genes Dev* **16**, 1446-65.

**Ornitz, D. M., Xu, J., Colvin, J. S., McEwen, D. G., MacArthur, C. A., Coulier, F., Gao, G. and Goldfarb, M.** (1996). Receptor specificity of the fibroblast growth factor family. *J Biol Chem* **271**, 15292-7.

**Orr-Urtreger, A., Bedford, M. T., Burakova, T., Arman, E., Zimmer, Y., Yayon, A., Givol, D. and Lonai, P.** (1993). Developmental localization of the splicing alternatives of fibroblast growth factor receptor-2 (FGFR2). *Dev Biol* **158**, 475-86.

**Ovchinnikov, D. A., Selever, J., Wang, Y., Chen, Y. T., Mishina, Y., Martin, J. F. and Behringer, R. R.** (2006). BMP receptor type IA in limb bud mesenchyme regulates distal outgrowth and patterning. *Dev Biol* **295**, 103-15.

**Padgett, R. W., Savage, C. and Das, P.** (1997). Genetic and biochemical analysis of TGF beta signal transduction. *Cytokine Growth Factor Rev* **8**, 1-9.

**Pajni-Underwood, S., Wilson, C. P., Elder, C., Mishina, Y. and Lewandoski, M.** (2007). BMP signals control limb bud interdigital programmed cell death by regulating FGF signaling. *Development* **134**, 2359-68.

**Pang, D. and Thompson, D. N.** (2011). Embryology and bony malformations of the craniovertebral junction. *Childs Nerv Syst* **27**, 523-64.

**Papaioannou, V. E. and Silver, L. M.** (1998). The T-box gene family. *Bioessays* **20**, 9-19.

**Pardali, K., Kurisaki, A., Moren, A., ten Dijke, P., Kardassis, D. and Moustakas, A.** (2000). Role of Smad proteins and transcription factor Sp1 in p21(Waf1/Cip1) regulation by transforming growth factor-beta. *J Biol Chem* **275**, 29244-56.

**Parr, B. A. and McMahon, A. P.** (1995). Dorsalizing signal Wnt-7a required for normal polarity of D-V and A-P axes of mouse limb. *Nature* **374**, 350-3.

**Parr, B. A., Shea, M. J., Vassileva, G. and McMahon, A. P.** (1993). Mouse Wnt genes exhibit discrete domains of expression in the early embryonic CNS and limb buds. *Development* **119**, 247-61.

**Partanen, J., Schwartz, L. and Rossant, J.** (1998). Opposite phenotypes of hypomorphic and Y766 phosphorylation site mutations reveal a function for Fgfr1 in anteroposterior patterning of mouse embryos. *Genes Dev* **12**, 2332-44.

**Pautou, M. P. and Kieny, M.** (1973). [Ecto-mesodermic interaction in the establishment of dorso-ventral polarity in the chick embryo foot]. *C R Acad Sci Hebd Seances Acad Sci D* **277**, 1225-8.

**Pinson, K. I., Brennan, J., Monkley, S., Avery, B. J. and Skarnes, W. C.** (2000). An LDL-receptor-related protein mediates Wnt signalling in mice. *Nature* **407**, 535-8.

**Pizette, S., Abate-Shen, C. and Niswander, L.** (2001). BMP controls proximodistal outgrowth, via induction of the apical ectodermal ridge, and dorsoventral patterning in the vertebrate limb. *Development* **128**, 4463-74.

**Pizette, S. and Niswander, L.** (1999). BMPs negatively regulate structure and function of the limb apical ectodermal ridge. *Development* **126**, 883-94.

**Pizette, S. and Niswander, L.** (2000). BMPs are required at two steps of limb chondrogenesis: formation of prechondrogenic condensations and their differentiation into chondrocytes. *Dev Biol* **219**, 237-49.

**Prahlad, K. V., Skala, G., Jones, D. G. and Briles, W. E.** (1979). Limbless: a new genetic mutant in the chick. *J Exp Zool* **209**, 427-34.

**Rallis, C., Bruneau, B. G., Del Buono, J., Seidman, C. E., Seidman, J. G., Nissim, S., Tabin, C. J. and Logan, M. P.** (2003). Tbx5 is required for forelimb bud formation and continued outgrowth. *Development* **130**, 2741-51.

**Rallis, C., Del Buono, J. and Logan, M. P.** (2005). Tbx3 can alter limb position along the rostrocaudal axis of the developing embryo. *Development* **132**, 1961-70.

**Rancourt, D. E., Tsuzuki, T. and Capecchi, M. R.** (1995). Genetic interaction between hoxb-5 and hoxb-6 is revealed by nonallelic noncomplementation. *Genes Dev* **9**, 108-22.

**Riddle, R. D., Ensini, M., Nelson, C., Tsuchida, T., Jessell, T. M. and Tabin, C.** (1995). Induction of the LIM homeobox gene Lmx1 by WNT7a establishes dorsoventral pattern in the vertebrate limb. *Cell* **83**, 631-40.

**Riddle, R. D., Johnson, R. L., Laufer, E. and Tabin, C.** (1993). Sonic hedgehog mediates the polarizing activity of the ZPA. *Cell* **75**, 1401-16.

**Robb, E. A., Gitter, C. L., Cheng, H. H. and Delany, M. E.** (2011). Chromosomal mapping and candidate gene discovery of chicken developmental mutants and genome-wide variation analysis of MHC congenics. *J Hered* **102**, 141-56.

**Robledo, R. F., Rajan, L., Li, X. and Lufkin, T.** (2002). The Dlx5 and Dlx6 homeobox genes are essential for craniofacial, axial, and appendicular skeletal development. *Genes Dev* **16**, 1089-101.

**Rodriguez-Esteban, C., Schwabe, J. W., De La Pena, J., Foys, B., Eshelman, B. and Izpisua Belmonte, J. C.** (1997). Radical fringe positions the apical ectodermal ridge at the dorsoventral boundary of the vertebrate limb. *Nature* **386**, 360-6.

**Roelink, H. and Nusse, R.** (1991). Expression of two members of the Wnt family during mouse development--restricted temporal and spatial patterns in the developing neural tube. *Genes Dev* **5**, 381-8.

**Ros, M. A., Lopez-Martinez, A., Simandl, B. K., Rodriguez, C., Izpisua Belmonte, J. C., Dahn, R. and Fallon, J. F.** (1996). The limb field mesoderm determines initial limb bud anteroposterior asymmetry and budding independent of sonic hedgehog or apical ectodermal gene expressions. *Development* **122**, 2319-30.

**Rosello-Diez, A., Ros, M. A. and Torres, M.** (2011). Diffusible signals, not autonomous mechanisms, determine the main proximodistal limb subdivision. *Science* **332**, 1086-8.

**Roux, P. P. and Blenis, J.** (2004). ERK and p38 MAPK-activated protein kinases: a family of protein kinases with diverse biological functions. *Microbiol Mol Biol Rev* **68**, 320-44.

**Rowe, D. A., Cairns, J. M. and Fallon, J. F.** (1982). Spatial and temporal patterns of cell death in limb bud mesoderm after apical ectodermal ridge removal. *Dev Biol* **93**, 83-91.

**Runko, A. P. and Sagerstrom, C. G.** (2003). Nlz belongs to a family of zinc-finger-containing repressors and controls segmental gene expression in the zebrafish hindbrain. *Dev Biol* **262**, 254-67.

**Rutledge, J. C., Shourbaji, A. G., Hughes, L. A., Polifka, J. E., Cruz, Y. P., Bishop, J. B. and Generoso, W. M.** (1994). Limb and lower-body duplications induced by retinoic acid in mice. *Proc Natl Acad Sci U S A* **91**, 5436-40.

**Sahara, S., Kawakami, Y., Izpisua Belmonte, J. C. and O'Leary, D. D.** (2007). Sp8 exhibits reciprocal induction with Fgf8 but has an opposing effect on anterior-posterior cortical area patterning. *Neural Dev* **2**, 10.

**Sakaguchi, M., Sonegawa, H., Nukui, T., Sakaguchi, Y., Miyazaki, M., Namba, M. and Huh, N. H.** (2005). Bifurcated converging pathways for high Ca2+- and TGFbeta-induced inhibition of growth of normal human keratinocytes. *Proc Natl Acad Sci U S A* **102**, 13921-6.

**Saunders, J. W. and Gasseling, M. T.** (1968). Ectodermal-mesenchymal interactions in the origin of limb symmetry. In *Epitethelial-Mesenchimal interactions*, (ed. R. Fleischmayer and R. E. Billingham), pp. 78–97. Baltimore: Williams & Wilkins.

**Saunders, J. W., Jr.** (1948). The proximo-distal sequence of origin of the parts of the chick wing and the role of the ectoderm. *J Exp Zool* **108**, 363-403.

**Saunders, J. W., Jr. and Reuss, C.** (1974). Inductive and axial properties of prospective wing-bud mesoderm in the chick embryo. *Dev Biol* **38**, 41-50.

**Schaeper, N. D., Prpic, N. M. and Wimmer, E. A.** (2010). A clustered set of three Sp-family genes is ancestral in the Metazoa: evidence from sequence analysis, protein domain structure, developmental expression patterns and chromosomal location. *BMC Evol Biol* **10**, 88.

**Scherer, S. W., Poorkaj, P., Massa, H., Soder, S., Allen, T., Nunes, M., Geshuri, D., Wong, E., Belloni, E., Little, S. et al.** (1994). Physical mapping of the split hand/split foot locus on chromosome 7 and implication in syndromic ectrodactyly. *Hum Mol Genet* **3**, 1345-54.

**Scherz, P. J., Harfe, B. D., McMahon, A. P. and Tabin, C. J.** (2004). The limb bud Shh-Fgf feedback loop is terminated by expansion of former ZPA cells. *Science* **305**, 396-9.

**Scherz, P. J., McGlinn, E., Nissim, S. and Tabin, C. J.** (2007). Extended exposure to Sonic hedgehog is required for patterning the posterior digits of the vertebrate limb. *Dev Biol* **308**, 343-54.

**Schimmang, T., Lemaistre, M., Vortkamp, A. and Ruther, U.** (1992). Expression of the zinc finger gene Gli3 is affected in the morphogenetic mouse mutant extra-toes (Xt). *Development* **116**, 799-804.

**Schwarz-Romond, T., Asbrand, C., Bakkers, J., Kuhl, M., Schaeffer, H. J., Huelsken, J., Behrens, J., Hammerschmidt, M. and Birchmeier, W.** (2002). The ankyrin repeat protein Diversin recruits Casein kinase Iepsilon to the beta-catenin degradation complex and acts in both canonical Wnt and Wnt/JNK signaling. *Genes Dev* **16**, 2073-84.

**Searls, R. L. and Janners, M. Y.** (1971). The initiation of limb bud outgrowth in the embryonic chick. *Dev Biol* **24**, 198-213.

**Sekine, K., Ohuchi, H., Fujiwara, M., Yamasaki, M., Yoshizawa, T., Sato, T., Yagishita, N., Matsui, D., Koga, Y., Itoh, N. et al.** (1999). Fgf10 is essential for limb and lung formation. *Nat Genet* **21**, 138-41.

**Selever, J., Liu, W., Lu, M. F., Behringer, R. R. and Martin, J. F.** (2004). Bmp4 in limb bud mesoderm regulates digit pattern by controlling AER development. *Dev Biol* **276**, 268-79.

**Shamseldin, H. E., Faden, M. A., Alashram, W. and Alkuraya, F. S.** (2012). Identification of a novel DLX5 mutation in a family with autosomal recessive split hand and foot malformation. *J Med Genet* **49**, 16-20.

**Sheth, R., Gregoire, D., Dumouchel, A., Scotti, M., Pham, J. M., Nemec, S., Bastida, M. F., Ros, M. A. and Kmita, M.** (2013). Decoupling the function of Hox and Shh in developing limb reveals multiple inputs of Hox genes on limb growth. *Development* **140**, 2130-8.

**Shubin, N. H.** (2002). Origin of evolutionary novelty: examples from limbs. *J Morphol* **252**, 15-28.

**Sidow, A., Bulotsky, M. S., Kerrebrock, A. W., Birren, B. W., Altshuler, D., Jaenisch, R., Johnson, K. R. and Lander, E. S.** (1999). A novel member of the F-box/WD40 gene family, encoding dactylin, is disrupted in the mouse dactylaplasia mutant. *Nat Genet* **23**, 104-7.

**Sifakis, S., Basel, D., Ianakiev, P., Kilpatrick, M. and Tsipouras, P.** (2001). Distal limb malformations: underlying mechanisms and clinical associations. *Clin Genet* **60**, 165-72.

**Simeone, A., Acampora, D., Pannese, M., D'Esposito, M., Stornaiuolo, A., Gulisano, M., Mallamaci, A., Kastury, K., Druck, T., Huebner, K. et al.** (1994). Cloning and characterization of two members of the vertebrate Dlx gene family. *Proc Natl Acad Sci U S A* **91**, 2250-4.

**Soriano, P.** (1999). Generalized lacZ expression with the ROSA26 Cre reporter strain. *Nat Genet* **21**, 70-1.

**Soshnikova, N., Zechner, D., Huelsken, J., Mishina, Y., Behringer, R. R., Taketo, M. M., Crenshaw, E. B., 3rd and Birchmeier, W.** (2003). Genetic interaction between Wnt/beta-catenin and BMP receptor signaling during formation of the AER and the dorsal-ventral axis in the limb. *Genes Dev* **17**, 1963-8.

**Stratford, T., Horton, C. and Maden, M.** (1996). Retinoic acid is required for the initiation of outgrowth in the chick limb bud. *Curr Biol* **6**, 1124-33.

**Summerbell, D.** (1974). Interaction between the proximo-distal and antero-posterior co-ordinates of positional value during the specification of positional information in the early development of the chick limb-bud. *J Embryol Exp Morphol* **32**, 227-37.

**Summerbell, D. and Lewis, J. H.** (1975). Time, place and positional value in the chick limb-bud. *J Embryol Exp Morphol* **33**, 621-43.

**Summerbell, D., Lewis, J. H. and Wolpert, L.** (1973). Positional information in chick limb morphogenesis. *Nature* **244**, 492-6.

**Sun, X., Lewandoski, M., Meyers, E. N., Liu, Y. H., Maxson, R. E., Jr. and Martin, G. R.** (2000). Conditional inactivation of Fgf4 reveals complexity of signalling during limb bud development. *Nat Genet* **25**, 83-6.

**Sun, X., Mariani, F. V. and Martin, G. R.** (2002). Functions of FGF signalling from the apical ectodermal ridge in limb development. *Nature* **418**, 501-8.

**Supp, D. M., Witte, D. P., Branford, W. W., Smith, E. P. and Potter, S. S.** (1996). Sp4, a member of the Sp1-family of zinc finger transcription factors, is required for normal murine growth, viability, and male fertility. *Dev Biol* **176**, 284-99.

**Suzuki, A., Kaneko, E., Maeda, J. and Ueno, N.** (1997). Mesoderm induction by BMP-4 and -7 heterodimers. *Biochem Biophys Res Commun* **232**, 153-6.

**Szeto, D. P., Rodriguez-Esteban, C., Ryan, A. K., O'Connell, S. M., Liu, F., Kioussi, C., Gleiberman, A. S., Izpisua-Belmonte, J. C. and Rosenfeld, M. G.** (1999). Role of the Bicoid-related homeodomain factor Pitx1 in specifying hindlimb morphogenesis and pituitary development. *Genes Dev* **13**, 484-94.

**Tabin, C.** (1995). The initiation of the limb bud: growth factors, Hox genes, and retinoids. *Cell* **80**, 671-4.

**Tabin, C. and Wolpert, L.** (2007). Rethinking the proximodistal axis of the vertebrate limb in the molecular era. *Genes Dev* **21**, 1433-42.

**Tabin, C. J.** (1991). Retinoids, homeoboxes, and growth factors: toward molecular models for limb development. *Cell* **66**, 199-217.

**Takada, S., Stark, K. L., Shea, M. J., Vassileva, G., McMahon, J. A. and McMahon, A. P.** (1994). Wnt-3a regulates somite and tailbud formation in the mouse embryo. *Genes Dev* **8**, 174-89.

**Takeuchi, J. K., Koshiba-Takeuchi, K., Suzuki, T., Kamimura, M., Ogura, K. and Ogura, T.** (2003). Tbx5 and Tbx4 trigger limb initiation through activation of the Wnt/Fgf signaling cascade. *Development* **130**, 2729-39.

**Talamillo, A., Delgado, I., Nakamura, T., de-Vega, S., Yoshitomi, Y., Unda, F., Birchmeier, W., Yamada, Y. and Ros, M. A.** (2010). Role of Epiprofin, a zinc-finger transcription factor, in limb development. *Dev Biol* **337**, 363-74.

**Tamai, K., Semenov, M., Kato, Y., Spokony, R., Liu, C., Katsuyama, Y., Hess, F., Saint-Jeannet, J. P. and He, X.** (2000). LDL-receptor-related proteins in Wnt signal transduction. *Nature* **407**, 530-5.

**Tanaka, M., Tamura, K., Noji, S., Nohno, T. and Ide, H.** (1997). Induction of additional limb at the dorsal-ventral boundary of a chick embryo. *Dev Biol* **182**, 191-203.

**Tarchini, B. and Duboule, D.** (2006). Control of Hoxd genes' collinearity during early limb development. *Dev Cell* **10**, 93-103.

**te Welscher, P., Zuniga, A., Kuijper, S., Drenth, T., Goedemans, H. J., Meijlink, F. and Zeller, R.** (2002). Progression of vertebrate limb development through SHH-mediated counteraction of GLI3. *Science* **298**, 827-30.

**Temtamy, S. A. and McKusick, V. A.** (1978). The genetics of hand malformations. *Birth Defects Orig Artic Ser* **14**, i-xviii, 1-619.

**ten Dijke, P., Yamashita, H., Ichijo, H., Franzen, P., Laiho, M., Miyazono, K. and Heldin, C. H.** (1994). Characterization of type I receptors for transforming growth factor-beta and activin. *Science* **264**, 101-4.

**Tickle, C. and Munsterberg, A.** (2001). Vertebrate limb development--the early stages in chick and mouse. *Curr Opin Genet Dev* **11**, 476-81.

**Tickle, C.** (2003). Patterning systems--from one end of the limb to the other. *Dev Cell* **4**, 449-58.

**Tickle, C., Alberts, B., Wolpert, L. and Lee, J.** (1982). Local application of retinoic acid to the limb bond mimics the action of the polarizing region. *Nature* **296**, 564-6.

**Tickle, C., Lee, J. and Eichele, G.** (1985). A quantitative analysis of the effect of all-trans-retinoic acid on the pattern of chick wing development. *Dev Biol* **109**, 82-95.

**Tickle, C. and Munsterberg, A.** (2001). Vertebrate limb development--the early stages in chick and mouse. *Curr Opin Genet Dev* **11**, 476-81.

**Todt, W. L. and Fallon, J. F.** (1984). Development of the apical ectodermal ridge in the chick wing bud. *J Embryol Exp Morphol* **80**, 21-41.

**Topczewski, J., Sepich, D. S., Myers, D. C., Walker, C., Amores, A., Lele, Z., Hammerschmidt, M., Postlethwait, J. and Solnica-Krezel, L.** (2001). The zebrafish glypican knypek controls cell polarity during gastrulation movements of convergent extension. *Dev Cell* **1**, 251-64.

**Towers, M., Mahood, R., Yin, Y. and Tickle, C.** (2008). Integration of growth and specification in chick wing digit-patterning. *Nature* **452**, 882-6.

**Treichel, D., Schock, F., Jackle, H., Gruss, P. and Mansouri, A.** (2003). mBtd is required to maintain signaling during murine limb development. *Genes Dev* **17**, 2630-5.

**Verheyden, J. M. and Sun, X.** (2008). An Fgf/Gremlin inhibitory feedback loop triggers termination of limb bud outgrowth. *Nature* **454**, 638-41.

**Vogel, A., Rodriguez, C. and Izpisua-Belmonte, J. C.** (1996). Involvement of FGF-8 in initiation, outgrowth and patterning of the vertebrate limb. *Development* **122**, 1737-50.

**Vogel, A., Rodriguez, C., Warnken, W. and Izpisua Belmonte, J. C.** (1995). Dorsal cell fate specified by chick Lmx1 during vertebrate limb development. *Nature* **378**, 716-20.

**Wanek, N., Gardiner, D. M., Muneoka, K. and Bryant, S. V.** (1991). Conversion by retinoic acid of anterior cells into ZPA cells in the chick wing bud. *Nature* **350**, 81-3.

**Wang, B., Fallon, J. F. and Beachy, P. A.** (2000). Hedgehog-regulated processing of Gli3 produces an anterior/posterior repressor gradient in the developing vertebrate limb. *Cell* **100**, 423-34.

**Wang, C. K., Omi, M., Ferrari, D., Cheng, H. C., Lizarraga, G., Chin, H. J., Upholt, W. B., Dealy, C. N. and Kosher, R. A.** (2004). Function of BMPs in the apical ectoderm of the developing mouse limb. *Dev Biol* **269**, 109-22.

**Wehrli, M., Dougan, S. T., Caldwell, K., O'Keefe, L., Schwartz, S., Vaizel-Ohayon, D., Schejter, E., Tomlinson, A. and DiNardo, S.** (2000). arrow encodes an LDL-receptor-related protein essential for Wingless signalling. *Nature* **407**, 527-30.

**Weinstein, M., Xu, X., Ohyama, K. and Deng, C. X.** (1998). FGFR-3 and FGFR-4 function cooperatively to direct alveogenesis in the murine lung. *Development* **125**, 3615-23.

**Weng, D. Y., Zhang, Y., Hayashi, Y., Kuan, C. Y., Liu, C. Y., Babcock, G., Weng, W. L., Schwemberger, S. and Kao, W. W.** (2008). Promiscuous recombination of LoxP alleles during gametogenesis in cornea Cre driver mice. *Mol Vis* **14**, 562-71.

**Werner, S., Duan, D. S., de Vries, C., Peters, K. G., Johnson, D. E. and Williams, L. T.** (1992). Differential splicing in the extracellular region of fibroblast growth factor receptor 1 generates receptor variants with different ligand-binding specificities. *Mol Cell Biol* **12**, 82-8.

**Whitman, M.** (1997). Signal transduction. Feedback from inhibitory SMADs. *Nature* **389**, 549-51.

**Wimmer, E. A., Frommer, G., Purnell, B. A. and Jackle, H.** (1996). buttonhead and D-Sp1: a novel Drosophila gene pair. *Mech Dev* **59**, 53-62.

**Winnier, G., Blessing, M., Labosky, P. A. and Hogan, B. L.** (1995). Bone morphogenetic protein-4 is required for mesoderm formation and patterning in the mouse. *Genes Dev* **9**, 2105-16.

**Wong, Y. L., Behringer, R. R. and Kwan, K. M.** (2012). Smad1/Smad5 signaling in limb ectoderm functions redundantly and is required for interdigital programmed cell death. *Dev Biol* **363**, 247-57.

**Wurst, W., Auerbach, A. B. and Joyner, A. L.** (1994). Multiple developmental defects in Engrailed-1 mutant mice: an early mid-hindbrain deletion and patterning defects in forelimbs and sternum. *Development* **120**, 2065-75.

**Xu, X., Weinstein, M., Li, C., Naski, M., Cohen, R. I., Ornitz, D. M., Leder, P. and Deng, C.** (1998). Fibroblast growth factor receptor 2 (FGFR2)-mediated reciprocal regulation loop between FGF8 and FGF10 is essential for limb induction. *Development* **125**, 753-65.

**Yamaji, N., Celeste, A. J., Thies, R. S., Song, J. J., Bernier, S. M., Goltzman, D., Lyons, K. M., Nove, J., Rosen, V. and Wozney, J. M.** (1994). A mammalian serine/threonine kinase receptor specifically binds BMP-2 and BMP-4. *Biochem Biophys Res Commun* **205**, 1944-51.

**Yamashita, H., ten Dijke, P., Huylebroeck, D., Sampath, T. K., Andries, M., Smith, J. C., Heldin, C. H. and Miyazono, K.** (1995). Osteogenic protein-1 binds to activin type II receptors and induces certain activin-like effects. *J Cell Biol* **130**, 217-26.

**Yang, A., Schweitzer, R., Sun, D., Kaghad, M., Walker, N., Bronson, R. T., Tabin, C., Sharpe, A., Caput, D., Crum, C. et al.** (1999). p63 is essential for regenerative proliferation in limb, craniofacial and epithelial development. *Nature* **398**, 714-8.

**Yang, Y., Drossopoulou, G., Chuang, P. T., Duprez, D., Marti, E., Bumcrot, D., Vargesson, N., Clarke, J., Niswander, L., McMahon, A. et al.** (1997). Relationship between dose, distance and time in Sonic Hedgehog-mediated regulation of anteroposterior polarity in the chick limb. *Development* **124**, 4393-404.

**Yang, Y. and Niswander, L.** (1995). Interaction between the signaling molecules WNT7a and SHH during vertebrate limb development: dorsal signals regulate anteroposterior patterning. *Cell* **80**, 939-47.

**Yoda, A., Oishi, I. and Minami, Y.** (2003). Expression and function of the Ror-family receptor tyrosine kinases during development: lessons from genetic analyses of nematodes, mice, and humans. *J Recept Signal Transduct Res* **23**, 1-15.

**Yu, K. and Ornitz, D. M.** (2008). FGF signaling regulates mesenchymal differentiation and skeletal patterning along the limb bud proximodistal axis. *Development* **135**, 483-91.

**Zakany, J. and Duboule, D.** (1999). Hox genes in digit development and evolution. *Cell Tissue Res* **296**, 19-25.

**Zembrzycki, A., Griesel, G., Stoykova, A. and Mansouri, A.** (2007). Genetic interplay between the transcription factors Sp8 and Emx2 in the patterning of the forebrain. *Neural Dev* **2**, 8.

**Zeng, L., Fagotto, F., Zhang, T., Hsu, W., Vasicek, T. J., Perry, W. L., 3rd, Lee, J. J., Tilghman, S. M., Gumbiner, B. M. and Costantini, F.** (1997). The mouse Fused locus encodes Axin, an inhibitor of the Wnt signaling pathway that regulates embryonic axis formation. *Cell* **90**, 181-92.

**Zeng, X., Goetz, J. A., Suber, L. M., Scott, W. J., Jr., Schreiner, C. M. and Robbins, D. J.** (2001). A freely diffusible form of Sonic hedgehog mediates long-range signalling. *Nature* **411**, 716-20.

**Zhang, H. and Bradley, A.** (1996). Mice deficient for BMP2 are nonviable and have defects in amnion/chorion and cardiac development. *Development* **122**, 2977-86.

**Zhao, C. and Meng, A.** (2005). Sp1-like transcription factors are regulators of embryonic development in vertebrates. *Dev Growth Differ* **47**, 201-11.

**Zhao, X., Sirbu, I. O., Mic, F. A., Molotkova, N., Molotkov, A., Kumar, S. and Duester, G.** (2009). Retinoic acid promotes limb induction through effects on body axis extension but is unnecessary for limb patterning. *Curr Biol* **19**, 1050-7.

**Zhu J, Nakamura E, Nguyen MT, Bao X, Akiyama H, Mackem S**. (2008). Uncoupling Sonic hedgehog control of pattern and expansion of the developing limb bud. *Dev. Cell..***14**,624-32

**Zou, H., Choe, K. M., Lu, Y., Massague, J. and Niswander, L.** (1997). BMP signaling and vertebrate limb development. *Cold Spring Harb Symp Quant Biol* **62**, 269-72.

**Zou, H. and Niswander, L.** (1996). Requirement for BMP signaling in interdigital apoptosis and scale formation. *Science* **272**, 738-41.

**Zuniga, A., Haramis, A. P., McMahon, A. P. and Zeller, R.** (1999). Signal relay by BMP antagonism controls the SHH/FGF4 feedback loop in vertebrate limb buds. *Nature* **401**, 598-602.

# AGRADECIMIENTOS

Hay tantas personas a las que debo estar agradecido por su apoyo a lo largo de estos cuatro años, que me resultaría muy difícil saber por donde empezar. Aun así, intentando ser breve, esta tesis no puede terminar sin unas palabras de agradecimiento hacia las personas que han marcado mi estancia en Santander.

En primer lugar, quiero agradecer a Marian y a Federica todo lo que me han enseñado sobre biología del desarrollo y sobre ciencia en general. Me siento muy agradecido de poder decir que he tenido como directoras no solo a unas grandes investigadoras, sino también unas personas cercanas y con las que poder discutir. Del mismo modo, me gustaría agradecerles todos los consejos que durante este tiempo me han dado.

No me puedo olvidar de todos los compañeros de laboratorio: Marisa, Mª Félix, Marta, Patricia, Paula, Lucia, Carlos, Rushi, Marian T., Antonio, Sara, Irene, Mamen y Mar. Muchas gracias por haber sido además de compañeros, grandes amigos. Me considero afortunado por haber compartido estos años con vosotros, todos en mayor o menor medida, habéis sido muy importantes y habéis marcado de forma especial mi estancia aquí.

También me gustaría agradecer en general el ambiente de compañerismo que existe entre los diferentes departamentos de la facultad y del recién inaugurado IBBTEC, a todos y cada uno de los becarios (que son muchos y me seria imposible agradecerles a todos sin dejarme seguramente alguno por el camino) siempre dispuestos a escuchar y a ayudar en lo que estuviese en su mano. Gracias a todos, aquí me tendréis siempre para lo que necesitéis.

Por último, pero no por ello menos especial quiero agradecer a mi familia y amigos en general , y a mis padres y a mi amama en particular, su paciencia e incondicional apoyo durante estos cuatro años, porque sin ellos esto no hubiese sido posible. Laura, por supuesto que no me olvido de ti, siempre has estado ahí ayudándome a conseguir lo que me proponía y esta última vez no ha sido menos, siempre te estaré agradecido por tu comprensión y alegría, solo puedo decirte:

*- UBI TU - IBI EGO-*